Stony Brook University

Utilization of Energy Analytics to Reduce Energy Waste in the Manufacturing Environment

A Dissertation presented

by

Michael P Brundage

to

The Graduate School

in Partial Fulfillment of the

Requirements

for the Degree of

Doctor of Philosophy

in

Mechanical Engineering

(Design & Manufacturing)

Stony Brook University

August 2015

Stony Brook University

The Graduate School

Michael P Brundage

We, the dissertation committee for the above candidate for the

Doctor of Philosophy degree, hereby recommend

acceptance of this dissertation

Professor Qing Chang - Advisor
Associate Professor - Mechanical Engineering

Professor Imin Kao - Committee Chair
Professor - Mechanical Engineering

Professor Shikui Chen - Committee Member
Associate Professor - Mechanical Engineering

Dr Jorge Arinez - Outside Member
Lab Group Manager - General Motors

This dissertation is accepted by the Graduate School

Charles Taber
Dean of the Graduate School

Utilization of Energy Analytics to Reduce Energy Waste in the Manufacturing Environment

by

Michael P Brundage

Doctor of Philosophy

in

Mechanical Engineering

(Design & Manufacturing)

Stony Brook University

2015

Current manufacturing facilities lack proper performance indicators that can accurately pinpoint areas of energy inefficiency on the manufacturing line. In studying the production dynamics, it is realized that not every disruption event causes permanent production loss for the manufacturing line. Each downtime event is categorized as non-effective (not causing permanent production loss) and effective (causing permanent production loss). This directly leads to the concept of the opportunity window, which is the largest amount of time a machine can be turned off without causing the slowest machine to become blocked or starved. The recovery time is also analyzed, which is the amount of time it takes the system to recover back to the original state after a downtime event. The opportunity window and recovery time are proven to be constant for a given line configuration in a deterministic scenario.

Building upon the study of the production dynamics, this dissertation establishes new indices that utilize readily available, real sensor information from the production line, such as buffer levels, machine throughput, etc., to find the machine that is the least energy efficient. This is the machine that causes the line to waste the most energy without producing parts. The energy structure of the production line is analyzed to better understand the complex system dynamics and to find the root cause of the energy inefficiencies. A baseline energy consumption is established, which is the least amount of energy that is needed to produce a certain number of parts on the line. Using this knowledge, the new sustainable manufacturing performance indicators are defined to properly monitor the performance of the line. These indices utilize the energy structure to illustrate the static (energy used when there are no downtime events) and dynamic (energy lost due to downtime) portions of the

energy consumption. The static portion of the energy structure is broken down further to find the optimal minimum energy consumption per part. This is a virtual scenario where each machine runs as a standalone machine and has no energy wasted due to unnecessary machine interactions. This provides plant managers with a quantitative self-benchmark for measuring system performance. The concepts of the downtime energy bottleneck and the rated power bottleneck are introduced and proven analytically. The downtime energy bottleneck is the machine that leads to the biggest energy waste reduction when prioritized for reactive maintenance. The rated power bottleneck is the machine, which when replaced, leads to the largest reduction in energy waste. These methods are verified using simulation studies in Simulink/MATLAB.

Furthering the study of the energy indices, the production line dynamics are analyzed from an energy economics point of view. A return on investment strategy is introduced, which allows for the largest return on investment when replacing a machine or part with a more energy efficient version. The energy profit bottleneck is defined as the machine that leads to the largest increase in profit when prioritized for reactive maintenance. These concepts are used with an opportunity window control scheme to maximize overall profit in the manufacturing facility.

The production line dynamics are integrated with the heating, ventilation, and air conditioning system to further reduce overall energy demand of the manufacturing plant. By merging the two largest energy consumers within the facility, we shift electrical demand to minimize the energy costs. The cooling load is analyzed to reduce the overall effect of the production system on the HVAC system. The opportunity window control methodology is utilized to further reduce electricity costs with minimal throughput impact on the production.

In the future, an optimal control methodology will be developed that utilizes Markov decision process to maximize profits, while minimizing energy demand. The issue of data uncertainty will be addressed by introducing a Kalman Filter into the system.

Contents

List of Figures

List of Tables

List of Abbreviations

This is a list of all abbreviations and their subsequent definitions used throughout the dissertation. The page numbers refer to the page on which each abbreviation is first defined.

Abbreviation	Definition	Page
ASHRAE	American Society of Heating, Refrigeration and Air Conditioning Engineers	87
BE	Break Even Point	63
BLAST	Building Loads Analysis and System Thermodynamics	91
CTF	Conduction Transfer Functions	91
DE-BN	Downtime Energy Bottleneck	28
EMCS	Energy Management Control Systems	18
EP-BN	Energy Profit Bottleneck	53
EPP	Energy per Part	29
ESO	Energy Savings Opportunity	18
KPI	Key Performance Indicator	14
HVAC	Heating, Ventilation, and Air Conditioning	5
MCBF	Mean Cycles Between Failure	43
MDP	Markov Decision Process	118
MTTR	Mean Time to Repair	38
OW	Opportunity Window	20
PMV	Predicted Mean Vote	103
PPD	Predicted Percentage Dissatisfied	103
PPL	Permanent Production Loss	20
RTSM	Radiant Time Series Method	88
ROI	Return on Investment	61
RP-BN	Rated Power Bottleneck	28
SMPI	Sustainable Manufacturing Performance Indicator	28
TH-BN	Throughput Bottleneck	58
WIP	Work in Progress	34

Acknowledgements

This research was funded by the National Science Foundation under CAREER AWARD CMMI-1351160.

Chapter 1

Introduction

1.1 Motivation

Reducing energy waste in manufacturing facilities is a primary goal of manufacturing companies as sustainability and green processes are becoming more prevalent. Over the past 60 years, the energy consumption in the industrial sector has more than doubled to approximately 30 quadrillion BTU in the United States, which was 31% of all energy used in 2011 [1]. This is illustrated in Fig. 1.1 & 1.2. This accounts for more than $100 Billion spent

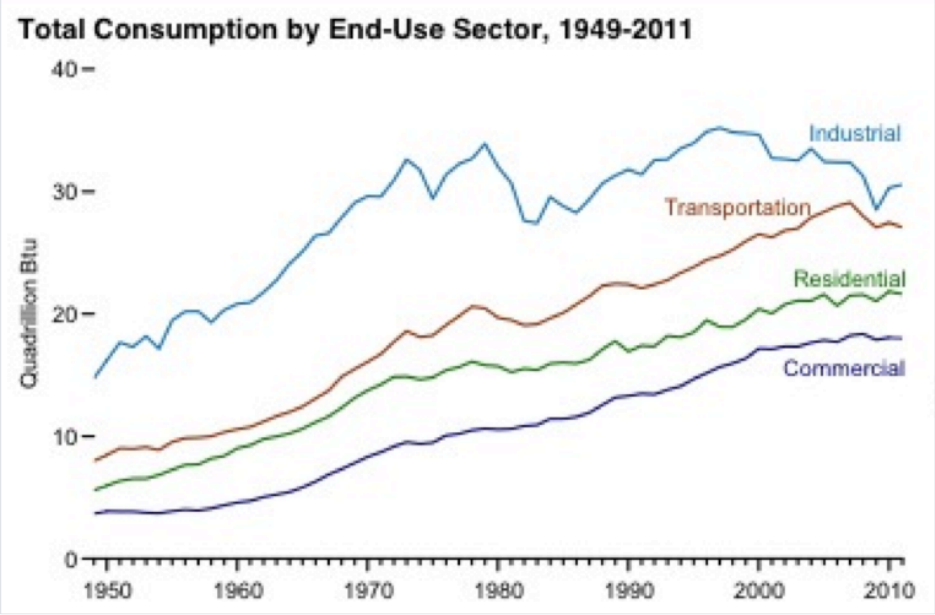

Figure 1.1: Energy Consumption Trends by End-Use Sector

in energy usage alone. Energy consumption in the industrial sector of the United States is projected to grow at an annual rate of 0.8% per year, which is the largest projected increase among any sector within the country. In 2013, the energy consumption within industry was 31.15 quadrillion BTU; by 2020 it is projected to reach 35.76 quadrillion BTU [2, 3]. From

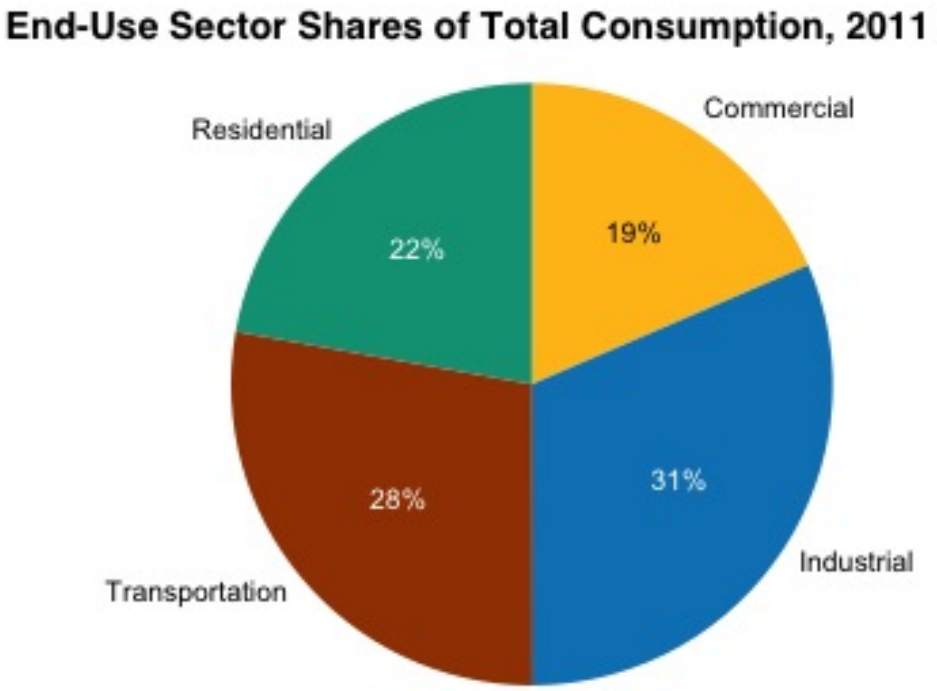

Figure 1.2: Energy Consumption End Use Comparision

2006 - 2010, the average energy price for electricity usage within the manufacturing sector has increased 3% [4]. The largest energy consumer in the manufacturing facility is the production line, which consumes approximately 75% of the energy used by the plant [5]. This is shown in Fig. 1.3.

An effective approach to achieve sustainability in a manufacturing facility is demand

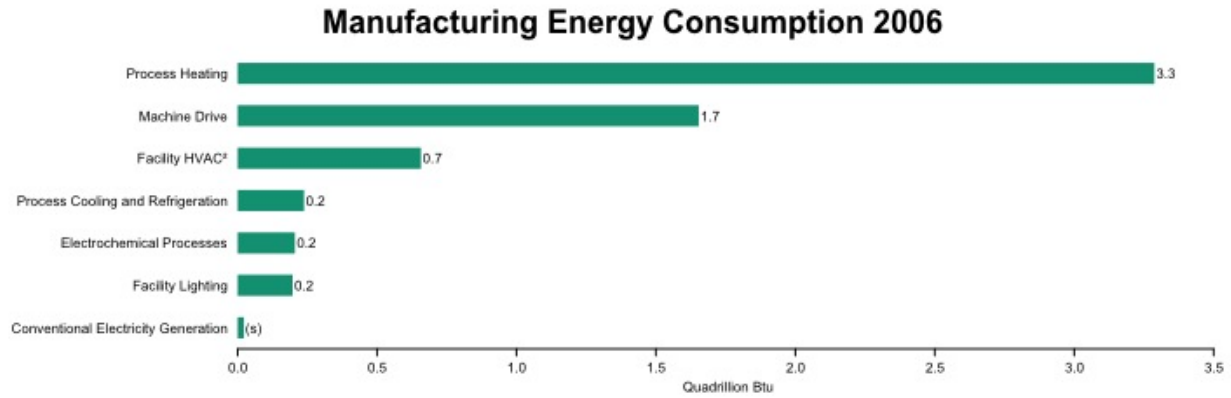

Figure 1.3: Manufacturing Energy Consumption

side management. Demand side management focuses on reducing the electrical demand within the manufacturing environment. There are two approaches to demand side management: electricity demand response and energy efficiency improvement [6]. Energy demand response focuses on shifting patterns of electricity usage due to the variable cost of energy. This dissertation focuses on energy efficiency improvement, where the energy consumption is reduced without sacrificing production system output. This is achieved by exploring the energy dynamics of the production system in relation to output produced.

Manufacturing companies lack the proper performance indicators to illustrate the energy performance of the production line. Most manufacturing facilities track machine performance by monitoring energy consumption per part, which, when utilized alone, does not properly reflect the energy efficiency of that machine [7]. This is due to the nonlinearity of the production system, which makes it difficult to quantify individual downtime incidents on the line. Another problem with this method is that it operates under the assumption that each machine's energy usage is monitored. This is not always the case in the manufacturing industry as it is nearly impossible to monitor individual energy usage within a complex system [8]. This dissertation focuses on exploring the dynamic energy structure to dissect the energy consumption per part to better illustrate energy inefficiencies by creating new sustainable manufacturing performance indicators (SMPI).

Previous research efforts have revealed that 85% of energy in a manufacturing environment is utilized for functions not related to the production of parts [9]. We need to better understand the energy structure in a manufacturing facility: knowing not only how much energy is consumed, but how the energy is consumed. The energy structure can be broken down into two parts: energy used for value adding processes, i.e. when parts are being produced by the production line, and energy waste that is not related to the production of parts. Understanding the energy structure is the first step in locating energy waste in the manufacturing facility.

1.2 Problems Addressed and Solutions

In this work energy analytics are developed for the manufacturing environment using readily available sensor data to reduce energy waste.

The production dynamics are analyzed to categorize disruption events into events that cause permanent production loss (effective downtime events) and events that have no impact on production throughput (non-effective downtime events). An effective downtime event is any disruption event that causes the slowest machine to break down or become blocked or starved, which disrupts the overall production of the line and causes permanent production loss. This directly leads to the concept of the opportunity window, which is the longest amount of time a machine can be down without causing permanent production loss. The opportunity window is shown to be constant for a given line configuration in a deterministic scenario. Furthermore, the recovery time is introduced, which is the amount of time it takes for the buffers to recover back to their original state after a downtime event. The upper bound of recovery time is also shown to be constant for a deterministic scenario with a given line configuration.

The production dynamic analysis is expanded to study the dynamic energy structure of the production line. The dynamic energy structure is broken down into two portions: the static portion (the energy consumed in the production of parts) and the dynamic portion (the energy wasted when the line is not producing parts). The static portion is further analyzed to show the energy waste due to unsynchonizations on the line and to show the minimum energy consumption that is achievable. This is a virtual scenario when each machine is running standalone, meaning there are no interactions from other machines. This analysis directly leads to the creation of the sustainable manufacturing performance indicators, which provide a quantitative self-benchmark for manufacturers to measure system performance. To further diagnose energy inefficiencies on the machine level the downtime energy bottleneck and the rated power bottleneck are created. These bottlenecks provide the plant manager with the tools to identify which machines produce the most energy waste.

An energy economic analysis is introduced that focuses on maximizing profit in the manufacturing environment. The energy profit bottleneck is introduced, which identifies the machine that, when prioritized for reactive maintenance, leads to the largest increase in profits. A return on investment strategy is developed that allows a plant manager to replace a machine or part with a more energy efficient version to achieve the largest return on investment based on energy cost savings. These concepts are used in conjunction with an opportunity window control methodology to maximize profits without sacrificing production throughput.

To further improve energy efficiency and increase overall profit, a new model is introduced that merges the two largest consumers in the manufacturing facility: the production line and the heating, ventilation, and air conditioning system (HVAC). By merging these two systems and using energy opportunity windows, certain machines can be shut down at strategic times to lower overall heat loads. This not only reduces the overall energy consumption by the production line, but also reduces the energy consumption of the HVAC system. The production impact on the HVAC cooling load is analyzed and reduced using an opportunity window control methodology.

In the future, an optimal control strategy will be developed using Markov decision process to minimize energy costs, while increasing overall profits for the manufacturing facility. The topic of data uncertainty will also be addressed through the use of a Kalman Filter.

The rest of this dissertation is structured as follows: a thorough literature review is presented in Chapter 2. Chapter 3 discusses the production dynamics and quantifies the systematic impact of disruption events. The energy dynamic structure is analyzed and the energy analytics are defined in Chapter 4. An energy economic analysis is presented in Chapter 5. Chapter 6 provides a control methodology that merges opportunity window control with bottleneck mitigation to increase overall profit of the line. In Chapter 7, the integrated HVAC and production system is discussed. Lastly, Chapter 8 discusses the conclusions and future work.

1.3 System Description, Notations, and Assumptions

A serial production line consists of a series of machines in sequence with inline buffers. A sequence of operations is performed on unfinished products in a predetermined order. A serial manufacturing system is represented in Fig. 1.4, consisting of M machines (represented by the rectangles) and M-1 buffers (represented by the circles). Continuous flow models are

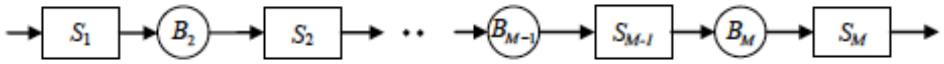

Figure 1.4: A Serial Production Line with M Machines and M-1 Buffers

adopted in this dissertation. The continuous flow model treats the quantity of jobs in the buffer as varying continuously from zero to the capacity of the buffer as opposed to integer steps. This model was adopted for the ease of math expressions and analysis, since the system dynamics can be conveniently expressed as integral or differential equations. The actual system dynamics are not affected by this assumption regardless of whether the system is continuous or discrete [10]-[13]. The following notations are adopted in this dissertation:

- $b_m(t), m = 2,3,...,M,$ denotes the buffer level of buffer B_m at time t.
- $\vec{e}_{j,i} = (j, t_i, d_i)$, $i = 1,2...,\eta_j$, $j = 1,2,...,M$, represents the i^{th} downtime event for machine j, which occurs at time t_i for a duration of d_i time units.
- $\vec{e}_j = \{\vec{e}_{j,1},\vec{e}_{j,2},...,\vec{e}_{j,\eta_j}\}$ $j = 1,2,...,M$, denotes a sequence of downtime events for machine j where η_j is the number of downtime events at machine j.
- $\vec{E} = \{\vec{e}_1,\vec{e}_2,...,\vec{e}_M\}$ denotes a sequence of downtime events for the line.
- $\frac{1}{\tau_j}$, $j = 1, 2, ..., M$ is the rated speed of machine j.
- $s_j(t)$, $j = 1, 2, ..., M$ is the actual processing speed of machine j at time t.

- $\int_0^t s_j(t')dt', j = 1, 2, ...M$ is the production volume of machine j from [0,t) without any downtime events.
- $\int_0^t s_j(t', \vec{E})dt', j = 1, 2, ...M$ is the production volume of machine j from [0,t) subject to a set of downtime events, $\vec{E}$.
- M^* denotes the slowest machine on the line.
- $W_j(t), j$ = 1,2,...,M, represents the opportunity window of machine j at time t.
- d_i^* is the largest possible downtime duration that does not lead to permanent production loss for the i^{th} failure event.
- $\vec{D}^n$ represents a set including η_j^n number of non-effective downtime events.
- $\vec{D}^e$ represents a set including η_j^e number of effective downtime events.
- $T_r(j, \vec{e}_{j,i})$ is the recovery time of machine j after the downtime event $\vec{e}_{j,i}$.
- $T_f(j)$ is the amount of time it takes the system to recover back to the full opportunity window state when the maximum energy savings opportunity is taken at machine j.
- $P_{pp,j}, j$ = 1,2,...,M, denotes the rated power consumption of machine j while the machine produces parts.
- $T_{pp,j}, j$ = 1,2,...,M, represents the time machine j produces parts.
- $P_{id,j}, j$ = 1,2,...,M, denotes the rated power consumption of machine j while the machine is idle due to being blocked/starved.
- α_j, j = 1,2,...,M, is the percentage of power consumed during idling as compared to the power consumption during the production of parts for machine j.
- $T_{id,j}, j$ = 1,2,...,M, represents the time machine j is idle.
- $T_{id,j}^D, j$ = 1,2,...,M, is the time machine j is idle due to downtime.

- $T^{U}_{id,j}, j = 1,2,...,M,$ represents the time machine j is idle due to unsynchronization.
- $P_{w,j}, j = 1,2,...,M,$ denotes the power during warm up for machine j.
- $T_{w,j}, j = 1,2,...,M,$ represents the time machine j is warming up.
- $\beta_j, j = 1,2,...,M,$ is the percentage of power consumed during warm up as compared to the power consumption during the production of parts for machine j.
- $T_{off,j}, j = 1,2,...,M,$ is the time machine j is off.
- $E,$ denotes the energy consumption of the line at time T.
- $EC(t),$ denotes the actual instantaneous energy consumption of the line at time t.
- $EC_j(t), j = 1,2,...,M,$ denotes the actual instantaneous energy consumption of machine j at time t.
- PC denotes the production count of the line at time T.
- $t_{p,j}, j = 1, ..., M,$ is the minimum amount of time machine j would produce the number of parts processed by the slowest machine in [0,T) if machine j was running as a standalone machine.
- EPP is the energy consumption per part of the line in the time period [0,T).
- EPP_h is the energy consumption per part of the line in the time period [0,T) without downtime events.
- $EPP_{h,sa}$ is the energy consumption per part of the line in the time period [0,T) if each machine was standalone.
- $EPP_{h,int}$ is the energy consumption per part of the line in the time period [0,T) due to interactions between machines.

- $EPP_j(t), j$ = 1,2,...,M, is the actual instantaneous energy consumption per part produced at machine j in the time period [0,t).
- $SMPI_{DT}$ is the sustainable manufacturing performance indicator that measures the line's performance with reference to the case with no downtime events.
- $SMPI_{SA}$ is the sustainable manufacturing performance indicator that measures the line's performance with reference to the optimal minimum scenario.
- e_j, j = 1,2,...,M, is the efficiency of machine j.
- CTR_j^k is the cost to replace a part k within machine j. The scenario where the entire machine j is replaced is represented by $k = 0$.
- c_p is the cost per part produced in $\$/part$.
- CE, represents the total cost of energy for the production line.
- c_e^l, l = 1,2,...,c, denotes the cost of energy per kWh for the time period $[t_{l-1}, t_l)$.
- c_d is the demand cost if the production count does not meet demand.
- c_b is the back log cost if the production count is below demand.
- c_i is the inventory cost if the production count is above demand.
- $c_{rep,j}^k$ is cost to replace part k at machine j.
- $N_{m,j}^k$ represents the number of maintenance workers required to replace part k in machine j.
- $t_{R,j}^k$ is the repair time required to replace part k in machine j.
- $c_{Main,j}$ is the cost per hour of a maintenance worker at machine j.
- $C_{Reg,j}$ is the cost per hour of a maintenance worker at machine j if the maintenance is performed during a regular shift.

- $C_{OT,j}$ is the cost per hour of a maintenance worker at machine j if the maintenance is performed during an overtime shift.
- ROI_j^k denotes the expected return on investment for replacing part k within machine j in [0,T).
- BE_j^k represents the expected number of days for an investment to replace part k at machine j to break even.
- $\eta_{OW,j}$ is the number of inserted downtime events at machine j.
- $t_{OW,j}$ is the length of one inserted downtime event at machine j.
- E_{pr} is the energy consumption of the production line.
- $Q(t)$ is the cooling load provided by the heating, ventilation, and air condition system at time t.
- $Q^r(t)$ is the radiative cooling load provided by the heating, ventilation, and air condition system at time t.
- $Q^c(t)$ is the convective cooling load provided by the heating, ventilation, and air condition system at time t.
- $Q_M(t)$ is the cooling load caused by the machines on the production line at time t.
- C_M is the percentage of the machine heat load that is convective.
- R_M is the percentage of the machine heat load that is radiative.
- TC is the thermal comfort of the building occupants. It is based on the Fanger PMV model.

The following assumptions are adopted in this dissertation:

1. Each machine j has a rated speed, $\frac{1}{\tau_j}$, $j = 1, 2, ..., M$, where τ_j is the cycle time of the machine. An operational machine can process jobs at a speed that is no greater than its rated speed. The machine can be viewed as operating at a duty cycle less than one when its speed is constrained by other machines, i.e. a machine is blocked/starved by another machine. We denote $s_j(t), j = 1, 2, .., M$, as the actual processing speed of machine j at time t. The production volume of machine j from [0,t) is represented by $\int_0^t s_j(t', \vec{E})dt', j = 1, 2, ...M$.

2. A machine is starved if it is operational and its upstream buffer is empty.

3. A machine is blocked if it is operational and its downstream buffer is full.

4. A machine cannot breakdown if it is blocked or starved.

5. The first machine, $j = 1$, is never starved and the last machine, $j = M$, is never blocked.

6. Each buffer $B_2, B_3, ..., B_M$ has a finite capacity. $B_2, B_3, ..., B_M$ also denotes the maximum capacity of the buffer.

7. $M^* = argmin_{j=1,...M} \frac{1}{\tau_j}$ represents the slowest machine in the line and it is unique.

8. Each machine will run at its power rating, $P_{pp,j}$, when up and producing parts and will consume no power when turned off.

9. A machine will run at its power rating, $P_{id,j}$, when starved/blocked and not producing parts. $P_{id,j}$ is a percentage (α_j) of $P_{pp,j}$, where $P_{id,j} = \alpha_j P_{pp,j}$, $0 \leq \alpha_j \leq 1$.

10. Machine j has a warmup time of $t^i_{w,j}$ for the i^{th} downtime event, where $t^i_{w,j} \sim exp(\omega_j)$ and ω_j is the mean time machine j warms up. During the warm up period, machine j consumes energy at a rate of $P_{w,j}$. $P_{w,j}$ is a percentage (β_j) of $P_{pp,j}$, where $P_{w,j} = \beta_j P_{pp,j}$, $\beta_j \geq 0$.

Chapter 2

Literature Review

In this chapter a thorough literature review is provided for the dissertation. Section 2.1 provides literature review on the dynamics of the production system and Section 2.2 discusses literature related to energy and economic indicators in the manufacturing industry. In Section 2.3 various control methodologies for the production line are discussed. Section 2.4 provides works that are related to HVAC control, which will be addressed in Chapter 7. In Section 2.5 we summarize the conclusions from the literature review.

2.1 Production Dynamics

Previous research dealing with the impact of disruption events is severely limited. Many of the existing literatures focus on utilizing stochastic modeling or simulation methods [14]-[17]. Recently, there have been data driven methods to quantify the effect of disruption events on overall production throughput for serial production lines [14, 18, 19]. A network based modeling methodology is created in [17] to investigate the impact of disruption events on the operation of a supply chain. The authors create a disruption analysis network, which models how disruptions or changes dissipate throughout the system and they quantify the impact of these events.

Langer et al. discuss disruption management within the manufacturing industry [20]. They propose a methodology to reduce disruption events on a system level. This method uses a cooperative distributed problem solving approach that is supported by a multi-agent system framework. In [15], the authors consider the propagation of disruption events and the capability of the system to recover from these events. The throughput settling time and

the overtime to recover are defined, which are two measures of resilience for the production system. The authors use an approximation method with system decomposition to expand these measures to general multi-stage systems.

This dissertation uses event based analysis to quantify the impacts of downtime events using online measured data, such as machine downtime, buffer levels, etc. Chang et al. discuss the effect of a single isolated downtime event on system throughput [14]. It has been proven that the downtime event will only affect system productivity if the event causes the slowest machine to break down or become blocked or starved. This is expanded in [19] to a general scenario where multiple disruption events can occur throughout the production line. It indicates that there is permanent production loss if the disruption event duration is larger than a certain threshold. This causes the system to lose production throughput can never be recovered. The analysis in this dissertation expands upon this research to include each machine's warm up period after a machine breakdown.

2.2 Energy & Economic Indicators

Researchers have only recently started to focus on energy management in the manufacturing environment. Most previous research efforts have studied quality control and maintaining throughput without explicitly considering energy consumption of the production line [21, 22]. These studies treat energy consumption as a byproduct of production instead of using it as the main driver in the decision process. They only treat energy consumption as another cost term in an optimization problem instead of assessing what is usable energy and what is energy waste. However, in [23] it is discovered that there is a positive effect of environmental and energy improvement investment on production growth. To achieve sustainability within the manufacturing sector, it is necessary not only to focus on throughput targets, but also to focus on reducing the overall energy demand of the facility.

There have been recent studies on the creation of sustainable indicators for the manufacturing facility, but these vary greatly from industry to industry. Haapala et al. review various sustainability indicators and manufacturing processes, but provide no methodology on how to reduce energy consumption within the facility [24]. A fuzzy-based sustainable manufacturing assessment model is developed for sustainability of small and medium enterprises in [25], however this only applies to a select number of sustainability indicators and cannot be expanded to more generalized systems. Despeisse et al. investigate the strategic direction and practices of manufacturing facilities to extract the mechanisms behind these practices to formulate sustainable manufacturing tactics [26]. This method relies on simulation modeling to guide the plant manager in decision making, but it does not explicitly consider economic impacts.

General Electric developed an energy treasure hunt method to find "non-operation waste" in their factory by scheduling weekend and daily shutdown plans [27]. The problem with this method is that it was based on a "trial and error" manual procedure that required the expert knowledge of the inspector to find ways to cut down on energy waste in the plant. Many companies within the manufacturing industry have focused on creating a unified energy dashboard to illustrate energy usage in a manufacturing plant. Companies like Siemens and Rockwell have created energy dashboards that provide information to plant managers using their own key performance indicators (KPI), which do not properly address problem areas on the floor [28, 29]. They utilize final production count and total energy consumption, but do not take into account any random downtime events that affect production processes. This makes it impossible to determine the root cause of energy inefficiency in the system.

While these KPIs do not properly assess energy inefficiencies, there have been many studies considering the evaluation of energy consumption and energy saving opportunities over the last decade [30]. In [31], Joung et al. categorize various sustainability indicators

within the manufacturing industry. They categorize indicators by the following criteria: measurable, relevant, understandable, reliable/usable, and data accessible. The indicators provided in this work fit all of the given criteria.

The overall efficiency has been defined in [32] as the benefit over the total effort. This has been further expanded for specific industries, such as the method presented by Dietmair and Veri [33]. They have created an index that is capable of calculating efficiency for a cutting operation by analyzing the energy needed versus the actual energy of the machine. However, this idea is limited and cannot be applied to processes that cannot be accurately modeled.

The overall equipment efficiency indicator was created using techniques from lean manufacturing. However, this is a heuristic measure and it is unable to capture the variability in the system [34]. This was expanded to find the energy efficiency of a casting production system, but it is difficult to model for other processes within manufacturing [35]. A decomposition method was proposed in [36] for a continuous flow model described by general Markovian fluid models. This method studies the effect of partial and complete blocking and starvation phenomena throughout the system. The challenge with this strategy is the decomposition method is time consuming as well as computationally intense, preventing it from being implemented in real time.

A different method for analyzing energy usage is trend decomposition [37]. Trend decomposition is a very practical method for determining decreases in energy efficiency, but there is no standard generally agreed upon for which method is the best. There are four different methods that are generally used depending on different conditions [38]. It is necessary to know which constraints to employ for the analysis, otherwise the method will not be accurate. Hammond and Norman attempt to reduce carbon emissions in the United Kingdom by using decomposition analysis [39]. However, this method cannot be used in real time to

diagnose problems.

Another research area uses engineering models to analyze energy usage in a manufacturing facility. A "bottom-up" method is utilized to determine if emerging technologies will reduce the energy consumption in the facility [40]. This method can react to changes in demand and fuel prices. However, it is difficult to apply in many manufacturing facilities since creating an accurate model is difficult and time consuming. The gap between energy efficiency performance measurement in scientific literature and industry is investigated in [41]. Bunse et al. interviewed over 100 industry experts who stated that the measurement of energy efficiency needed to be converted to monetary values to communicate directly where money could be saved. Another hurdle for implementing energy efficiency improvement is the difficulty of measuring energy indicators [42]. The method developed in this dissertation provides the plant manager with the quantitative tools that utilize readily available sensor data to directly provide energy and economic indicators. A control methodology that uses real sensor data is also introduced to reduce the overall energy cost with minimal impact to production.

2.3 Production Control Methodologies

The control and improvement of production systems is important in the analysis of the energy dynamics of the production system. In the last few decades there have been multiple literatures devoted to this topic. Caifen and Shao-kun present an optimization algorithm to maximize machine utilization and reduce work in progress [43]. However, this method is for planning purposes and cannot be utilized in real-time control. In [44], a real-time production planning and control algorithm is introduced for job shop systems, but this work does not incorporate energy consumption into their model. Chen et al. create an energy efficient, greedy-algorithm scheduling procedure that optimizes start up and shut down times of machines for a paint shop [45]. However, the control capability and benefit is very limited by

only controlling the shut down sequence of machines. In practice, real-time feedback control based scheduling is more desirable than offline optimization because the optimized solutions are normally sensitive to system parameters, which often leads to errors.

Production scheduling and control research has become more prevalent in the last decade [46]-[50]. In [51], an optimal policy is found by making decisions on pricing, the level of modularity, and customer returns under a mean-variance formulation for a mass customization system. Hu et al. discuss the real-time optimal control of a serial production line, however the disruption events must be known in advance [52]. Game-theoretic models are developed to determine the optimal price decisions and competitive capacity for build-to-order manufacturers that are facing time-dependent demands in [53]. Shen et al. reviewed literature on manufacturing scheduling and process planning and concluded that agent-based approaches have advantages such as scalability, robustness, and modularity [54]. However, these methods are usually developed for simple systems. Optimal scheduling and control cannot be solved analytically for complex production systems, since neither computational nor analytical solutions are achievable [55].

The work presented in this manuscript introduces a method that can be used for any serial production line, regardless of the production process. This method uses readily available sensor data in the analysis of the energy dynamics of a line to identify and mitigate the energy waste in the facility. A control algorithm is created to reduce this energy waste, while minimizing throughput impact to the production line. Together with bottleneck mitigation, the control methodology can be used to maximize profit for the manufacturing facility.

2.4 HVAC Control

The operation and control of HVAC systems has significant impacts on the energy and cost efficiency of buildings. In [56], a cost effective strategy is introduced to improve energy

consumption by determining set points of local loop controllers used in a multi-zone HVAC system. An optimization process is used in [57] to automatically change the settings of the HVAC system in accordance with changes in outside temperature and building operation. A robust model predictive control scheme is developed in [58] to deal with various constraints on the HVAC system, such as the rate limit of actuators. In [59], facility improvement and life cycle costs related to the HVAC system alone in automotive manufacturing are studied. At the system level, comprehensive building automation systems and building energy management control systems (EMCS) are utilized to allow the possibility of enhancing and optimizing the operation and control of HVAC systems [60]. In a manufacturing facility, the EMCS usually does not communicate with the production system. One method of satisfying the energy reduction goal in a manufacturing environment had production work groups develop specific actions in their area, such as tracking and shutting off unused lights, fans and other equipment when production turns off, and develop weekend and daily shutdown plans and manage the leak tag program [61]. However, this method is a heuristic based process and cannot be used for continuous improvement.

Previous methods that coordinate the production line with the HVAC system focus on modeling and designing the HVAC around the production system [62, 63]. To the best of our knowledge, there are very few studies that have addressed the integrated modeling and control of the production operations in coordination with the HVAC system to improve overall manufacturing system energy efficiency. This dissertation presents a method for controlling the HVAC set points in combination with the energy savings opportunities (ESO) for the production line.

2.5 Conclusion

Despite these efforts, the study of the dynamic energy structure of the production line is severely limited. Most researchers analyze energy or production separately, however, the

uncertainties on the production line impact energy consumption as well as throughput. Thus, total energy consumption is only a measure of total energy, which does not carry any explicit information about throughput. In this paper, we link the throughput dynamic and energy dynamic. We treat energy consumption per part as a dynamic system, which is a complex function of each machine's up time, down time, buffer levels, machine rated power, machine idle time power consumption, etc. Then for a realized production trajectory, we analyze the physical meaning of its homogeneous solution. From this, we develop the sustainable manufacturing performance indicators, which is the energy efficiency index. This index describes the energy structure, i.e., how much energy is wasted without producing parts. Building on this analysis, we present an energy economic analysis to provide analytical tools for the plant manager to make decisions on overall profit of the facility. This differs from previous research because the methods presented in this manuscript use readily available, online sensor data to provide a quantitative self-benchmark to monitor system performance. By using this methodology, a control algorithm is created that will maximize overall profit, while minimizing throughput impact. The production system is then coupled with the HVAC system to create a control methodology to reduce overall energy costs by merging the two dynamic systems.

Chapter 3

Analysis of Production Dynamics

3.1 Introduction

To analyze the energy dynamics of a production line, it is necessary to understand the effect of random downtime events on the system. In this section, we focus on the impact of disruption events on a serial production line. We begin by analyzing and categorizing which downtime events cause disruptions to overall production, thus resulting in permanent production loss (PPL). We then extend our analysis to analytically prove the expected opportunity window (OW) and recovery time in a deterministic system.

3.2 Impact of Downtime Events on Overall System Throughput

In this section, we analyze the impacts of disruption events on the production line. When there are random downtime events in the system, not every one of them will contribute to permanent production loss. This leads to the concept of the opportunity window, $W_j(T_d)$, which is defined as the longest amount of time machine j can be down at time T_d without resulting in PPL [14, 19, 64]. This is seen below in (3.1):

$$W_j(T_d) = sup\{d \geq 0 : s.t. \exists T^*(d), \int_0^T s_M(t')\,\mathrm{d}t' = \int_0^T s_M(t', \vec{e}_{j,i})\,\mathrm{d}t', \forall T \geq T^*(d)\}, \quad (3.1)$$

where $\int_0^T s_M(t')\,\mathrm{d}t'$ and $\int_0^T s_M(t', \vec{e})\,\mathrm{d}t'$ are the production counts of the end of line machine, M, at time T with and without the inserted downtime event, $\vec{e}_{j,i} = (j, t_i, d_i)$, respectively. $T^*(d)$ signifies the potential dependency of T^* on d. Thus, the largest possible downtime duration that does not lead to permanent production loss, d_i^*, for the i^{th} failure event, $\vec{e}_{j,i}$,

can be found in (3.2) [64]:

$$d_i^* = inf\{d \geq 0 : s.t.\tau_{M^*} \int_{t_i}^{t_i+d} s_{M^*}(t'; \vec{E})\mathrm{d}t' = W_j(t_i)\}, \tag{3.2}$$

where $W_j(t_i)$ is the opportunity window of machine j as defined in (3.1), M^* is the slowest machine on the line, and d_i^* is the time it takes the buffers between machine j and M^* to become full if $j > M^*$ or empty if $j < M^*$. The production volume of the slowest machine between t_i and $t_i + d$ is $\int_{t_i}^{t_i+d} s_{M^*}(t'; \vec{E})\mathrm{d}t'$ and $\vec{E} = \{\vec{e}_1,\vec{e}_2,...,\vec{e}_M\}$ is a sequence of downtime events for the line.

In [64] it was shown that if the downtime event is greater than the value in (3.2), then it is an effective downtime event contributing to a permanent production time loss of $d_i - d_i^*$. If the downtime duration is less than the above value ($d_i \leq d_i^*$), it is referred to as a non-effective downtime event since there is no PPL. However, this is under the assumption that the warm up time ($t_{w,j}^i$) of machine j is equal to zero for the i^{th} downtime event. Since a machine is consuming energy without producing parts during this warm up time period, it must be taken into account when analyzing the production system energy consumption. The period that machine j does not produce parts is $d_i + t_{w,j}^i$. Let $\vec{D}^e$ represent a set of η_j^e number of effective downtime events and $\vec{D}^n$ represent a set of η_j^n number of non-effective downtime events, then $\forall d_i$:

$$d_i \in \begin{cases} \vec{D}^n, & d_i \leq (d_i^* - t_{w,j}^i), \quad i = 1...\eta_j \\ \vec{D}^e, & d_i > (d_i^* - t_{w,j}^i), \quad i = 1...\eta_j, \end{cases}$$

where:

$$\eta_j = \eta_j^e + \eta_j^n.$$

Thus, an effective downtime event leads to permanent production time loss of $d_i - d_i^* + t_{w,j}^i$.

3.3 Expected Energy Opportunity Window

From the analysis of the opportunity window, it is noticed that the maximum opportunity window for any machine is closely related to the location of the machine. Since inserted opportunity windows have no permanent production impact to the system, the system with inserted opportunity windows should recover to its original state after a certain period of time. We will show that the expected opportunity window and recovery time for an arbitrary machine are constant for a given line configuration when there are no random downtime events.

Proposition 1: *If all machines operate without any random downtime, the energy opportunity window can be described as the following:*

$$d_i^*(t) = \begin{cases} \tau_{M^*} \sum_{k=j+1}^{M^*} b_k(t), & j < M^* \\ 0, & j = M^* \\ \tau_{M^*} \sum_{k=M^*+1}^{j} (B_k - b_k(t)), & j > M^* \end{cases}$$

Proof:

For a serial production line with all machines working without random downtime events, the end-of-line production volume is equal to the production volume of the slowest machine. The case for when $j = M^*$ is proved by contradiction. Suppose the opportunity window of the slowest machine M^* at time T_d is not zero, i.e., $W_{M^*}(T_d) > 0$. Then for any downtime event (M^*, T_d, d_i) with $0 < d_i \leq W_{M^*}(T_d)$, the difference between the undisturbed and disturbed production volume of the end-of-line machine M is nonzero, which contradicts the definition of the opportunity window. Actually, it is obvious that for a serial production line with all machines operating without downtime, any inserted downtime event at the slowest machine will cause a production loss at the end-of-line machine M.

For the case when $j < M^*$, an equivalent condition requires that the duration of the stoppage event at the slowest machine M^* be equal to zero to allow for no production loss at

machine M. Considering the line segment between machine m and machine M^*, as shown in Fig. 1.4, we insert a downtime event, $\vec{e}_{j,i} = (j, T_d, d_i)$ at machine j with duration d_i at time T_d. Immediately after machine j is down, there is no flow into this line segment until time $T_d + d_i$. Applying the principle of conservation of flow during time interval $(T_d, T_d + d_i]$ yields:

$$\int_{T_d}^{T_d+d_i} s_j(t, \vec{e}_{j,i})\mathrm{dt} - \int_{T_d}^{T_d+d_i} s_{M^*}(t, \vec{e}_{j,i})\mathrm{dt} = \sum_{k=j+1}^{M^*} b_k(T_d + d_i; \vec{e}_{j,i}) - \sum_{k=j+1}^{M^*} b_k(T_d; \vec{e}_{j,i}),$$

where $s_j(t, \vec{e}_{j,i}) = 0, t \in (T_d, T_d + d_i]$. In the case when $j < M^*$, the slowest machine will operate at a constant rate $s_{M^*} = 1/\tau_M^*$ until $\sum_{k=j+1}^{M^*} b_k(T_d; \vec{e}_{j,i})$ becomes zero. Note that the slowest machine M^* will never be blocked because all of the machines downstream have higher processing rates and there is no other downtime events except $\vec{e}_{j,i} = (j, T_d, d_i)$ as we have assumed. The buffer content between machine j and M^* will gradually drain at a constant rate of $1/\tau_{M^*}$. Therefore, the time it takes for all the buffers between machine j and the slowest machine M^* to become empty is:

$$d_i^* = \tau_{M^*} \sum_{k=j+1}^{M^*} b_k(T_d),$$

since $b_k(T_d) = b_k(T_d; \vec{e}_{j,i}), \forall k = 2, ..., M^*$. If the downtime duration d_i is greater than $d_i^* - t_{w,j}^i$ then the slowest machine will be starved. This will eventually lead to a production loss equal to $(d_i - d_i^* + t_{w,j}^i)/\tau_M^*$. Therefore, in the case when $j < M^*$, the opportunity window of machine j is $W_j(T_d) = d_i^*$. Analogously, one can also prove the case when $j > M^*$. □

This indicates when all machines are running without random downtime the energy savings opportunity window will be constant if always taken at the same buffer content level (b_k). The maximum energy savings opportunity is realized when the buffers upstream of the slowest machine go from full to empty and the downstream buffers go from empty to full. The next section will introduce the concept of recovery time, which is the amount of time it

takes the buffers to recover back to their original state after a downtime event.

3.4 Maximum Upper Bound of Recovery Time

In this section, we prove the maximum upper bound of recovery time in a system with deterministic downtime. This is the scenario when the buffers upstream of the slowest machine go from empty to full and the downstream buffers go from full back to empty. The recovery time after a downtime event is introduced:

$$T_r(j, \vec{e}_{j,i}) = inf\{\Delta T \geq 0 \; s.t. \int_0^T s_j(t)\mathrm{dt} = \int_0^T s_j(t, \vec{e_{j,i}})\mathrm{dt}, \forall T \geq \Delta T + T_d + d_i\},$$

where $\int_0^T s_j(t)\mathrm{dt}$ and $\int_0^T s_j(t, \vec{e}_{j,i})\mathrm{dt}$ are the production count of machine j at time T, with and without downtime event $\vec{e}_{j,i} = (j, T_d, d_i)$. All downtime will be realized in the form of taking the maximum opportunity window at machine j.

Proposition 2 *If all machines operate without any random downtime, the upper bound of recovery time is a fixed length for machine j, depending on its location and buffer capacities. After machine j takes its maximum d_i^*, the upper bound of recovery time can be described as follows:*

$$T_r(j, d_i^*) = \begin{cases} \frac{\sum_{k=j+1}^{M^*}(B_k)}{min\{\frac{1}{\tau_1}, \ldots, \frac{1}{\tau_{M^*-1}}\} - \frac{1}{\tau_{M^*}}}, & j < M^* \\ \infty, & j = M^* \\ \frac{\sum_{k=M^*+1}^{j}(B_k)}{min\{\frac{1}{\tau_{M^*+1}}, \ldots, \frac{1}{\tau_M}\} - \frac{1}{\tau_{M^*}}}, & j > M^* \end{cases}$$

Proof:

As discussed previously, if the downtime event is an effective downtime event then the recovery time is infinite. Similar to the energy opportunity window, the recovery time of each machine depends on the location of said machine in relation to the slowest machine in the

line. If we start with the downstream machines, $j > M^*$, by conservation of flow we have:

$$\int_0^T s_j(t)\mathrm{dt} = \int_0^T s_{M^*}(t)\mathrm{dt} - \sum_{k=M^*+1}^{j} (b_k(T) - b_k(0))$$
$$\int_0^T s_j(t;\vec{e}_{j,i})\mathrm{dt} = \int_0^T s_{M^*}(t;\vec{e}_{j,i})\mathrm{dt} - \sum_{k=M^*+1}^{j} (b_k(T;\vec{e}_{j,i}) - b_k(0;\vec{e}_{j,i})).$$

Because the slowest machine is unique per our assumption, we know that:

$$\frac{1}{\tau_{M^*}} < min\{\frac{1}{\tau_{M^*+1}}, ...\frac{1}{\tau_M}\}.$$

When there are no inserted downtime events, the total buffer level between the slowest machine M^* and the machine j decreases at a rate at least as fast as $min\{\frac{1}{\tau_{M^*+1}}, ..., \frac{1}{\tau_M}\} - \frac{1}{\tau_{M^*}}$ and if we choose $T_1^* = \frac{\sum_{k=M^*+1}^{j}(b_k(0))}{min\{\frac{1}{\tau_{M^*+1}},...,\frac{1}{\tau_M}\}-\frac{1}{\tau_{M^*}}}$, then we have:

$$\int_0^T s_j(t)\mathrm{dt} = \int_0^T s_{M^*}(t)\mathrm{dt} + \sum_{k=M^*+1}^{j} (b_k(0)), \forall T > T_1^*.$$

When there is an inserted downtime event $\vec{e}_{j,i}$, if we choose $T_2^* = T_d + d_i + \frac{\sum_{k=M^*+1}^{j}(b_k(T_d+d_i;\vec{e}_{j,i}))}{min\{\frac{1}{\tau_{M^*+1}},...,\frac{1}{\tau_M}\}-\frac{1}{\tau_{M^*}}}$, we obtain:

$$\int_0^T s_j(t;\vec{e}_{j,i})\mathrm{dt} = \int_0^T s_{M^*}(t;\vec{e}_{j,i})\mathrm{dt} - \sum_{k=M^*+1}^{j} (b_k(0;\vec{e}_{j,i})), \forall T > T_2^*.$$

As long as the system starts with the same exact initial conditions, i.e., $b_k(0) = b_k(0;\vec{e}_{j,i}), \forall k = M^*+1, ..., M$, we have $\forall T > T^* = max\{T_1^*, T_2^*\}$. Thus:

$$\int_0^T s_j(t)\mathrm{dt} - \int_0^T s_j(t;\vec{e}_{j,i})\mathrm{dt} = \int_0^{T_d+d_i} (s_{M^*}(t) - s_{M^*}(t;\vec{e}_{j,i}))\mathrm{dt} + \int_{T_d+d_i}^{T} (s_{M^*}(t) - s_{M^*}(t;\vec{e}_{j,i}))\mathrm{dt} = \frac{d_i}{\tau_{M^*}},$$

since $s_{M^*}(t;\vec{e}_{j,i}) = 1/\tau_{M^*}, t \notin (T_d, T_d+d_i]$ and $s_{M^*}(t;\vec{e}_{j,i}) = 0, t \in (T_d, T_d+d_i]$. Because we are looking for the upper bound of recovery time immediately after the maximum opportunity window is taken, we know the buffer contents will be full downstream of the slowest machine.

This leads to the upper bound of recovery time of machine j after machine j is down for the maximum length of the opportunity window, d_i^*:

$$T_r(j, d_i^*) = \frac{\sum_{k=M^*+1}^{j}(B_k)}{min\{\frac{1}{\tau_{M^*+1}}, ..., \frac{1}{\tau_M}\} - \frac{1}{\tau_{M^*}}}. \tag{3.3}$$

Similarly, if we take the line segment when $j < M^*$, if we choose $T^* = max\{T_1^*, T_2^*\}$, with $T_1^* = \frac{\sum_{k=j+1}^{M^*}(B_k - b_k(0))}{min\{\frac{1}{\tau_1}, ..., \frac{1}{\tau_{M^*-1}}\} - \frac{1}{\tau_{M^*}}}$ and $T_2^* = \frac{\sum_{k=j+1}^{M^*}(B_k - b_k(T_d + d; \vec{e}_{j,i}))}{min\{\frac{1}{\tau_1}, ..., \frac{1}{\tau_{M^*-1}}\} - \frac{1}{\tau_{M^*}}}$, we obtain:

$$\int_0^T s_j(t)\mathrm{dt} = \int_0^T s_{M^*}(t)\mathrm{dt} + \sum_{k=j+1}^{M^*}(B_k - b_k(0))$$
$$\int_0^T s_j(t; \vec{e}_{j,i})\mathrm{dt} = \int_0^T s_{M^*}(t; \vec{e}_{j,i})\mathrm{dt} + \sum_{k=j+1}^{M^*}(B_k - b_k(0; \vec{e}_{j,i})).$$

Taking the difference of the two above equations yields:

$$\int_0^T s_j(t)\mathrm{dt} - \int_0^T s_j(t; \vec{e}_{j,i})\mathrm{dt} = \frac{d_i}{\tau_{M^*}}.$$

Since we are looking to find the upper bound of recovery time after the maximum opportunity is taken, we know that the buffer contents will be empty at said time. This leads to the recovery time for $j < M^*$ in (3.4):

$$T_r(j, d_i^*) = \frac{\sum_{k=j+1}^{M^*}(B_k)}{min\{\frac{1}{\tau_1}, ..., \frac{1}{\tau_{M^*-1}}\} - \frac{1}{\tau_{M^*}}}. \tag{3.4}$$

This ends the proof of the maximum upper bound of recovery time. □

This proves to be an important result because it is leads to the calculation of the minimum amount of time to allow between subsequent energy opportunity windows:

$$T_f(j) = d_i^* + T_r(j, d_i^*), \tag{3.5}$$

where T_f is the amount of time it takes the system to recover back to the next full opportunity window state when taking the maximum energy opportunity window.

3.5 Conclusions

In this chapter, we analyzed the production dynamics of the manufacturing system. The expected opportunity window and the maximum upper bound of recovery time are both proven analytically. The random disruption events on the production system are categorized into events that cause permanent production loss (effective downtime events), and events that do not cause PPL (non-effective downtime events). This will be studied further in the next chapter when we analyze the energy analytics of the manufacturing line.

Chapter 4

Energy Analytics of the Manufacturing Line

4.1 Introduction

After analyzing the effect of disruption events on the system, it is important to understand how downtime impacts energy consumption and the energy structure of the production line. Studying the energy structure determines the portion of energy consumed while producing parts and the portion of energy wasted due to random downtime events that cause permanent production loss. The energy structure is analyzed using measurable and readily available information from the production line such as buffer contents, production count, power, etc. This information is utilized in the development of the Sustainable Manufacturing Performance Indicators (SMPI). These indicators provide a quantitative self-benchmark method to correctly monitor the performance of the production line. To identify energy inefficiencies on the machine level, two bottlenecks are introduced: the Downtime Energy Bottleneck (DE-BN) and the Rated Power Bottleneck (RP-BN).

4.2 Dynamic Energy Structure of the Production Line

In analyzing the energy structure, it is necessary to address how each machine operates in a time period [0,T):

$$T = T_{pp,j} + T_{id,j} + T_{off,j} + T_{w,j}, \tag{4.1}$$

where $T_{pp,j}$ is the amount of time machine j is on and producing parts and $T_{id,j}$ is the time that machine j is on, but is idle due to being blocked/starved. $T_{off,j}$ is the time that machine j is not operational, and $T_{w,j}$ is the time the machine is warming up. While the machine is on and producing parts, machine j consumes power at a rate of $P_{pp,j}$. During its warm up

time it consumes $P_{w,j}$ and it consumes zero power during the period of time the machine is off. We can assume that the power consumed during idling is a percentage of the power consumed during the production of parts:

$$P_{id,j} = \alpha_j P_{pp,j}, \qquad 0 \leq \alpha_j \leq 1.$$

The same assumption can be made for the power consumed during warm up, however the warm up power is not always less than the power consumed during the production of parts:

$$P_{w,j} = \beta_j P_{w,j}, \qquad \beta_j \geq 0.$$

The idling time of machine j is broken into two parts:

$$T_{id,j} = T_{id,j}^{D} + T_{id,j}^{U},$$

where $T_{id,j}^{D}$ is the idling time only due to downtime events and $T_{id,j}^{U}$ is the amount of time machine j idles due only to machine rated speed unsynchronizations.

The total energy consumption and the production throughput need to be linked to analyze the energy efficiency. Therefore energy consumption per part (EPP) is used. EPP for a production line is a complicated function of production line parameters such as each machine's speed, rated power, buffer capacity, downtime distribution, etc. Therefore, EPP is treated as a dynamic system. In analyzing the energy structure, the interactions among the different production processes are treated as "internal forces," while the random disruption events are considered "external forces." The state space equation for this system is represented by (4.2):

$$\frac{d\,[EPP]}{dt} = f(t, EPP(t), U(t)), \tag{4.2}$$

where $U(t) = \vec{E} = [\vec{e_1}, ..., \vec{e_M}]$ denotes a sequence of random disruption events during period [0,T). To solve the state space equation (4.2), we consider the following homogeneous and non-homogeneous functions:

$$\frac{d\,[EPP]}{dt} = f(t, EPP(t)) \tag{4.3}$$

$$\frac{d\,[EPP]}{dt} = f(t, EPP(t), U(t)), \tag{4.4}$$

Equation (4.3) describes a virtual scenario when there are no random downtime events in the system. When there are no disruption events each machine will be on for the entirety of the time period. We can assume that the analysis begins when all of the machines are turned on. The production count of the line is constrained by the base cycle time of the slowest machine [65], therefore, the homogeneous solution for the time period [0,T) is denoted in (4.5):

$$EPP_h = \frac{\sum_{j=1}^{M} P_{pp,j}\Big[T - (1-\alpha_j)T_{id,j}^U\Big]}{\frac{1}{\tau_{M^*}}T} \tag{4.5}$$

The idle time due only to rated speed unsynchronizations cannot be calculated explicitly. An iterative procedure is used to calculate $T_{id,j}^U$. Analyzing the virtual scenario when there are no downtime events, the slowest machine, M^*, never idles due to machine unsynchronizations, therefore $T_{id,M^*}^U = 0$. To solve for $T_{id,j}^U$ for all other machines, we begin by studying the machines upstream of the slowest machine ($j < M^*$):

1. Set initial values: $k = 1$, $t_{id}^u(1) = 0$, $PP_j^u(1) = 1$, $ID_j^u(1) = 0$, $s_j = \frac{1}{\tau_j}$, $t_0 = 0$.

2. Start with machine j and calculate when it is blocked from machines downstream ($j < i$):

$$\int_{t_0}^{t_0+t_{i,j}} s_j(t)dt - \int_{t_0}^{t_0+t_{i,j}} s_i(t)dt = \sum_{z=j+1}^{i} B_z - b_z(t_0)$$

Next, check when machine j becomes starved from machines upstream ($j > i$):

$$\int_{t_0}^{t_0+t_{i,j}} s_i(t)dt - \int_{t_0}^{t_0+t_{i,j}} s_j(t)dt = \sum_{z=i+1}^{j} b_z(t_0)$$

Solve for $t_{i,j}$, which is the time machine j becomes blocked or starved by machine i:

$$t_{i,j} = \begin{cases} \dfrac{\sum_{z=j+1}^{i} B_z - b_z(t_0)}{s_j - s_i}, & C1 \\ \infty, & C2 \\ \dfrac{\sum_{z=i+1}^{j} b_z(t_0)}{s_i - s_j}, & C3, \end{cases}$$

where $C1 = (j < i \;\&\; s_i < s_j)$, $C2 = (i = j) \mid (i < j \;\&\; s_j \geq s_i) \mid (i > j \;\&\; s_i \geq s_j)$, and $C3 = (j > i \;\&\; s_j < s_i)$.

3. Find the smallest $t_{i,j}$, by calculating the minimum of the set, $T^u = \{t_{i,j}\}_{i,j=1}^{M^*-1}$

$$t^u_{i^m,j^m} = min(T^u),$$

Thus, machine(s) j^m becomes blocked or starved by machine(s) i^m at $t^u_{i^m,j^m}$. It is possible that multiple machines become blocked/starved at the same time.

4. Set the next element in the vector, $\vec{t^u_{id}}$:

$$t^u_{id}(k+1) = t^u_{i^m,j^m} + t^u_{id}(k).$$

5. Calculate the buffer level of B_m, $m = 2, ..., M^*$ at time $t^u_{id}(k+1)$:

$$b_m(t^u_{id}(k+1)) = (s_{m-1} - s_m)t^u_{i^m,j^m} + b_m(t^u_{id}(k)).$$

6. Reset actual processing speed of idle machines:

$$s_j = \begin{cases} s_{i^m}, & j = j^m, \quad j = 1...M^* - 1 \\ s_j, & j \neq j^m, \quad j = 1...M^* - 1, \end{cases}$$

   and calculate the percentage of time machine j is producing parts or is idle:

$$PP^u_j(k+1) = \frac{s_j}{\frac{1}{\tau_j}},$$
$$ID^u_j(k+1) = \frac{\frac{1}{\tau_j} - s_j}{\frac{1}{\tau_j}}.$$

7. Calculate the time machine j is idle from rated speed unsynchonizations:

$$T^U_{id,j} = (ID^u_j)T, \quad j = 1...M^* - 1.$$

8. Set $t_0 = t^u_{id}(k+1)$, $\forall\ i = 1, ..., M^* - 1$, $j = 1, ..., M^* - 1$

9. If $s_j \neq rs_{M^*}$, $\forall\ j = 1, ..., M^* - 1$ then $k = k + 1$ and return to step 2.
   If $s_j = rs_{M^*}$, $\forall\ j = 1, ..., M^* - 1$ then end algorithm.

Similarly, one can solve for the unsynchronized idle time of machines downstream of the slowest machine using a similar procedure. To solve for (4.4), the scenario when there is a sequence of random downtime events ($\vec{E}$) on the production line, it is necessary to find the

overall energy consumption:

$$E = \sum_{j=1}^{M} (P_{pp,j} T_{pp,j} + P_{id,j} T_{id,j} + P_{w,j} T_{w,j}), \tag{4.6}$$

where $T_{pp,j}$ is the time that machine j produces parts:

$$T_{pp,j} = \tau_j \int_0^T s_j(t'; \vec{E}) dt'.$$

and where $T_{id,j} = T - T_{off,j} - T_{w,j} - T_{pp,j}$. $T_{off,j}$ is:

$$T_{off,j} = \sum_{k=1}^{\eta_j} d_k,$$

and the warm up time is represented below:

$$T_{w,j} = \sum_{k=1}^{\eta_j} t_{w,j}^k,$$

where η_j is the number of downtime events at machine j and $t_{w,j}^k$ is the length of time machine j warms up after the k^{th} breakdown. The production count of the line is:

$$PC = \frac{1}{\tau_{M^*}} \Big(T - \bigcup_{i \in n^s} [t_i + d_{i^*}, t_i + d_i + t_{w,j}^i) \Big), \tag{4.7}$$

where $n^s = \{i = 1, ..., \eta_j \ s.t. \ d_i \in \vec{D}^e\}$. To understand the derivation of the production count, we look at the i^{th} downtime event at machine j: $\vec{e}_{j,i} = (j, t_i, d_i)$. If $d_i \in \vec{D}^e$, then the permanent production time loss is equivalent to $d_i - d_i^* + t_{w,j}^i$. We thus attribute the idling of machine M^* during the time interval $[t_i + d_i^*, t_i + d_i + t_{w,j}^i)$ to $\vec{e}_{j,i} = (j, t_i, d_i)$. Under a sequence of downtime events, $\vec{E} = \{\vec{e}_1, \vec{e}_2, ..., \vec{e}_M\}$, the slowest machine stops during [0,T) for $\cup_{i \in n^s} [t_i + d_{i^*}, t_i + d_i + t_{w,j}^i)$, where $j = 1, ..., M$. It is possible for two different downtime events to result in overlapping stoppage intervals. Therefore, this term cannot simply be written as the summation of the duration of the reconstructed stoppage intervals without

imposing some conditions. However, this information can be measured using sensor data since this term is the time the slowest machine, M^*, is not producing parts. Therefore, the general solution of EPP is:

$$EPP = \frac{\sum_{j=1}^{M} P_{pp,j}\left[T - \sum_{k=1}^{\eta_j}[d_k - (1+\beta_j)t_{w,j}^k] - (1-\alpha_j)T_{id,j}\right]}{PC}. \tag{4.8}$$

This analysis of the energy dynamics of the production system can be utilized to properly illustrate the performance of the production system.

4.2.1 Energy Consumption due to Machine Interactions

While the homogeneous portion is the scenario in which the line runs without any downtime events, it is still not the absolute minimum energy consumption per part that can be achieved. By analyzing the homogeneous solution there are two portions: the portion if each machine is standalone ($EPP_{h,sa}$) and the energy consumed due to machine interactions ($EPP_{h,int}$):

$$EPP_h = EPP_{h,sa} + EPP_{h,int}. \tag{4.9}$$

There are situations when certain machines will be producing parts, while the production count of the overall line is not increasing. If each machine was standalone then this leads to the optimal minimum energy consumption per part: the situation in which each machine produces the same number of parts as the slowest machine and then immediately turns off without producing extra work in progress (WIP).

Consider a virtual scenario where each machine has no interactions with each other and treating this as a dynamic system where the interactions between machines are considered "external forces," the dynamics can be represented as:

$$\frac{d\left[EPP_h\right]}{dt} = f(t, EPP_h(t), I(t)), \tag{4.10}$$

where EPP_h is the energy consumption per part produced without downtime events and $I(t)$ is the interactions between machines. To solve the state space equation in (4.10) we present the following homogeneous and non-homogeneous functions:

$$\frac{d\left[EPP_h\right]}{dt} = f(t, EPP_h(t)) \tag{4.11}$$

$$\frac{d\left[EPP_h\right]}{dt} = f(t, EPP_h(t), I(t)), \tag{4.12}$$

Equation (4.11) represents a virtual scenario when each machine is running standalone, producing the same number of parts as the slowest machine. However, each machine's production time will be different: once the machine produces the same amount of parts as the slowest machine, it turns off. This is the theoretical minimum energy consumption per part that can be achieved in the system. To solve for the standalone case in (4.11), we introduce the variable $t_{p,j}$, which is the minimum amount of time machine j would produce the number of parts processed by the slowest machine in [0,T) if machine j was running as a standalone machine:

$$t_{p,j} = \tau_j \int_0^T s_{M^*}(t')dt'. \tag{4.13}$$

This directly leads to the standalone case:

$$EPP_{h,sa} = \frac{\sum_{j=1}^{M} P_{pp,j} t_{p,j}}{\frac{1}{\tau_{M^*}} T}. \tag{4.14}$$

Using (4.5), (4.9), and (4.14) leads to the portion wasted due to machine variations and interactions:

$$EPP_{h,int} = \frac{\sum_{j=1}^{M} P_{pp,j}\left[(T - T_{id,j}^U - t_{p,j}) + \alpha_j T_{id,j}^U\right]}{\frac{1}{\tau_{M^*}} T}. \tag{4.15}$$

In the scenario without any downtime events, the $EPP_{h,int}$ provides the energy consumption per part caused by machine interactions and unsychronous operation due to capacity

variation. The first term in the numerator of (4.15) is the energy consumed due to WIP and the second term is the energy consumed because of unsynchronized idling. The standalone solution represents the energy consumption per part for a virtual scenario as if each machine was running standalone without capacity variation constraints from other machines.

4.3 Sustainable Manufacturing Performance Indicators

Using the analysis of the dynamic energy structure leads to the creation of the SMPI. Two SMPIs are created: one that illustrates the line's performance in reference to the case with no downtime events, the other compares the current performance to the optimal minimum energy consumption per part. The first SMPI is the ratio of the energy consumption per part without downtime events (EPP_h) to the overall energy consumption per part (EPP) for the entire production line ($SMPI_{DT}$):

$$\begin{aligned} SMPI_{DT} &= \frac{(EPP_h)}{(EPP)} \\ &= \frac{T_{pp,M^*}\sum_{j=1}^{M} P_{pp,j}\left[T-(1-\alpha_j)T^U_{id,j}\right]}{T\sum_{j=1}^{M} P_{pp,j}\left[T-\sum_{k=1}^{\eta_j}[d_k-(1+\beta_j)t^k_{w,j}]-(1-\alpha_j)T_{id,j}\right]}. \end{aligned} \tag{4.16}$$

The $SMPI_{DT}$ accurately shows how the line is performing in comparison to the static portion of the energy consumption per part where there are no downtime events. This shows how much energy is being wasted due to disruption events. There are three scenarios to discuss with this SMPI:

Case 1: $SMPI_{DT} < 1$

This is when the production line is consuming more energy per part produced than in the scenario when there are no downtime events. This is due to the permanent production loss from effective downtime events causing the slowest machine to be blocked or starved.

Case 2: $SMPI_{DT} = 1$

This shows the situation when the production line is producing parts with an energy consumption equal to the amount if the machines were running at one hundred percent efficiency. However, there can be more energy savings since it is possible to turn off certain machines without affecting the throughput of the line. This is shown in case 3.

Case 3: $SMPI_{DT} > 1$

This illustrates that the line is producing parts with less energy consumption than the homogeneous case with no downtime events. The best case scenario is when the line has an energy consumption per part equal to that of the standalone, homogenous portion of the energy consumption per part. This is the minimum energy consumption per part produced that can be achieved.

To show how the production line is performing compared to the minimum amount of energy consumption per part that can be achieved (the ratio of the $EPP_{h,sa}$ to EPP), the $SMPI_{SA}$ is introduced:

$$\begin{aligned} SMPI_{SA} &= \frac{(EPP_{h,sa})}{(EPP)} \\ &= \frac{T_{pp,M^*} \sum_{j=1}^{M} P_{pp,j} t_{p,j}}{T \sum_{j=1}^{M} P_{pp,j} \left[T - \sum_{k=1}^{\eta_j} [d_k - (1+\beta_j) t_{w,j}^k] - (1-\alpha_j) T_{id,j} \right]}. \end{aligned} \tag{4.17}$$

This indicator has the limits of [0,1], where 0 indicates the case when each individual machine's downtime events cause the slowest machine to be blocked or starved. The best case scenario ($SMPI_{SA} = 1$) will be achieved when the production line is consuming energy per part at the same rate as the standalone case of the homogeneous solution. While these two indicators are useful as a self bench-mark of a production line for energy efficiency performance, there still needs to be a method to dissect the energy inefficiencies at the machine

level. The next section addresses this issue with the introduction of the downtime energy bottleneck and the rated power bottleneck.

4.4 Downtime Energy Bottleneck

The DE-BN allows a plant manager to allocate maintenance workers to the machine which will lead to the largest decrease in energy waste for the production line. It uses real sensor data that is readily available from the manufacturing facility to calculate the machine with the most energy waste.

4.4.1 Analytical Proof

Definition 1: *Consider the serial production line as presented in Fig. 5.4.1, machine j, $j = 1, ..., M$, is the DE-BN if:*

$$\frac{\partial(EPP)}{\partial d_j} > \frac{\partial(EPP)}{\partial d_z}, \quad \forall z \neq j. \tag{4.18}$$

This implies that machine j is the DE-BN if an infinitesimal improvement in its mean downtime (∂d) (a small change in Mean Time to Repair, MTTR) leads to the largest decrease in energy consumption per part for the entire production line, as compared with a similar improvement of any other machine in the system.

Proposition 1: *Machine j is the DE-BN if j is the machine with the largest percent energy waste and the highest percent permanent production loss. This is illustrated by the following:*

$$A_j + B_j > A_z + B_z, \quad \forall z \neq j, \tag{4.19}$$

where:

$$A_l = \frac{-\eta_l P_{pp,l}}{\sum_{j=1}^{M} P_{pp,j}\Big[T - \sum_{k=1}^{\eta_j}[d_k - (1+\beta_j)t_{w,j}^k] - (1-\alpha_j)T_{id,j}\Big]}$$

$$B_l = \frac{\eta_l^e}{T - \bigcup_{i\in n^s}[t_i + d_{i^*}, t_i + d_i + t_{w,j}^i)}, \quad l = 1, 2, ..., M.$$

Proof:

For the serial production line considered with all machines operating with random downtime events, the general form of the energy consumption per part for the production line as seen in (4.8) must be used. To find the partial derivative of the energy consumption per part with respect to mean downtime, the DE-BN as a function of downtime (d) defined in (4.18) is used in conjunction with the quotient rule for partial differential equations:

$$\frac{\partial(EPP)}{\partial d_j} = \frac{\partial(\frac{E}{PC})}{\partial d_j} = \frac{(PC)(\frac{\partial E}{\partial d_j}) - (E)(\frac{\partial PC}{\partial d_j})}{(PC)^2}, \tag{4.20}$$

where E is energy consumption of the line, PC is the production count of the line, $\frac{\partial E}{\partial d_j}$ is the partial derivative of energy consumption with respect to mean downtime duration, and $\frac{\partial PC}{\partial d_j}$ is the partial derivative of production count with respect to mean downtime duration. The energy consumption as well as the production count were defined in (4.6) and (4.7) respectively. Manipulating (4.6) gives:

$$E = \sum_{j=1}^{M} P_{pp,j}\Big[T - \sum_{k=1}^{\eta_j}[d_k - (1+\beta_j)t_{w,j}^k] - (1-\alpha_j)T_{id,j}\Big] \tag{4.21}$$

To find the partial derivatives of energy consumption with respect to downtime we use the definition of a derivative:

$$\frac{\partial E}{\partial d_j} = \lim_{\partial d_j \to 0} \frac{E(d_j + \partial d_j) - E(d_j)}{\partial d_j}, \tag{4.22}$$

where $E(d_j)$ is found above in (4.21), and $E(d_j + \partial d_j)$ for machine j is:

$$E(d_j + \partial d_j) = \sum_{j=1}^{M} P_{pp,j}\Big[T - \sum_{k=1}^{\eta_j}[d_k - (1+\beta_j)t^k_{w,j}] - (1-\alpha_j)T_{id,j}\Big] - (\partial d_j)\,(\eta_j P_{pp,j})\,. \quad (4.23)$$

It is important to note here that for a small change, ∂d_j, in each downtime event there is no change in $T_{id,j}$ due to the fact that the machine can never break down when idle. Plugging (4.23) and (4.21) into (4.22) gives the partial derivative of energy consumption with respect to mean downtime duration:

$$\frac{\partial E}{\partial d_j} = -\eta_j P_{pp,j}. \quad (4.24)$$

To find the partial derivative for production count of the line with respect to the mean downtime, we first manipulate (4.7) and take the derivative:

$$\frac{\partial PC}{\partial d_j} = -\frac{\partial}{\partial d_j}\Big\{\frac{1}{\tau_{M^*}} \bigcup_{i \in n^s} [t_i + d_{i^*}, t_i + d_i + t^i_{w,j})\Big\}. \quad (4.25)$$

In order to solve (4.25), it is necessary to study the effect of downtime at machine j on the production count of machine M^*. This is the permanent production loss (PPL) caused by machine j:

$$\frac{\partial PC}{\partial d_j} = -\frac{\partial PPL}{\partial d_j} = -\lim_{\partial d_j \to 0} \frac{PPL(d_j + \partial d_j) - PPL(d_j)}{\partial d_j}. \quad (4.26)$$

By changing the MTTR of machine j by a small infinitesimal amount, we can assume that this small change will not cause any non-effective downtime event to become an effective downtime event. To find the permanent production loss caused by machine j, it is necessary to look at the effect of downtime events at machine j. The permanent production time loss of the downtime event $\vec{e}_{j,i} = (j, t_i, d_i)$, $\forall\ d_i \in \vec{D}^e$, is $d_i - d^*_i + t^i_{w,j}$. The permanent production loss for the event $\vec{e}_{j,i}$ is $(d_i - d^*_i + t^i_{w,j})/\tau_{M^*}$, which is the number of parts lost by the production line due to this downtime event. Therefore, the permanent production loss for machine j when subject to a sequence of downtime events $\vec{e}_j = \{\vec{e}_{j,1}, \vec{e}_{j,2}, ..., \vec{e}_{j,\eta_j}\}$ is equivalent to the

summation of the stoppage intervals caused by machine j:

$$PPL(d_j) = \frac{\sum_{i=1}^{\eta_j^e} d_i - d_i^* + t_{w,j}^i}{\tau_{M^*}}. \tag{4.27}$$

The PPL caused by machine j is simply the summation of stoppage intervals caused by machine j since there cannot be overlapping downtime events at a single machine. This is because a machine cannot break down when already non-operational. By changing the mean downtime of machine j by a small amount, ∂d_j, leads to (4.28):

$$PPL(d_j + \partial d_j) = \frac{\sum_{i=1}^{\eta_j^e} d_i + \partial d_j - d_i^* + t_{w,j}^i}{\tau_{M^*}}. \tag{4.28}$$

Thus, by substituting (4.27) and (4.28) into (4.26):

$$\frac{\partial PC}{\partial d_j} = -\sum_{i=1}^{\eta_j^e} \frac{1}{\tau_{M^*}} = -\frac{\eta_j^e}{\tau_{M^*}}. \tag{4.29}$$

Comparing machine j to all other machines using the DE-BN definition in (4.20) and providing some manipulation gives:

$$\frac{(\frac{\partial E}{\partial d_j})}{E} - \frac{(\frac{\partial PC}{\partial d_j})}{PC} > \frac{(\frac{\partial E}{\partial d_z})}{E} - \frac{(\frac{\partial PC}{\partial d_z})}{PC}, \quad \forall z \neq j. \tag{4.30}$$

And thus machine j is the DE-BN if it satisfies the following:

$$A_j + B_j > A_z + B_z \quad \forall z \neq j.$$

This completes the proof. □

These results give the plant manager a quantitative tool in selecting which machine to prioritize with reactive maintenance. The DE-BN can be identified by using readily available

sensor data. Improving the DE-BN leads to the largest improvement in the EPP and largest decrease in energy waste as compared to the same improvement to any other machine on the line.

4.4.2 Numerical Validation

The simulation studies are performed using a model built in Simulink/MATLAB. The model is a continuous flow model, which means that the buffers vary continuously, as opposed to integer steps. As stated earlier, this does not affect the dynamics of the system. For these scenarios, the model is initially run for one 8 hour period of warmup, which is the time needed for system to reach a steady state. The model is then run for the time horizon [0,T) of $T = 8$ hours for each shift with a time step of 0.005 min. Once the simulation is completed all necessary data is recorded and saved. The simulation studies utilize 1000 different line combinations to test the effectiveness of the DE-BN method against other industry standards. The simulation model is a 15 Machine, 14 Buffer line. To create the 1000 line combinations, the rated speed, $\frac{1}{\tau_j}$ (parts/min), the efficiency, e_j, the buffer capacity, B_m (parts), and the power consumption, $P_{pp,j}$ (kW), are selected randomly and with equal probability from the following sets:

$$\begin{aligned}
\frac{1}{\tau_j} &\in \{1.0, 1.5, 2.0, 2.5, 3.0\} \quad j = 1, ..., M \\
e_j &\in \{0.80, 0.85, 0.90, 0.95, 0.99\} \quad j = 1, ..., M \\
P_{pp,j} &\in \{80, 100, 120\} \quad j = 1, ..., M \\
B_m &\in \{10, 30, 50\} \quad m = 2, ..., M.
\end{aligned}$$

These combinations include various scenarios as seen in industry, including, but not limited to, machines arranged in increasing efficiency or decreasing efficiency, systems with buffer capacity arranged with increasing or decreasing order, systems with machine efficiency or buffer capacity arranged based on a bowl or inverted bowl pattern, etc. The MTTR and the

Mean Cycles Between Failure (MCBF) are assumed to be exponentially distributed. The mean time to warm up, ω_j, is 1 minute. The MTTR for each machine is assumed to be 10 minutes and the MCBF is changed based on the efficiency of the machine. Each scenario was run for one 8 hour time period and the method from (4.19) is used to determine the DE-BN machine. Other production data is recorded, such as energy consumption, individual machine energy per part produced, etc. The line is then run for another 8 hour time period with one machine having a decrease in the MTTR (in this case a 10% decrease). This machine is selected based on the DE-BN measurement and various common industry measurements. For the remainder of the dissertation, we call these measurements "indicators". The $SMPI_{DT}$ is recorded to show how the 10% change in MTTR reduces the energy waste of the facility. This data is used to test the effectiveness of utilizing the DE-BN to decide which machine should have maintenance priority versus other indicators such as selecting the machine with the highest energy consumption per part or the machine with the highest overall energy consumption, etc. The results can be seen in Table 4.1, which summarizes the 1000 scenarios. The first column in Table 4.1 shows the different indicators. The "DE-BN" is the downtime

Table 4.1: Downtime Energy Bottleneck Indicators

Indicator	Total EC (kWh)	Total PC	Avg EC (kWh)	Avg PC	% Δ $SMPI_{DT}$
Baseline	10,963,911	602,883	10,953	602	-
DE-BN	11,002,349	625,233	11,002	626	**3.01%**
Max EPP_j	10,981,621	613,164	10,982	613	1.39%
Min e_j	10,968,520	605,722	10,968	605	0.39%
Max $P_{pp,j}$	10,962,917	603,228	10,962	603	0.05%
Max EC_j	10,974,375	610,996	10,974	610	1.04%

energy bottleneck method discussed in the previous section. The "Max EPP_j" is the machine with the maximum energy consumption per part produced at machine j. The "Max EC_j" is the machine with the maximum energy consumption. "Min e_j" is the machine with the

lowest efficiency, where the efficiency is calculated by:

$$e_j = \frac{\frac{MCBF}{\tau_j}}{\frac{MCBF}{\tau_j} + MTTR}. \tag{4.31}$$

The "Max $P_{pp,j}$" is the machine with the maximum rated power consumption. Column two shows the total energy for the 1000 scenarios, while column three shows the total production count. The average energy consumption for the 1000 scenarios is shown in column four, and the average production count is displayed in column five. Column six shows the change in $SMPI_{DT}$ for the entire production line when the given indicator is used to select which machine to repair as compared to the baseline. The DE-BN is ranked number 1, having an increase in production of 22,350 parts, which is more than double the amount of the number 2 ranked indicator, i.e., the EPP_j. With a small energy consumption increase dedicated to the production of parts, the DE-BN method leads to an energy waste decrease of 3.24% which is also more than double the energy waste decrease of the rank 2 indicator. To show the effectiveness of the proposed approach across various cases we randomly pull out the results for 10 different line combinations. These scenarios can be found in Appendix A.

4.5 Rated Power Bottleneck

The RP-BN provides the plant manager with the information necessary to change an individual machine on the production line with one that is more energy efficient to achieve the largest decrease in energy waste. This provides a method for utilizing the readily available sensor data to calculate the RP-BN.

4.5.1 Analytical Proof

Definition 2: *Consider the serial production line in Fig. 5.4.1, machine j, $j = 1, ..., M$, is the RP-BN if:*

$$\frac{\partial(EPP)}{\partial P_j} > \frac{\partial(EPP)}{\partial P_z}, \quad \forall z \neq j. \tag{4.32}$$

This implies that machine j is the RP-BN if an infinitesimal improvement in its rated power while producing parts (∂P_j) leads to the largest decrease in energy consumption per part for the entire production line, as compared with a similar improvement of any other machine in the system.

Proposition 2: *Machine j is the RP-BN if machine j satisfies the following:*

$$\begin{aligned} &T - \sum_{k=1}^{\eta_j}[d_k - (1+\beta_j)t_{w,j}^k] - (1-\alpha_j)T_{id,j} > \\ &T - \sum_{k=1}^{\eta_z}[d_k - (1+\beta_z)t_{w,z}^k] - (1-\alpha_z)T_{id,z}, \quad \forall z \neq j. \end{aligned} \tag{4.33}$$

Proof:

Once again consider a serial production line with all machines operating with random down-time events. To find the partial derivative of the energy consumption per part with respect to rated power we use the quotient rule for machine j:

$$\frac{\partial(EPP)}{\partial P_j} = \frac{\partial(\frac{E}{PC})}{\partial P_j} = \frac{(PC)(\frac{\partial E}{\partial P_j}) - (E)(\frac{\partial PC}{\partial P_j})}{(PC)^2}.$$

Since production count is not a function of rated power, the partial derivative of production count with respect to rated power is zero, which leads to:

$$\frac{\partial(\frac{E}{PC})}{\partial P_j} = \frac{(\frac{\partial E}{\partial P_j})}{(PC)}. \tag{4.34}$$

The equation for production count can be found in (4.7) and the equation for energy consumption is above in (4.21). $E(P_j + \partial P_j)$ for machine j is:

$$\begin{aligned}
&E(P_j + \partial P_j) = \\
&\sum_{i=1}^{M} P_{pp,i} \left(T - \sum_{k=1}^{\eta_j} [d_k - (1+\beta_j) t_{w,j}^k] - (1-\alpha_j) T_{id,j} \right) \\
&+ (\partial P_j) \left(T - \sum_{k=1}^{\eta_j} [d_k - (1+\beta_j) t_{w,j}^k] - (1-\alpha_j) T_{id,j} \right).
\end{aligned} \tag{4.35}$$

Plugging this into (4.34) along with (4.6) gives:

$$\frac{\partial E}{\partial P_j} = T - \sum_{k=1}^{\eta_j} [d_k - (1+\beta_j) t_{w,j}^k] - (1-\alpha_j) T_{id,j}. \tag{4.36}$$

Comparing machine j to the other machines on the line using the RP-BN definition in (4.32) gives:

$$(\frac{\partial E}{\partial P_j}) > (\frac{\partial E}{\partial P_z}), \quad \forall z \neq j. \tag{4.37}$$

Plugging in (4.36):

$$\begin{aligned}
&\left(T - \sum_{k=1}^{\eta_j} [d_k - (1+\beta_j) t_{w,j}^k] - (1-\alpha_j) T_{id,j} \right) > \\
&\left(T - \sum_{k=1}^{\eta_z} [d_k - (1+\beta_z) t_{w,z}^k] - (1-\alpha_z) T_{id,z} \right), \quad \forall z \neq j.
\end{aligned}$$

This completes the proof. □

4.5.2 Numerical Validation

The same one thousand scenarios as with the DE-BN in Sec 4.4.2 are run to test the effectiveness of the RP-BN. Once again to create the 1000 line combinations, the rated speed, $\frac{1}{\tau_j}$ (parts/min), the efficiency, e_j, the buffer capacity, B_m (parts), and the power consumption,

$P_{pp,j}$ (kW), are selected randomly and with equal probability from the following sets:

$$\frac{1}{\tau_j} \in \{1.0, 1.5, 2.0, 2.5, 3.0\} \quad j = 1, ..., M$$

$$e_j \in \{0.80, 0.85, 0.90, 0.95, 0.99\} \quad j = 1, ..., M$$

$$P_{pp,j} \in \{80, 100, 120\} \quad j = 1, ..., M$$

$$B_m \in \{10, 30, 50\} \quad m = 2, ..., M.$$

However, rather than making a change to the MTTR, there is a change to the power consumption, $P_{pp,j}$, of an individual machine. The power consumption is reduced by 30 kW. The mean time to warmup, ω_j, is 1 min. The RP-BN is tested against the same indicators as seen in Table 4.1. This study assumes one 8 hour shift per day for a one year period since the machine is being replaced and machines cannot be replaced on a daily basis, therefore it is a long-term decision. The average yearly results can be seen in Table 4.2 for the 1000 scenarios. Note that the production count is not included since the RP-BN only leads to an energy savings. The RP-BN is ranked number one, which leads to a savings of 85,252

Table 4.2: Rated Power Bottleneck Indicators

Indicator	Average Yearly EC (kWh)	% Change $SMPI_{DT}$
Baseline	3,717,779	-
RP-BN	3,632,526	**2.29%**
Max EPP_j	3,640,076	2.09%
Min e_j	3,647,165	1.90%
Max $P_{pp,j}$	3,646,277	1.92%
Max EC_j	3,638,593	2.16%

kWh. It saves over 6,000 kWh more than the the second ranked indicator, i.e. "Max EC_j". Although these indicators result in similar energy waste reduction, the RP-BN method is always ranked number one for all 1000 scenarios. To further show the effectiveness of the proposed approach across various cases we randomly pull out the results for 10 different line combinations, which can be found in Appendix A. By using readily available sensor

Table 4.3: Production Line Parameters: DE-BN & RP-BN Case Study

	m_1	m_2	m_3	m_4	m_5	m_6	m_7	m_8	m_9	m_{10}	m_{11}	m_{12}	m_{13}	m_{14}	m_{15}
$1/\tau$	5.3	5.8	4.1	6.6	4.4	4.8	4.8	5.5	3.1	5.2	6.3	5.4	6.2	5.5	7.8
MTTR	13	11	13	14	18	11	13	11	9	12	18	11	13	11	13
MCBF	200	210	205	255	200	205	215	200	290	200	255	200	205	275	200
e_j	74	77	79	73	71	79	77	77	91	76	69	77	71	82	66
P_{pp}	120	125	120	110	130	120	107	105	120	110	130	125	130	105	132
P_{id}	96	100	96	88	104	96	85.6	84	96	88	104	100	104	84	105
P_w	108	113	108	99	117	108	97	95	108	99	117	113	117	95	119
-	-	B_2	B_3	B_4	B_5	B_6	B_7	B_8	B_9	B_{10}	B_{11}	B_{12}	B_{13}	B_{14}	B_{15}
B_m	-	20	30	15	20	25	20	25	35	30	25	30	25	20	15

information, the RP-BN method can be implemented quickly and easily as compared to the industry measurements. Therefore, the RP-BN is a better quantitative indicator to decide where to invest money into more energy efficient machines on the production line.

4.6 Case Study

A real battery assembly line composed of 15 machines and 14 buffers is adopted for the case study to further demonstrate the method in this research. The system parameters are recorded from the real production line and the data is mocked up for confidential reasons. The mocked data is shown in Table 4.3. The mean time to warmup, ω_j, is 1 min. The MTTR and the MCBF are assumed to be exponentially distributed based on the real data. The rated speed, $\frac{1}{\tau_j}$, is in parts/min, the efficiency, e_j, is in percent (%), the buffer capacity, B_m, is in parts, the MTTR is in mins, the MCBF is in cycles, and the power consumption is in kW. To test the effectiveness of the DE-BN versus the other industry measures, the line is run for a one month period with one 8 hour shift per day. Each day, one machine is prioritized, for a 10% decrease in MTTR, based on the various indicators as presented in Table 4.1. The results for the entire month for each indicator are presented in Table 4.4. The baseline case is where no machine is given maintenance priority. It is important to note that

Table 4.4: Case Study: DE-BN Results

Indicator	$EC\ (kWh)$	PC	$SMPI_{DT}$
Baseline	385,758	27,517	0.685
DE-BN	388,091	29,470	0.730
Max EPP_j	386,472	28,273	0.703
Max EC_j	386,414	28,148	0.700
Max $P_{pp,j}$	385,828	27,697	0.690
Min e_j	385,828	27,697	0.690

for the case study, machine $j = 15$ is "Max $P_{pp,j}$" and "Min e_j", therefore the results for those indicators are equivalent. The DE-BN leads to an increase in production by approximately 2,000 parts, which is more than 1,000 parts over the next closest indicator (in this case EPP_j). For this additional 1000 parts, only minimal additional energy is consumed, which is dedicated to the production of parts. According to the $SMPI_{DT}$, a decrease of 4.5% on energy waste is achieved based on the DE-BN, while the rank 2 indicator results in a 1.5% energy waste reduction. While the decrease in energy waste is important, it is also necessary to explore how this will save money for the manufacturing facility by decreasing energy costs and increasing productivity. Considering only throughput gain and energy cost, the profit realized in the period [0,T) is seen below:

$$\begin{aligned} Profit &= Total\ Revenue - Total\ Cost \\ &= Throughput\ Gain - Energy\ Cost \end{aligned} \tag{4.38}$$

where total revenue is the throughput gain and the total cost is the energy cost. We will assume that the expenses to produce the part in terms of material and labor are included when the profit per part is calculated. It is assumed that there is a \$100 profit per part produced, based on mocked up data for the value of a battery pack, and that the energy cost is \$0.14 per kWh based on data from the Energy Information Administration for the

Northeast, United States [67]. Plugging these values into (4.38) gives:

$$Profit = (\$100) \int_0^T s_{M^*}(t'; \vec{E}) dt' - (\$0.14) EC(T), \tag{4.39}$$

where $EC(T)$ is the energy consumption of the entire line in the period [0,T). By prioritizing the DE-BN machine the plant will realize the largest total monthly profit. The results for the total monthly profit for each indicator as compared with the baseline case are seen in Table 4.5. As one can see, the DE-BN leads to a cost savings of more than $119,000 over

Table 4.5: Case Study: DE-BN Cost Savings

Indicator	Monthly Cost Savings ($)
DE-BN	**$194,935.53**
Max EPP_j	$75,493.11
Max EC_j	$62,978.36
Max $P_{pp,j}$	$17,991.67
Min e_j	$17,991.67

the EPP_j. For the study of the RP-BN the same battery production line in Table 4.3 is utilized. Since the RP-BN is used to replace a machine, the simulation is run for a one year period assuming one 8 hour shift per day. The line is then simulated for another year with one machine having a reduced energy consumption (30 kW decrease) based on the indicators presented in Table 4.2. This simulates a machine being replaced with a more energy efficient machine. The results for the entire year are shown in Table 4.6. The baseline case is where no machine is replaced. At first glance it appears that the indicators are all similar in reducing the $SMPI_{DT}$. However, the savings from utilizing the RP-BN leads to a 84,900 kWh yearly savings for the production facility. This is more than 24,800 kWh over the next closest indicator (in this case the machine with the maximum $P_{pp,j}$ and minimum e_j). The production count for each scenario remains the same since we assume the replaced machine will only have a reduced energy consumption. The RP-BN provides a better solution than any other indicators while still utilizing available sensor data. Investigating the monetary

Table 4.6: Case Study: RP-BN Results

Indicator	EC (kWh)	$SMPI_{DT}$
Baseline	4,688,487	0.6851
RP-BN	4,603,597	0.6980
Max $P_{pp,j}$	4,628,482	0.6936
Min e_j	4,628,482	0.6936
Max EPP_j	4,631,246	0.6940
Max EC_j	4,631,440	0.6940

savings will provide even more insight into the reason why the RP-BN is a more cost effective solution than the other indicators. The yearly cost savings for each indicator versus the baseline scenario is presented in Table 4.7. This research assumes that each machine has the

Table 4.7: Case Study: RP-BN Cost Savings

Indicator	Yearly Cost Savings ($)
RP-BN	**$11,884.54**
Max $P_{pp,j}$	$8,368.34
Min e_j	$8,368.34
Max EPP_j	$7,999.68
Max EC_j	$7,916.71

same cost to replace and therefore does not explicitly take into account return on investment. This will be addressed in the next chapter. These results compare the energy cost savings of the RP-BN versus other common indicators used in industry. The RP-BN leads to an increase of profit of approximately $11,880, which is $2,500 more than the case if the machine with the maximum power consumption is replaced. The RP-BN provides the machine which, when replaced, will lead to the most energy and cost savings on the production line.

4.7 Conclusions

This chapter investigates the dynamic energy structure of a serial production line to further mitigate the energy waste for the manufacturing facility. We formulate the framework of the

dynamic system to analyze the energy consumption per part, understanding how and where energy is wasted on the production line. The energy consumption per part has two portions: the static component, i.e., the energy consumed when there are no random downtime events (a virtual scenario) and the dynamic component, i.e., the energy consumed due to random downtime events. The energy structure is further analyzed to find the optimal minimum energy consumption per part for the production line.

This dynamic energy structure is then used to create the SMPI for the overall production line. This provides a quantitative self-benchmark method to correctly monitor the performance of the production line. The definition of the DE-BN and the RP-BN are introduced and the DE-BN and RP-BN are proven analytically. The DE-BN provides the plant manager with information on where to direct maintenance workers to lead to the most energy efficiency improvement, while the RP-BN will allow the plant manager to identify which machine can be replaced with a more energy efficient version.

Chapter 5

Energy Economic Analysis

5.1 Introduction

This chapter uses energy economic analysis to increase the overall profit of the manufacturing facility by reducing energy consumption with minimal throughput impact. This allows for the utilization of energy savings opportunities, where certain machines are powered off with minimal production impact. The energy profit bottleneck is identified, which is the machine that causes the biggest loss in profit on the line. A return on investment strategy is developed to give plant managers the quantitative tools to select the machine or part which, when replaced, will lead to the largest return on investment. Over the long term, this will lead to the largest decrease in energy costs. To increase profits on a daily basis, a control methodology is developed that uses energy opportunity windows to insert downtime events that have minimal production impact, but reduce the overall energy consumption. A simulation case study is performed to test the control methodology and the return on investment strategy to show the effect of both on the profit of the manufacturing facility.

5.2 Energy Profit Bottleneck

The Energy Profit Bottleneck (EP-BN) allows a plant manager to allocate maintenance workers to the machine that when repaired will lead to the largest increase in profit margin for the plant. The profit of the plant is considered in (5.16):

$$\begin{aligned} Profit =& Total\ Revenue - Total\ Cost \\ =& (PC)(c_p) - CE, \end{aligned} \tag{5.1}$$

where PC is the production count, CE is the total cost of energy used by the production line and c_p is the income per part. We will assume that the expenses to produce the part in terms of material and labor are already considered in the profit per part calculation. In this chapter, inventory cost is ignored, since the trade off between throughput and energy savings is the main concern. The cost of energy is calculated based on a time of use schedule. If we assume that the energy price per kWh from the electrical company is broken up into c time periods then the energy price per kWh can be represented by:

$$c_e^l(t) = \begin{cases} c_e^1, & t_0 \leq t < t_1, \\ c_e^2, & t_1 \leq t < t_2, \\ \vdots & \vdots \\ c_e^l, & t_{l-1} \leq t < t_l, \\ \vdots & \vdots \\ c_e^c, & t_{c-1} \leq t \leq t_c. \end{cases}$$

After manipulating the energy equation in (4.21), the total cost of energy, CE, is displayed below:

$$CE = \sum_{j=1}^{M} \sum_{l=1}^{c} \left[P_{pp,j} \Big(t_l - t_{l-1} - \sum_{k=1}^{\eta_{j,l}} [d_k^l - (1+\beta_j) t_{w,j}^i] - (1-\alpha_j) T_{id,j}^l \Big) \right] c_e^l, \tag{5.2}$$

where $\eta_{j,l}$is the number of downtime events at machine j and d_k^l is the amount of each downtime in the time period of $[t_{l-1}, t_l)$. We note that this accounts for all downtime that starts in the time period $[t_{l-1}, t_l)$ and we will attribute all downtime to this time period even if there is any overlap into the next time period, $[t_l, t_{l+1})$. In our experience, the cost difference is inconsequential if we attribute this downtime to one time period. The idle time in each time period is represented by $T_{id,j}^l$. The production count, PC, is represented in (4.7):

$$PC = \frac{1}{\tau_{M^*}} \Big(T - \bigcup_{i \in n^s} [t_i + d_{i^*}, t_i + d_i + t_{w,j}^i) \Big),$$

5.2.1 Analytical Proof

Definition 1: *If we consider the serial production line in Fig. 1, machine j, $j = 1, ..., M$, is the energy profit bottleneck (EP-BN) if:*

$$\left|\frac{\partial(Profit)}{\partial d_j}\right| > \left|\frac{\partial(Profit)}{\partial d_z}\right|, \quad \forall z \neq j. \tag{5.3}$$

This implies that machine j is the energy profit bottleneck if its infinitesimal improvement in its mean downtime (∂d_j) (a small change in Mean Time to Repair, MTTR) leads to the largest increase in profit for the production line, as compared with the same perturbation to any other machine in the system. Equation (5.3) utilizes absolute value in the formulation since for any decrease in MTTR the profit will increase. However, this definition cannot be easily used to identify the energy profit bottleneck. Therefore, we introduce Proposition 1.

Proposition 1: *Machine j is the energy profit bottleneck if $\forall z \neq j$, j satisfies the following:*

$$\left|\sum_{l=1}^{c} \eta_{j,l} P_{pp,j} c_e^l - \frac{\eta_j^e}{\tau_{M^*}} c_p\right| > \left|\sum_{l=1}^{c} \eta_{z,l} P_{pp,z} c_e^l - \frac{\eta_z^e}{\tau_{M^*}} c_p\right| \tag{5.4}$$

Proof:

If we consider the serial production line in Fig. 1 with all machines operating with random downtime, it is necessary to find the partial derivative of the profit with respect to mean downtime. The change in profit with respect to mean downtime is seen in (5.5):

$$\frac{\partial Profit}{\partial d_j} = \left(\frac{\partial PC}{\partial d_j}\right)(c_p) - \left(\frac{\partial CE}{\partial d_j}\right). \tag{5.5}$$

To find the partial derivative of energy cost with respect to mean downtime, we use the

definition of a derivative in (5.6):

$$\frac{\partial CE}{\partial d_j} = \lim_{\partial d_j \to 0} \frac{CE(d_j + \partial d_j) - CE(d_j)}{\partial d_j}, \tag{5.6}$$

where $CE(d_j + \partial d_j)$ is considered in (5.7):

$$\begin{aligned} CE(d_j + \partial d_j) = &\sum_{j=1}^{M} \sum_{l=1}^{c} \left[P_{pp,j} \left(t_l - t_{l-1} - \sum_{k=1}^{\eta_{j,l}} [d_k^l - (1+\beta_j) t_{w,j}^i] - (1-\alpha_j) T_{id,j}^l \right) \right] \\ &- \sum_{l=1}^{c} \eta_{j,l} P_{pp,j} \partial d_j c_e^l \end{aligned} \tag{5.7}$$

Thus, plugging in (5.7) and (5.2) into (5.6) gives the following:

$$\frac{\partial CE}{\partial d_j} = -\sum_{l=1}^{c} \eta_{j,l} P_{pp,j} c_e^l \tag{5.8}$$

Next, to find the partial derivative of production count, it is necessary to manipulate (4.7) and take the derivative with respect to mean downtime at machine j to obtain:

$$\frac{\partial PC}{\partial d_j} = -\frac{\partial}{\partial d_j} \left\{ \frac{1}{\tau_{M^*}} \bigcup_{i \in n^s} [t_i + d_{i^*}, t_i + d_i + t_{w,j}^i) \right\}. \tag{5.9}$$

Since $\cup_{i \in n^s} [t_i + d_{i^*}, t_i + d_i + t_{w,j}^i)$ is the time machine M^* is not producing parts, to find this derivative at machine j, it is necessary to find the permanent production loss caused by machine j, which leads to:

$$\frac{\partial PC}{\partial d_j} = -\frac{\partial PPL}{\partial d_j} = \lim_{\partial d_j \to 0} \frac{PPL(d_j) - PPL(d_j + \partial d_j)}{\partial d_j}. \tag{5.10}$$

To solve for (5.10), it is necessary to look at the effect of downtime events at machine j. By improving the mean downtime of machine j, which decreases the MTTR by a small infinitesimal amount, we can assume that this small change will not cause any non-effective downtime events to become effective downtime events. As stated earlier the permanent

production time loss of the downtime event $\vec{e}_{j,i} = (j, t_i, d_i)$, $\forall\ d_i \in \vec{D}^e$, is $d_i - d_i^* + t_{w,j}^i$. The permanent production loss for this event is $(d_i - d_i^* + t_{w,j}^i)/\tau_{M^*}$. This is the number of parts lost by the production line due to this downtime event. Since there cannot be overlapping events at a single machine because a machine cannot break down when already non-operational, the permanent production loss for machine j when subject to a sequence of downtime events, $\vec{e}_j = \{\vec{e}_{j,1}, \vec{e}_{j,2}, ..., \vec{e}_{j,\eta_j}\}$, is equivalent to the summation of the stoppage intervals caused by machine j:

$$PPL(d_j) = \frac{\sum_{i=1}^{\eta_j^e} d_i - d_i^* + t_{w,j}^i}{\tau_{M^*}}. \tag{5.11}$$

By changing the mean downtime of machine j by a small amount, ∂d_j, leads to (5.12):

$$PPL(d_j + \partial d_j) = \frac{\sum_{i=1}^{\eta_j^e} d_i + \partial d_j - d_i^* + t_{w,j}^i}{\tau_{M^*}}. \tag{5.12}$$

Thus, by substituting (5.11) and (5.12) into (5.10):

$$\frac{\partial PC}{\partial d_j} = -\sum_{1}^{\eta_j^e} \frac{1}{\tau_{M^*}} = -\frac{\eta_j^e}{\tau_{M^*}}, \tag{5.13}$$

Plugging (5.8) and (5.13) into (5.5) gives:

$$\frac{\partial Profit}{\partial d_j} = -\frac{\eta_j^e}{\tau_{M^*}}(c_p) + \sum_{l=1}^{c} \eta_{j,l} P_{pp,j} c_e^l. \tag{5.14}$$

Using (5.14) in the bottleneck definition, (5.3), yields $\forall z \neq j$:

$$\left| \sum_{l=1}^{c} \eta_{j,l} P_{pp,j} c_e^l - \frac{\eta_j^e}{\tau_{M^*}} c_p \right| > \left| \sum_{l=1}^{c} \eta_{z,l} P_{pp,z} c_e^l - \frac{\eta_z^e}{\tau_{M^*}} c_p \right|$$

This completes the proof. □

The EP-BN allows a plant manager to reduce downtime of the machine that leads to the largest increase in profit margin for the plant. The energy profit bottleneck can change dynamically, therefore it is necessary to find the proper amount of time to select the correct machine to repair. It is found in [20] that the optimal time to repair bottlenecks is on a daily basis, which is what is utilized in the control methodology with the EP-BN. It is important to note that the above energy profit indicator can be easily calculated based on sensor data from the plant information system, thus providing the plant manager with the information on which machine to reduce the overall downtime.

Remark 1: Note that the EP-BN is a more general case of the traditional throughput bottleneck (TH-BN). It is shown in [66], that machine j is a TH-BN if:

$$\eta_j^e > \eta_z^e, \quad \forall j \neq z. \tag{5.15}$$

The EP-BN will reduce to the TH-BN if $\frac{\eta_j^e}{\tau_{M^*}} c_p >> \sum_{l=1}^{c} \eta_{j,l} P_{pp,j} c_e^l$, which is the case when the income from production is much larger than the energy cost. Thus, the TH-BN is a special case of the EP-BN when energy cost is negligible, which is usually not the case. This EP-BN indicator explicitly considers the cost of energy and releases the assumption in the traditional throughput analysis that energy is "free" or not significant.

5.2.2 Numerical Validation

Extensive numerical simulations are performed to validate the EP-BN. The system analyzed for the case studies is composed of 15 Machines and 14 Buffers, which is based on a portion of a engine block line. The system parameters are recorded from the real production line and the mocked data is shown for confidential consideration and is shown in Table 5.1. The

time step for this simulation is $ts = 0.005\ min$. The MTTR and the MCBF are assumed to be exponentially distributed based on the observed production data. The profit of each part, is assumed to be c_p is \$100 per part based on the real value after it is mocked up for confidential reasons and the cost of energy, c_e^l, is assumed to be [67]:

$$c_e^l(t) = \begin{cases} \$0.08, & 00:00 \leq t < 06:00, \\ \$0.14, & 06:00 \leq t < 11:00, \\ \$0.24, & 11:00 \leq t < 19:00, \\ \$0.14, & 19:00 \leq t \leq 23:59. \end{cases}$$

The warm up time of each machine, $t_{w,j}$, is 1 minute. One hundred scenarios are simulated

Table 5.1: Production Line Parameters: EP-BN Case Study

	m_1	m_2	m_3	m_4	m_5	m_6	m_7	m_8	m_9	m_{10}	m_{11}	m_{12}	m_{13}	m_{14}	m_{15}
$1/\tau$	2.5	1.3	1.7	1.2	1.8	1.5	2.1	0.9	0.5	1.2	2.3	1.6	1.9	2.4	1.7
MTTR	13	11	13	14	18	11	13	11	9	12	18	11	13	11	13
MCBF	250	270	300	350	325	205	245	250	200	265	350	200	280	275	400
e_j	89	95	93	95	91	93	90	96	97	94	89	91	91	91	94
P_{pp}	25	30	21	25	40	10	43	40	17	45	28	25	15	21	30
P_{id}	17.5	21	14.7	17.5	28	7	30.1	28	11.9	31.5	19.6	17.5	10.5	14.7	21
P_w	30	36	25.2	30	48	12	51.6	48	20.4	54	33.6	30	18	25.2	36
-	-	B2	B3	B4	B5	B6	B7	B8	B9	B10	B11	B12	B13	B14	B15
B_m	-	20	30	15	20	25	20	25	35	30	25	30	25	20	15

to test the effectiveness of the EP-BN against other commonly used industry metrics, such as diverting maintenance workers to the machine with the highest energy consumption. The energy profit bottleneck is found using (5.4), while other production data, such as buffer content, block/starve, etc is used to calculate the other indicators. The line is then run for another 8 hours with one machine having the downtime reduced based on the indicators as seen in Table 5.2, thus reducing the machine's MTTR by 10%. The profit is recorded for each case and compared to the baseline scenario when there is no decrease in any machine's

Table 5.2: Energy Profit Bottleneck Identifiers

Indicator	Avg. EC (kWh)	Avg. PC	% Reduction $SMPI_{DT}$	Avg. Profit Increase ($)
Baseline	10,174	589	-	-
EP-BN	10,175	618	**3.88%**	**$2,784.60**
Min e_j	10,211	593	0.34%	$414.53
Max EPP_j	10,183	590	0.09%	$109.93
Max $P_{pp,j}$	10,200	590	-0.12%	$75.33
Max EC_j	10,181	590	0.03%	$52.71

MTTR, which gives the average cost savings. The results are seen in Table 5.2 for the profit increase. As one can see, reducing the downtime of the EP-BN leads to the biggest average cost savings at $2,784.60 daily, which is approximately $2,300 more daily than any of the other indicators. These findings show how the EP-BN provides plant managers with a quantitative method that uses readily available sensor data to prioritize the maintenance of the machine that will lead to the most profit for the manufacturing facility.

5.3 Return on Investment Analysis

To improve energy efficiency in the long term, it is sometimes necessary to upgrade certain machines or parts to more energy efficient versions. Plant managers lack the proper quantitative tools to select which machine or part to replace with a machine or part that has a reduced energy consumption. When selecting a part or machine to replace it is imperative that the investment leads to the most energy cost savings. We utilize energy economic analysis to determine the machine or part which, when replaced, leads to the largest return on investment. We remove the assumptions of no backlog or inventory cost and reanalyze the

profit in the time period [0,T):

$$\begin{aligned} Profit &= TotalRevenue \ - \ TotalCost \\ &= PC(c_p) - E(c_e) - |PC - D|(c_d) - CTR_j^k, \end{aligned} \tag{5.16}$$

where PC is the production count, which is measured by sensor data. The energy consumption of the production line is represented by E. The production demand of the plant in the time period [0,T) is D and c_e and c_p are cost of energy per kWh and the profit per part respectively. We assume that the cost of energy is static throughout the day for ease of math representation. We also assume that the expenses to produce the part in terms of material and labor are already considered in the profit per part. The cost to replace, CTR_j^k, is included if machine j is replaced with a more energy efficient machine or a part k is replaced within machine j to reduce energy consumption. We will denote the case $k = 0$ as the scenario when the entire machine is being replaced. The third term represents the cost incurred if production is less than demand ($PC < D$), leading to a back log cost or if production is greater than demand ($PC > D$), leading to an inventory cost. The demand cost, c_d, is calculated by:

$$c_d = \begin{cases} c_b, & PC < D, \\ 0, & PC = D, \\ c_i, & PC > D, \end{cases}$$

where c_i is the cost of inventory per part and c_b is the back log cost per part. To study the effect of replacing a part or machine, we use Return on Investment (ROI) analysis. Return on investment is used in financial analysis to compare the efficiency of different investments. The ROI is the benefit of an investment (return) divided by the cost of the investment [68]. The formula for ROI is displayed in Eq. 5.17:

$$ROI = \frac{(Gain\ from\ investment - Cost\ of\ investment)}{Cost\ of\ investment}. \tag{5.17}$$

When replacing a part or machine, the cost of investment is the cost to replace the machine j or a part k within machine j (CTR_j^k). The cost to replace is represented by:

$$CTR_j^k = Part\ Cost + Maintenance\ Cost + PPL\ Cost, \tag{5.18}$$

where the $Part\ Cost$ is the cost of the part or machine that is being replaced: $Part\ Cost = c_{rep,j}^k$. The $Maintenance\ Cost$ is represented by:

$$Maintenance\ Cost = N_{m,j}^k t_{R,j}^k c_{Main,j}, \tag{5.19}$$

where $N_{m,j}^k$ is the number of maintenance workers required at machine j to replace part k, $t_{R,j}^k$ is the time it takes to replace part k at machine j in hours, and $c_{Main,j}$ is the cost per hour for each maintenance person. The maintenance cost per person per hour depends if the maintenance is performed during a regular shift ($C_{Reg,j}$) or within an overtime shift ($C_{OT,j}$):

$$c_{Main,j} = \begin{cases} C_{Reg,j}, & during\ regular\ shift, \\ C_{OT,j}, & during\ overtime\ shift, \end{cases}$$

The last term in Eq. (5.18) is the permanent production loss cost. If the maintenance repair time ($t_{R,j}^k$) is longer than the opportunity window when the repair is being performed then there is production loss. If the maintenance is performed within the opportunity window duration then there is no cost due to permanent production loss. Therefore, the permanent production loss cost is represented by:

$$PPL\ Cost = \begin{cases} c_p(t_{R,j}^k - d_i^*)\frac{1}{\tau_{M^*}}, & t_{R,j}^k > d_i^*, \\ 0, & t_{R,j}^k \leq d_i^*, \end{cases}$$

The gain from the investment is the energy cost savings from replacing a part or the entire machine, which reduces the power consumption of machine j by an amount $\Delta P_{pp,j}$.

Therefore, the energy savings, ΔE_j^k, in the time period [0,T) is:

$$\Delta E_j^k = \Delta P_{pp,j}\left[T - \sum_{k=1}^{\eta_j}[d_k - (1+\beta_j)t_{w,j}^k] - (1-\alpha_j)T_{id,j}\right]. \tag{5.20}$$

Thus, the gain from investment is calculated in Eq. 5.21:

$$Gain\ from\ investment = c_e \Delta E_j^k, \tag{5.21}$$

and the return on investment in the time period [0,T) for replacing machine j or part k within machine j is:

$$ROI_j^k = \frac{(c_e \Delta E_j^k - CTR_j^k)}{CTR_j^k}. \tag{5.22}$$

Therefore, replacing a part within machine j or replacing the entire machine with a more energy efficient version (reducing $P_{pp,j}$ by an amount $\Delta P_{pp,j}$) will lead to the largest return on investment in [0,T) if:

$$ROI_j^k > ROI_z^k, \quad \forall z \neq j. \tag{5.23}$$

This analysis can be applied to any time period [0,T). By utilizing the ROI, the manager can select the machine or part with the largest return on investment for any time period. Another important identifier in economic analysis is the break-even point, which is the point at which the cost and the revenue are equal. This term uses return on investment to study how quickly the investment leads to a net gain in profit. In this scenario, this is the point when the energy cost saved is equivalent to the cost to replace the part or machine. Therefore, the expected number of days it takes for the investment to break even (BE) is:

$$BE_j^k = \frac{CTR_j^k}{c_e \overline{\Delta E}_j^k}, \tag{5.24}$$

where BE_j^k is the expected number of days it takes for the cost to replace part k within machine j to equal the energy cost savings at machine j. The average energy savings per

day is $\overline{\Delta E}_j^k$. It is important to note that the machine with the maximum ROI_j^k will always have the smallest BE_j^k for the time period [0,T). The BE_j^k gives an alternative indicator to illustrate the investment of replacing a machine or a part within the machine. These indicators provide the plant manager with the quantitative tools to select the machine or part which, when replaced, leads to the largest return on investment based on energy cost savings. While this method is useful in the long term, there still needs to be a control methodology to reduce overall energy consumption on a daily basis. This is addressed in the next section.

5.4 Case Study

To improve the energy efficiency on a daily basis, we introduce a control methodology to insert downtime events which lower energy consumption with minimal throughput impact. This leads to the largest increase in profit for the plant. We utilize the concept of the energy opportunity window to insert $\eta_{OW,j}$ number of downtime events each for a length of $t_{OW,j}$ at machine j, $j = 1, 2, ..., M$. This allows for various machines to be strategically turned off without affecting the overall throughput of the line and thus reducing energy consumption. The energy consumption of the production line with the inserted downtime events is represented by:

$$E = \sum_{j=1}^{M} P_{pp,j} \left[T - \sum_{k=1}^{\eta_j} d_k - \sum_{k=1}^{\eta_j + \eta_{OW,j}} (1 + \beta_j) t_{w,j}^k - \eta_{OW,j} t_{OW,j} - (1 - \alpha_j) T_{id,j} \right]. \tag{5.25}$$

To maximize the profit of the production facility in the period [0,T), it is necessary to select the length of the inserted opportunity windows ($t_{OW,j}$) and the number of opportunity windows ($\eta_{OW,j}$) at each machine:

$$\max_{\substack{\eta_{OW,j} \\ t_{OW,j} \\ j=1,2,...,M}} \quad Profit. \tag{5.26}$$

The profit equation is displayed in Eq. 5.16, where E is calculated from Eq. 5.25 and PC is found using production data. The demand is calculated by either external customer demand or by an internal standard if a certain level of inventory must be maintained. If the inserted energy opportunity window at machine j is too large, i.e. $t_{OW,j} > d_i^*$, it will lead to the slowest machine idling from being starved/blocked, thus leading to permanent production loss. Therefore, the inserted opportunity window must be less than d_i^*. If the energy opportunity window is too small, more energy will be consumed while the machine warms up than energy saved from turning off machine j. This results in a greater energy cost, which leads to the lower bound of $t_{OW,j}$:

$$\begin{aligned} t_{OW,j} P_{id,j} &> E[t_{w,j}^i] P_{w,j} \\ t_{OW,j} &> \frac{\omega_j \beta_j}{\alpha_j}. \end{aligned} \tag{5.27}$$

Thus, the length of the inserted opportunity window is bounded by:

$$\frac{\omega_j \beta_j}{\alpha_j} < t_{OW,j} < d_i^*, \quad j = 1, 2, ..., M, \quad i = 1, ..., \eta_{OW,j}. \tag{5.28}$$

This provides the bounds for $t_{OW,j}$, where the energy saved from the opportunity window must be larger than the expected energy consumed during the machine warm up period and must be less than the calculated opportunity window at that time.

The control methodology allows the buffer levels to reach a certain threshold ($B_{0,j}$) before taking the opportunity window and then turning the machine back on after $t_{OW,j}$. The pseudo code for the control algorithm is displayed below:

1. *Begin shift*
2. *Collect pertinent data from buffer levels and machine states*
3. *If* $b_j = B_{0,j}$, $\forall j < M^*$ *turn off machine* $j-1$ *for* $t_{OW,j-1}$.

(a) *After* $t_{OW,j-1}$ *turn on machine* $j-1$

4. *If* $b_j \neq B_{0,j}$, $\forall j < M^*$, *go to step 5*

5. *If* $b_j = B_{0,j}$, $\forall j > M^*$ *turn off machine* j *for* $t_{OW,j}$.

   (a) *After* $t_{OW,j}$ *turn on machine* j

6. *If* $b_j \neq B_{0,j}$, $\forall j > M^*$ *return to step 2.*

The control methodology is illustrated in Fig. 5.1. The buffer threshold, $B_{0,j}$, depends on a specific scenario for each production line. Based on our simulation studies and experience, we normally determine the threshold to be approximately 95% of the buffer capacity. In this specific example as shown in Fig. 5.1, the threshold $B_{0,j}$ is determined to be 50 parts, which is 95% of the buffer capacity. Once the buffer level reaches the threshold the machine is switched off for a period of 25 minutes and then it is switched back on. From our previous research, we found that $t_{OW,j}$ is approximately 95% of the upper bound. This pattern is repeated until the end of the shift. This example also displays a random disruption event approximately 350 minutes into the shift. When the machine is switched on after the inserted opportunity window, it experiences a random failure, thus causing the buffer level to take longer to reach the 50 part threshold. By following this control scheme, the risk of production loss is lowered for the manufacturing line. To solve for the length and number of inserted downtime events for each machine, an exhaustive search algorithm is utilized to maximize profit for the line. The results are shown in the simulation case study.

A real automotive production line composed of 15 machines and 14 buffers is adopted for the case study to further demonstrate the return on investment analysis. The system parameters are recorded from the real production data and are mocked up for confidential reasons. The mean time to repair (MTTR) and the mean cycles between failure (MCBF) are assumed to be exponentially distributed based on this real data. The production parameters are shown

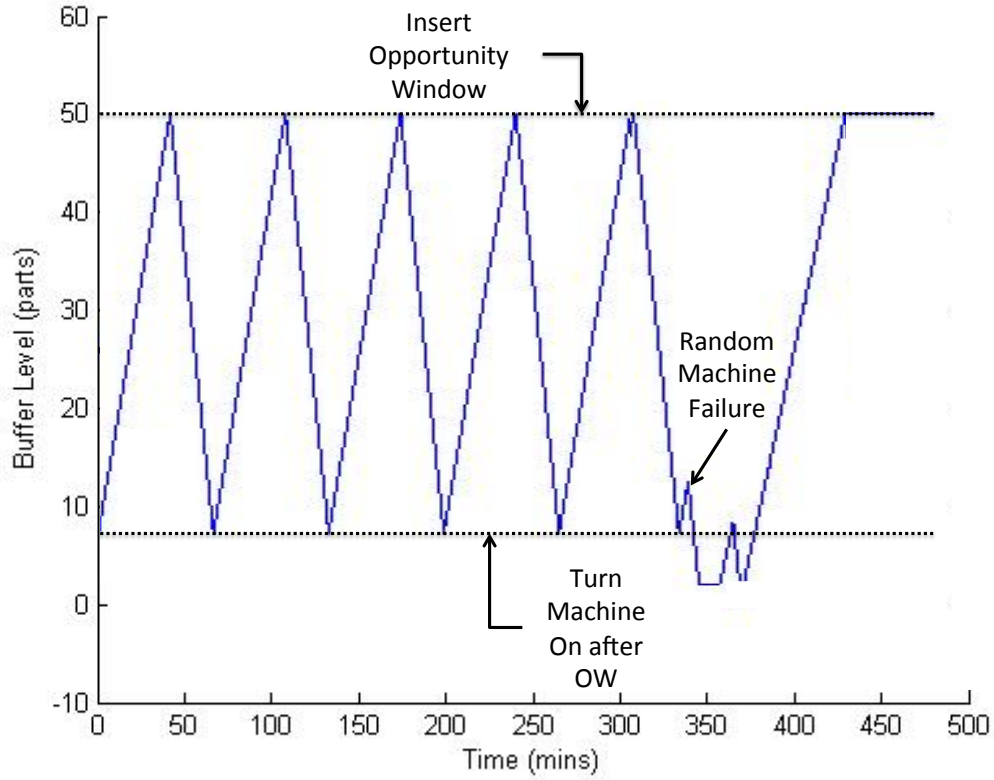

Figure 5.1: Control Methodology Buffer Thresholds

Table 5.3: Production Line Parameters: ROI Case Study

	m_1	m_2	m_3	m_4	m_5	m_6	m_7	m_8	m_9	m_{10}	m_{11}	m_{12}	m_{13}	m_{14}	m_{15}
$1/\tau$ (p/m)	2.5	1.3	1.7	1.2	1.8	1.5	2.1	0.9	0.5	1.2	2.3	1.6	1.9	2.4	1.7
MTTR (min)	13	11	13	14	18	11	13	11	9	12	18	11	13	11	13
MCBF (cyc)	250	270	300	350	325	205	245	250	100	265	350	200	280	275	400
Efficiency (%)	89	95	93	95	91	93	90	96	95	94	89	92	92	91	94
P_{pp} (kW)	25	30	21	25	40	10	43	40	17	45	28	25	15	21	30
Buffer	-	B_2	B_3	B_4	B_5	B_6	B_7	B_8	B_9	B_{10}	B_{11}	B_{12}	B_{13}	B_{14}	B_{15}
Capacity	-	20	30	15	20	25	20	25	35	30	25	30	25	20	15

in Table 5.3. The idle power is assumed to be 70% ($\alpha_j = 0.7$) of the power consumed during the production of parts and the warm up power is assumed to be 90% ($\beta_j = 0.9$) of the power consumed during the production of parts for each machine. The mean time to warm up time after the i^{th} downtime event is 1 minute ($\omega_j = 1$ min). The cost of energy is $\$0.14/kWh$ and the profit per part is \$50 per part. To test the return on investment strategy, three

Table 5.4: Economic Analysis

Option 1	m_1	m_2	m_3	m_4	m_5	m_6	m_7	m_8	m_9	m_{10}	m_{11}	m_{12}	m_{13}	m_{14}	m_{15}
ΔP_{pp} (kW)	1	2	2	2	2	1	4	2	2	3	2	2	1	2	2
CTR (\$)	1.2k	2.2k	2.1k	3.6k	2.1k	1.1k	4.1k	2.9k	4.6k	4.9k	2.4k	2.2k	1.1k	2.2k	2.3k
Option 2	m_1	m_2	m_3	m_4	m_5	m_6	m_7	m_8	m_9	m_{10}	m_{11}	m_{12}	m_{13}	m_{14}	m_{15}
ΔP_{pp} (kW)	1	2	2	2	2	1	4	2	2	3	2	2	1	2	2
CTR (\$)	1.5k	2.5k	2.4k	2.7k	2.2k	1.4k	4.2k	2.2k	2.2k	3.3k	2.3k	2.4k	1.2k	2.5k	2.6k
Option 3	m_1	m_2	m_3	m_4	m_5	m_6	m_7	m_8	m_9	m_{10}	m_{11}	m_{12}	m_{13}	m_{14}	m_{15}
ΔP_{pp} (kW)	7	10	5	7	10	2	12	9	5	11	5	7	4	3	8
CTR (\$)	23k	35k	21k	37k	23k	37k	49k	34k	20k	60k	23k	36k	25k	28k	35k

options are presented: option 1 is the scenario where a machine part is replaced with a more energy efficient version during a regular production shift, option 2 is the case where the same part is replaced, but during an overtime shift when there is no production, and option 3 is the situation when the entire machine is replaced with a more energy efficient version. We assume that $C_{Reg,j}$ is \$70 per hour and $C_{OT,j}$ is \$140 per hour for each machine. We also manage the replacement of the part during a regular shift when the machine has its maximum opportunity window therefore limiting production loss. The parameters for each option are shown in Table 5.4. The CTR is in thousands of dollar, i.e. 5k = \$5,000. We utilize Eq. 5.24 to calculate the expected number of days the investment will break even and then compare that with the simulation break even point for the investment. The results are shown in Fig. 5.2-5.4. The diamonds represent the theoretical break even point calculated with Eq. 5.24. The squares are the break even points from the simulation for each option. The results illustrate that the simulation break even point is within 10% error (as shown with the error bars) for each option and each machine. The best option is replacing a part during an overtime shift (option 2) for machine 9, which leads to an expected break even point of 997 days, while the simulation study is 951 days. The next section will use this return on investment analysis in conjunction with the opportunity window control scheme to maximize profits for the production line.

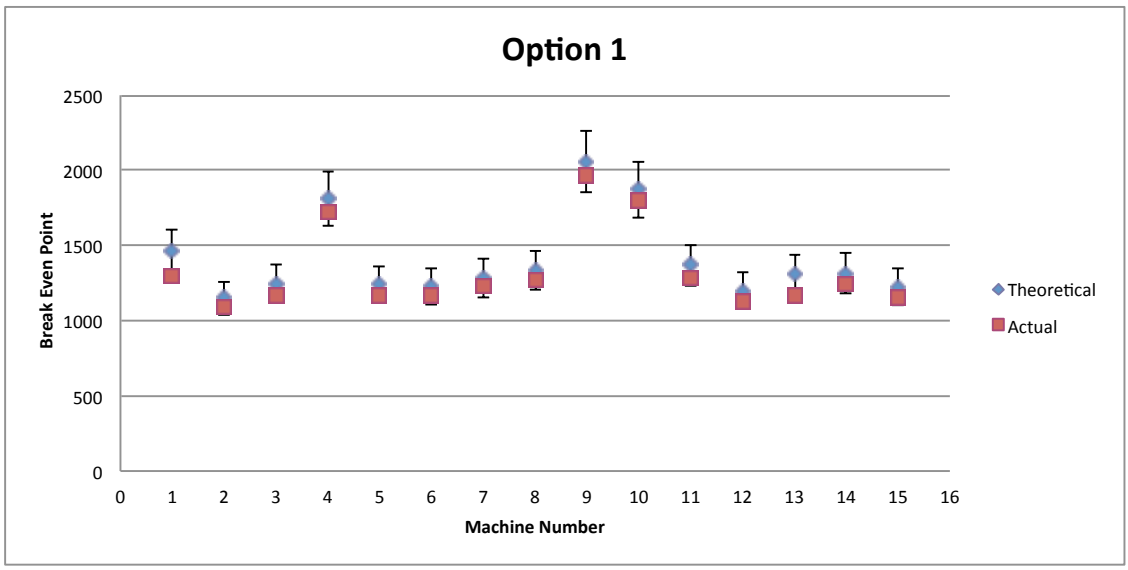

Figure 5.2: Break Even Results - Option 1

5.4.1 Opportunity Window Control Numerical Study

This study uses the same production line as seen in Table 5.3. The return on investment strategy is utilized in conjunction with the control methodology. The cost of energy is still $\$0.14/kWh$ and the profit per part is still \$50 per part. The back log cost, c_b, is \$15 per part and the inventory cost, c_i, is \$5 per part. The production line is run for a 5 year time period, assuming one 8 hour shift per day, with no opportunity window control methodology and no machines or parts replaced with upgraded versions. The profit for this 5 year period is calculated and recorded as the baseline scenario. One part in machine 9 is then replaced based on the break even and return on investment analysis as shown in Table 5.4. The opportunity window control methodology is then used and the line is simulated for another 5 year period with a part from machine 9 having been replaced with a more energy efficient version (2 kW reduced power consumption). The results are recorded and compared with the baseline scenario. Figure 5.5 displays the production count of the baseline scenario versus the control scenario. The demand is 230 parts per day, which is 83,950 parts per year, which is met by both the control and baseline situations. The baseline scenario produces 18,250

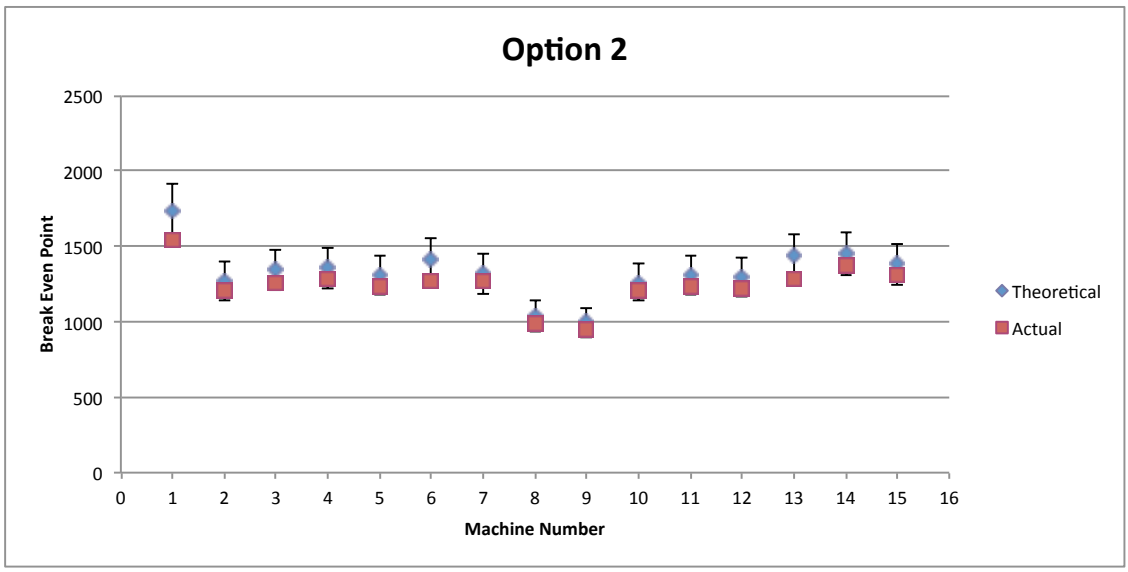

Figure 5.3: Break Even Results - Option 2

parts over the demand of the facility, while the control scenario produces 16,263 parts more than the demand. By reducing the number of parts produced past the demand threshold in the control scenario and replacing a part within machine 9, the overall energy consumption decreases by 1,519,404 kWh. Thus, running the opportunity window control scheme while replacing a part within machine 9 leads to a decreased energy consumption with no impact to the production demand. This leads to an overall profit increase of $121,107.364 over five years as displayed in Fig. 5.6.

5.5 Conclusions

This chapter investigates the energy economics of a manufacturing facility. The profit of the production plant is explored to include both production and energy costs. The energy dynamics of the production system are studied and incorporated into an energy economic analysis. Building on this analysis, the Energy Profit Bottleneck (EP-BN) is introduced and proven both analytically and numerically. This provides a method to correctly identify the machine that is causing the biggest loss in profit due to a lower production count and a high

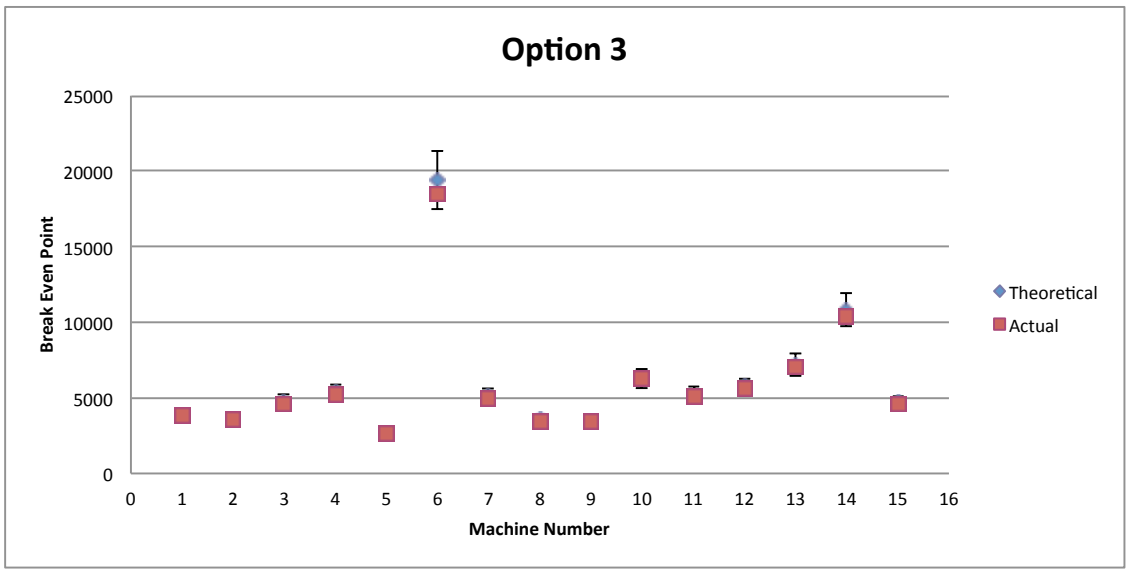

Figure 5.4: Break Even Results - Option 3

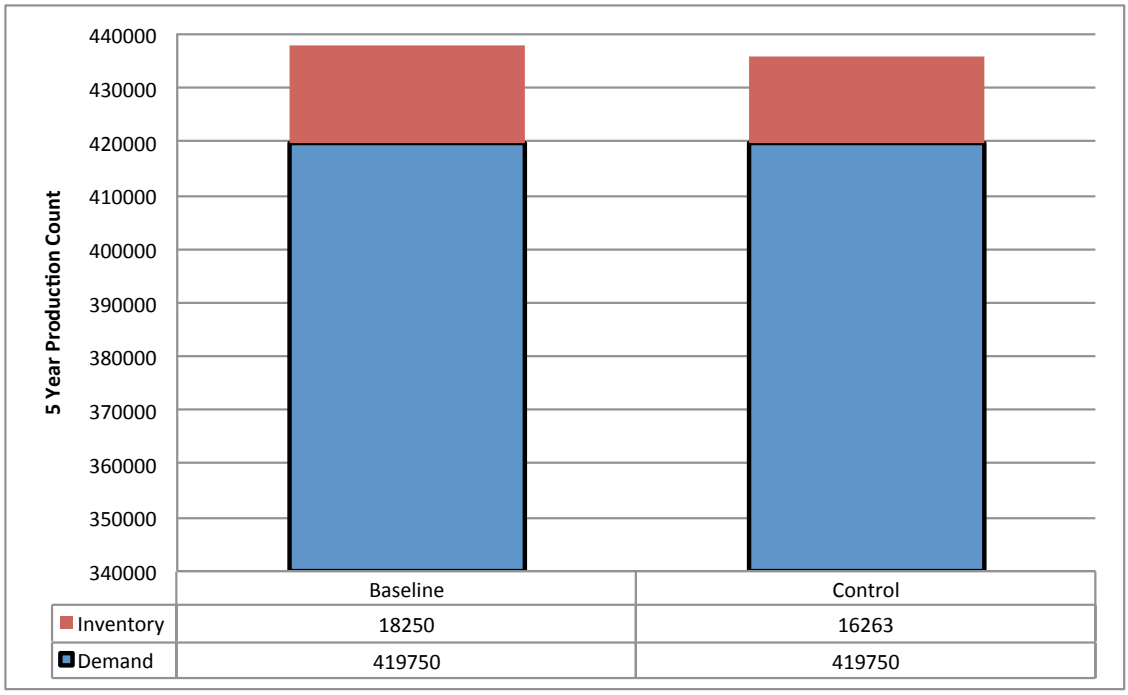

Figure 5.5: 5 Year Production Count

energy consumption. This directly leads to the return on investment analysis and break-even point for investing money into replacing a part or machine with a more energy efficient version. The analysis provides the plant manager with the quantitative tools to increase

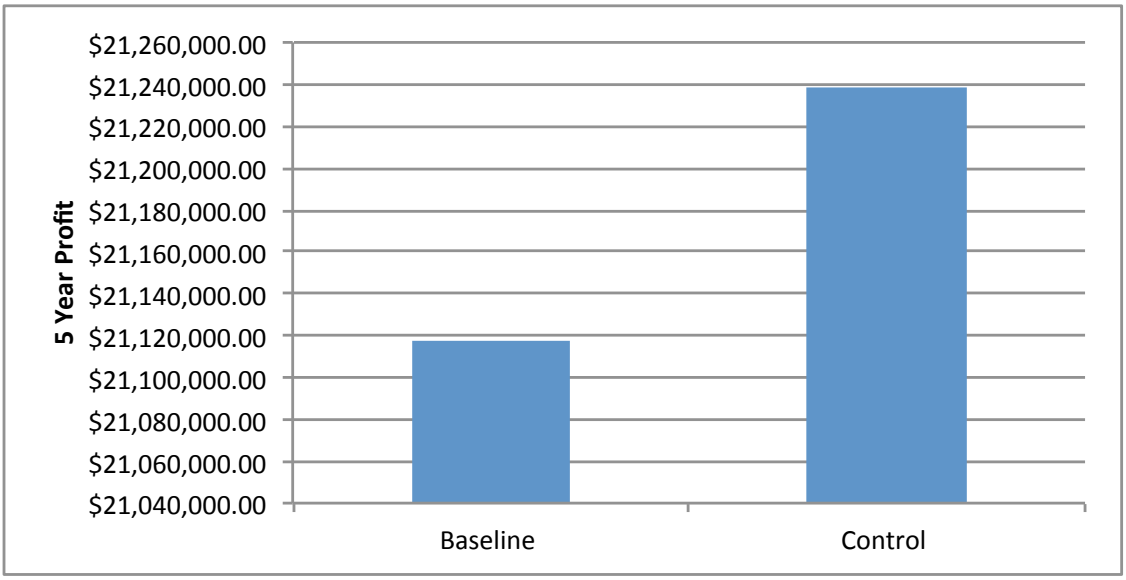

Figure 5.6: 5 Year Profit

profit in the long term by replacing the machine or part which will lead to the largest return on investment. To increase profit on a daily basis, a control methodology is introduced that utilizes inserted opportunity windows to reduce overall energy consumption with minimal throughput impact. A case study is performed to validate the energy economic method in conjunction with the opportunity window control scheme.

Chapter 6

Control Methodology

6.1 Introduction

The control methodology from the previous chapter is expanded to increase profit in a given time horizon [0,T). Previous studies have utilized supervisory control methods that mitigate throughput bottlenecks [18]. This control scheme combines bottleneck mitigation for the EP-BN as well as an opportunity window control methodology to decrease energy consumption while minimizing throughput loss. The feedback control diagram can be seen in Fig. 6.1. To maximize the profit of the production line, we must select the length of each opportunity

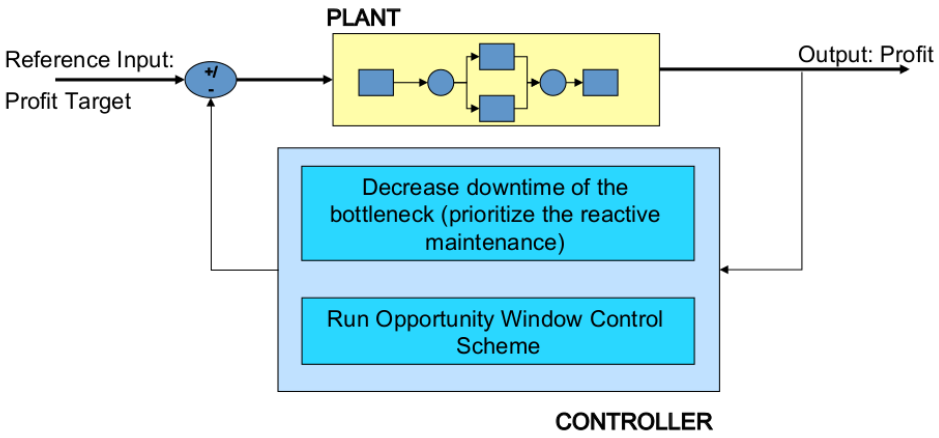

Figure 6.1: Control Diagram to Maximize Profit

window (t_{OW}), the length of the recovery time between each energy opportunity window (t_r), and the machine to reduce downtime (δd) such that we maintain a certain production threshold (PC_0):

$$\max_{\substack{t_{OW} \\ t_r \\ \delta d}} Profit, \quad s.t.\ PC \geq PC_0 \tag{6.1}$$

To achieve this goal, the overall control methodology is presented as follows:

1. Collect pertinent production data and determine which machine is the EP-BN for the day.
2. Reduce downtime (δd) of the EP-BN by prioritizing maintenance staff on the EP-BN.
3. Initialize t_{OW} and t_r based on the numerical study.
4. Run opportunity window control algorithm presented in Fig. 6.2 for period of [0,T).
5. If Production Count or Profit are below thresholds, recalculate t_{OW} and t_r based on the steps below:
   (a) If Production Count and Profit are below thresholds, reduce t_{OW} and t_r, & return to Step 4.
   (b) If Production Count is above the threshold, but the Profit is below the threshold, increase t_{OW} and reduce t_r, & return to Step 4.
   (c) If Production Count is below the threshold, but the Profit is above the threshold, reduce t_{OW} and increase t_r, & return to Step 4.
6. If Production Count and Profit are above desired values, reuse same values for t_{OW} and t_r & return to Step 4.

Numerical studies are performed to provide guidance for the initial selection of t_r and t_{OW}. The recovery time, t_r, is the amount of time between subsequent opportunity windows while the system recovers. The variable t_{OW} is the amount of time the machine is turned off during the opportunity window. The variable t_{OW} is a certain percentage of the maximum opportunity window, d_i^*. The method presented in Section IV is used to identify the EP-BN for the day. Once the EP-BN is identified, the downtime at that machine is reduced. This bottleneck mitigation is combined with an opportunity window control scheme, which

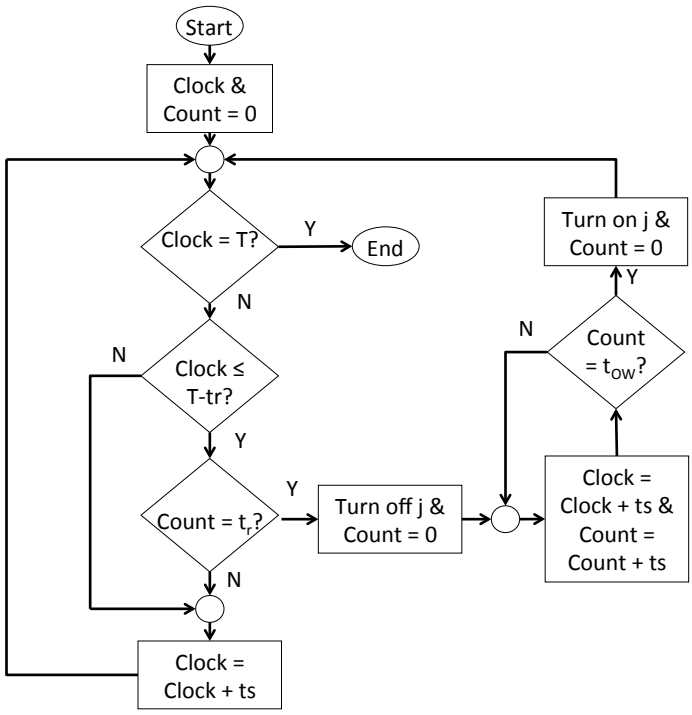

Figure 6.2: Opportunity Window Control Flow Chart for Machine j

is presented for machine j in Fig. 6.2. Every machine on the line will run the same algorithm, however the parameters will vary for each machine. It is important to find a rule for selecting the control parameters t_{OW} and t_r in a stochastic scenario. Since this is very difficult, if not impossible, to study analytically, numerical studies are necessary. Studies are performed to find the optimal percentage of t_r based on the analysis of the recovery time in a deterministic scenario, T_r, when taking successive opportunity windows. A numerical study is also performed to find the duration and frequency of the opportunity window in a stochastic scenario.

6.2 Numerical Studies for Control Parameters

The numerical studies for the control parameters utilize 1000 different line combinations to find guidance in selecting the parameters t_r and t_{OW}. The simulation utilizes a 6 Machine, 5 Buffer line. To create the 1000 simulations, the rated speed, $\frac{1}{\tau_j}$, the efficiency, e_j, and the

buffer capacity, B_m, are selected randomly and with equal probability from the following sets:

$$\frac{1}{\tau_j} \in \{3, 4, 5, 6\} \quad j = 1, ..., M$$

$$e_j \in \{0.70, 0.75, 0.80, 0.85, 0.90, 0.95, 1.00\} \quad j = 1, ..., M$$

$$B_m \in \{50, 70, 100\} \quad m = 2, ..., M.$$

6.2.1 Recovery Time

In order to have an effective feedback control scheme for the production line, it is necessary to find the appropriate recovery time for each machine so that successive opportunity windows can be taken with minimal throughput impact. It is important to find the smallest possible value of recovery time to allow for the maximum number of opportunity windows.

Numerical Fact 6.1: *To reduce the permanent production loss of the production line, the range of recovery time, t_r, is in practice between 150% and 200% of the value based on the upper bound of the deterministic scenario, T_r.*

Justification: From the 1000 simulations, 25 different line combinations ranging from Line 1A - Line 5E are shown in this dissertation. In Lines 1-5 the efficiency of the machines are changed, while in Lines A-E the rated speed of the machines are varied. For example, Line 1A will have the efficiencies presented in Line 1 and the machine speeds from Line A. The different lines can be seen in Table 6.1. For these 25 scenarios, each buffer has a capacity of 100 parts and the simulation is run for one 8 hour shift per day. The recovery time is calculated using the method presented in Eqn (3.3) and (3.4) for the deterministic case. The upper bound of the recovery time for a deterministic scenario, T_r is a fixed length for machine j after machine j takes its maximum opportunity window d_i^*. The deterministic

Table 6.1: Recovery Time Simulations

Line 1	m_1	m_2	m_3	m_4	m_5	m_6
$Efficiency(\%)$	95.00	95.00	95.00	95.00	95.00	95.00
Line 2	m_1	m_2	m_3	m_4	m_5	m_6
$Efficiency(\%)$	85.00	85.00	90.00	95.00	90.00	85.00
Line 3	m_1	m_2	m_3	m_4	m_5	m_6
$Efficiency(\%)$	95.00	95.00	90.00	85.00	90.00	95.00
Line 4	m_1	m_2	m_3	m_4	m_5	m_6
$Efficiency(\%)$	70.00	75.00	80.00	85.00	90.00	95.00
Line 5	m_1	m_2	m_3	m_4	m_5	m_6
$Efficiency(\%)$	100.00	95.00	95.00	90.00	90.00	85.00
Line A	m_1	m_2	m_3	m_4	m_5	m_6
s_j (parts/mins)	4.00	5.00	6.00	3.00	6.00	5.00
Line B	m_1	m_2	m_3	m_4	m_5	m_6
s_j (parts/mins)	4.00	5.00	4.00	3.00	4.00	5.00
Line C	m_1	m_2	m_3	m_4	m_5	m_6
s_j (parts/mins)	5.00	4.00	5.00	3.00	5.00	4.00
Line D	m_1	m_2	m_3	m_4	m_5	m_6
s_j (parts/mins)	6.00	5.00	4.00	3.00	4.00	5.00
Line E	m_1	m_2	m_3	m_4	m_5	m_6
s_j (parts/mins)	4.00	4.00	4.00	3.00	4.00	4.00

upper bound for the recovery time, T_r can be evaluated as follows:

$$T_r(j, d_i^*) = \begin{cases} \frac{\sum_{k=j+1}^{M^*}(B_k)}{min\{\frac{1}{\tau_1},\ldots,\frac{1}{\tau_{M^*-1}}\}-\frac{1}{\tau_{M^*}}}, & j < M^* \\ 0, & j = M^* \\ \frac{\sum_{k=M^*+1}^{j}(B_k)}{min\{\frac{1}{\tau_{M^*+1}},\ldots,\frac{1}{\tau_M}\}-\frac{1}{\tau_{M^*}}}, & j > M^*. \end{cases}$$

This value is based on a deterministic scenario and will be examined in the stochastic situation by multiplying by a percentage ranging from 25% to 600% to see how much recovery time needs to be allotted such that the permanent production loss is minimized when successive opportunity windows are taken. In each simulation, the full opportunity window is exercised followed by a certain percentage of T_r. The results for all 1000 lines can be seen

below in Table 6.2. The results for Lines 1A-1E can be seen in Fig. 6.3. The remaining line

Table 6.2: Recovery Time Results

% t_r	25	50	75	100	125	150
PPL	45.95%	34.62%	19.90%	15.66%	11.12%	4.95%
% t_r	175	200	225	250	275	300
PPL	4.05%	3.81%	3.84%	2.97%	3.36%	2.96%
% t_r	325	350	375	400	425	450
PPL	2.66%	2.09%	1.55%	1.23%	1.30%	1.09%
% t_r	475	500	525	550	575	600
PPL	0.85%	0.97%	1.27%	1.42%	1.08%	1.04%

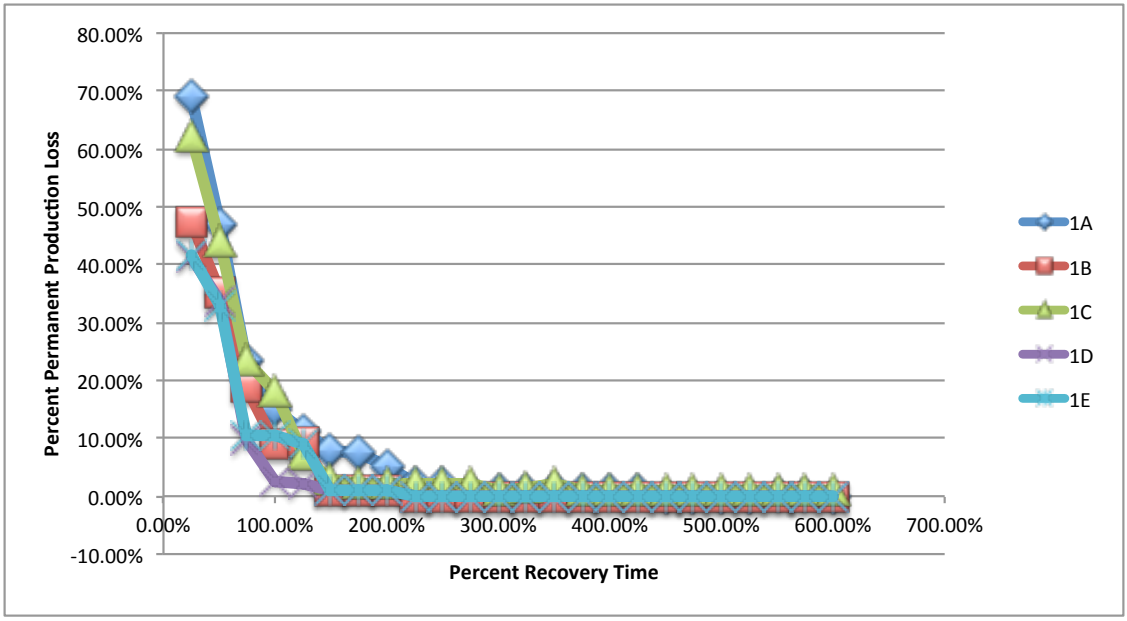

Figure 6.3: Recovery Time Lines 1A-1E

combinations can be found in Appendix B in Fig. B.1-B.4. The numerical study shows that the optimal amount of recovery time to allow between opportunity windows is between 150% and 200% of the deterministic upper bound of recovery time, T_r. Obviously, there is still some permanent production loss shown in this study, since inserting opportunity windows can be treated as inserting disturbances into the system. We are interested in finding a

scenario that allows for less than a 5% production loss. This is analogous to the settling time of a dynamic system. The settling time is defined as the time required for the response curve to reach and stay within a range of a certain percentage of the final value [69]. After taking an opportunity window, it is necessary to find the smallest recovery time that allows the production system to recover within 5% of the throughput when no opportunity window is utilized. This numerical study found that this recovery time is between 150% and 200% of T_r.

6.2.2 Length of the Opportunity Window

To find guidance for the variable t_{OW}, the same 1000 lines are run for one 8 hour shift per day for a one month period. The parameters t_{OW} and t_r are chosen randomly and with equal probability from the following sets:

$$t_{r,j} \in \{1.50, 1.60, 1.70, 1.80, 2.0\} \times T_r \quad j = 1, ..., M$$
$$t_{OW,j} \in \{0.30, 0.50, 0.70, 0.90, 0.95, 1.0\} \times d_i^* \quad j = 1, ..., M,$$

where d_i^* is the largest opportunity window of machine j. To find the baseline case, the control methodology is not utilized: there is no opportunity window control and the EP-BN is not mitigated. Next, the opportunity window control scheme is used for each machine in the production line, however the EP-BN is still not mitigated so that the focus is on t_{OW}. Ten scenarios are shown in this dissertation to illustrate the numerical findings. The recovery time is 150% of T_r for Scenarios 1-5 and 200% of T_r for Scenarios 6-10 which follows the numerical findings in the previous section. These scenarios can be seen in Table 6.3. The production throughput is recorded and compared with the baseline case and the results are presented in Fig. 6.4.

Fig. 6.4 shows that the lowest throughput loss is realized in Scenario 6 where t_{OW} is approximately 95% of d_i^*. From the analysis of all 1000 lines, it is found that taking the

Table 6.3: Opportunity Window Parameters

Scenario 1	m_1	m_2	m_3	m_4	m_5	m_6
t_{OW} (mins)	51.15	34.65	21.45	0	23.10	41.25
t_r(mins)	206.67	140.00	86.67	0	93.33	166.67
Scenario 2	m_1	m_2	m_3	m_4	m_5	m_6
t_{OW} (mins)	46.04	31.19	19.31	0	20.79	37.13
t_r(mins)	206.67	140.00	86.67	0	93.33	166.67
Scenario 3	m_1	m_2	m_3	m_4	m_5	m_6
t_{OW} (mins)	46.04	27.72	15.02	0	16.17	33.00
t_r(mins)	206.67	140.00	86.67	0	93.33	166.67
Scenario 4	m_1	m_2	m_3	m_4	m_5	m_6
t_{OW} (mins)	35.81	27.72	19.31	0	20.79	33.00
t_r(mins)	206.67	140.00	86.67	0	93.33	166.67
Scenario 5	m_1	m_2	m_3	m_4	m_5	m_6
t_{OW} (mins)	18.08	19.60	17.55	0	18.90	23.33
t_r(mins)	206.67	140.00	86.67	0	93.33	166.67
Scenario 6	m_1	m_2	m_3	m_4	m_5	m_6
t_{OW} (mins)	46.04	31.19	19.31	0	20.79	37.13
t_r(mins)	155.00	105.00	65.00	0	70.00	125.00
Scenario 7	m_1	m_2	m_3	m_4	m_5	m_6
t_{OW} (mins)	48.59	32.92	20.38	0	21.95	39.19
t_r(mins)	155.00	105.00	65.00	0	70.00	125.00
Scenario 8	m_1	m_2	m_3	m_4	m_5	m_6
t_{OW} (mins)	38.36	29.45	20.38	0	21.95	35.06
t_r(mins)	155.00	105.00	65.00	0	70.00	125.00
Scenario 9	m_1	m_2	m_3	m_4	m_5	m_6
t_{OW} (mins)	43.48	31.19	20.38	0	21.95	37.13
t_r(mins)	155.00	105.00	65.00	0	70.00	125.00
Scenario 10	m_1	m_2	m_3	m_4	m_5	m_6
t_{OW} (mins)	46.50	33.25	21.45	0	23.1	39.58
t_r(mins)	155.00	105.00	65.00	0	70.00	125.00

opportunity window less frequently for a longer duration and then waiting enough time for the system to recover results in a smaller throughput loss as opposed to taking it more frequently for a shorter duration.

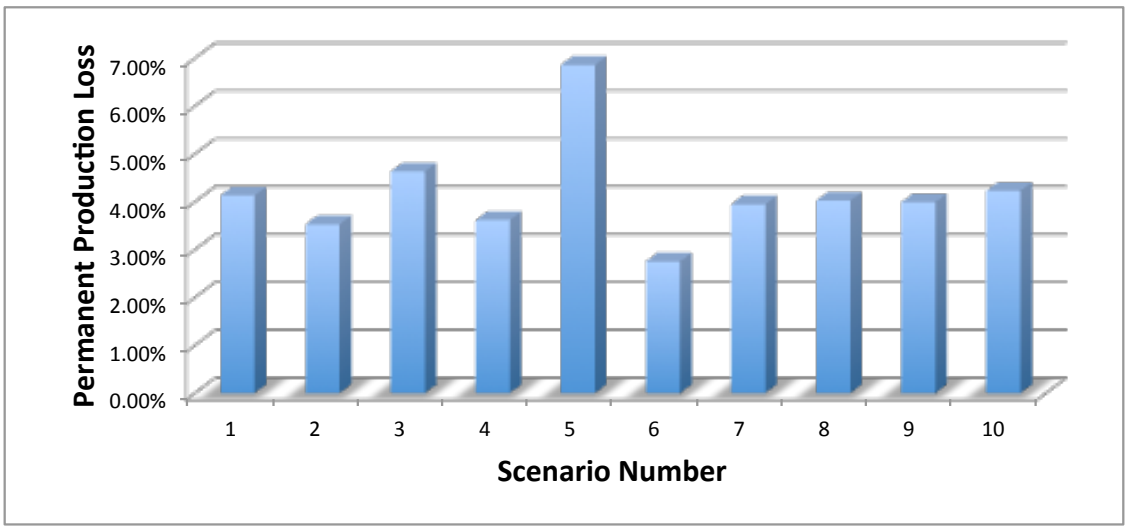

Figure 6.4: Frequency and Length of Opportunity Window Scenarios

6.3 Case Study

The system analyzed for the case study is composed of 15 Machines and 14 Buffers, which is based on a portion of an engine block line. The system parameters are recorded from the real production line and the mocked data is shown for confidential consideration and is shown in Table 6.4. The time step for this simulation is $ts = 0.005$ min. The MTTR and the MCBF are assumed to be exponentially distributed based on the observed production data. The profit of each part, is assumed to be c_p is \$100 per part based on the real value after it is mocked up for confidential reasons and the cost of energy, c_e is assumed to be [67]:

$$c_e^l(t) = \begin{cases} \$0.08, & 00:00 \leq t < 06:00, \\ \$0.14, & 06:00 \leq t < 11:00, \\ \$0.24, & 11:00 \leq t < 19:00, \\ \$0.14, & 19:00 \leq t \leq 23:59. \end{cases}$$

The mean warm up time of each machine, ω_j, is 1 minute. The production line is run for one 8 hour shift per day for a one month period without utilizing the control methodology presented. This is established as the baseline case. For the EP-BN mitigation, the pertinent

Table 6.4: Production Line Parameters: Control Case Study

	m_1	m_2	m_3	m_4	m_5	m_6	m_7	m_8	m_9	m_{10}	m_{11}	m_{12}	m_{13}	m_{14}	m_{15}
$1/\tau$	2.5	1.3	1.7	1.2	1.8	1.5	2.1	0.9	0.5	1.2	2.3	1.6	1.9	2.4	1.7
MTTR	13	11	13	14	18	11	13	11	9	12	18	11	13	11	13
MCBF	250	270	300	350	325	205	245	250	200	265	350	200	280	275	400
e_j	89	95	93	95	91	93	90	96	97	94	89	91	91	91	94
P_{pp}	25	30	21	25	40	10	43	40	17	45	28	25	15	21	30
P_{id}	17.5	21	14.7	17.5	28	7	30.1	28	11.9	31.5	19.6	17.5	10.5	14.7	21
P_w	30	36	25.2	30	48	12	51.6	48	20.4	54	33.6	30	18	25.2	36
-	-	B2	B3	B4	B5	B6	B7	B8	B9	B10	B11	B12	B13	B14	B15
B_m	-	20	30	15	20	25	20	25	35	30	25	30	25	20	15

data is recorded and the EP-BN machine is identified for the day. The production line is then run by reducing the previous day's EP-BN's MTTR by 10% and utilizing the presented control scheme. If there is a decrease in profit from the baseline case with no control or there is more than a 5% loss in production count, the control variables are varied by changing t_{OW} or t_r by 5%. The results can be seen below in Table 6.5 with 95% confidence interval included. By using the control methodology and mitigating the EP-BN daily there is an increase of profit of \$9,431.12. The average production count for the baseline case is 234 parts per day, while for the monthly bottleneck and opportunity window control case it is 236 parts per day. This is equivalent to a 1.0% production count increase daily. By using the control methodology with daily EP-BN mitigation there is a savings of 716.74 kWh per day. Another important result of utilizing the control methodology is the decrease of energy waste for the production line. The $SMPI_{DT}$ is recorded daily for the baseline case and is compared to the control scenario with the EP-BN mitigation in Fig. 6.5. The daily EP-BN mitigation saves an average of 45% of energy waste daily. As one can see the daily EP-BN mitigation in conjunction with the opportunity window control algorithm leads to less energy waste as well as a higher net profit while also increasing production. This is due to the energy savings from the opportunity window control as well as the production increase from the daily bottleneck mitigation.

Table 6.5: EP-BN Case Study Results

	No Control	EP-BN & OW Control
Avg Daily EC (kWh)	2,700.52	1,983.78
95% CI EC (kWh)	[2696.12, 2704.91]	[1973.68, 1993.89]
Total Monthly EC (kWh)	81,015.57	59,413.5
Avg Daily PC $(Parts)$	234	236
95% CI PC $(Parts)$	[232.31, 235.68]	[234.62, 236.91]
Total Monthly PC $(Parts)$	6,990	7,080
Avg Daily Profit ($)	$22,913.86	$23,228.23
95% CI Profit ($)	[$22,745.98, $23,081.73]	[$23,115.17, $23,341.29]
Total Monthly Profit ($)	$687,415.70	$696,846.82

6.4 Conclusions

In this chapter a control methodology is introduced to reduce energy consumption while minimizing throughput impact. This leads to an increase in profit for the manufacturing facility. Numerical studies are performed to illustrate the advantages of turning machines off by utilizing their opportunity windows to reduce both costs and energy. A case study is performed to illustrate the effectiveness of the EP-BN and the control methodology.

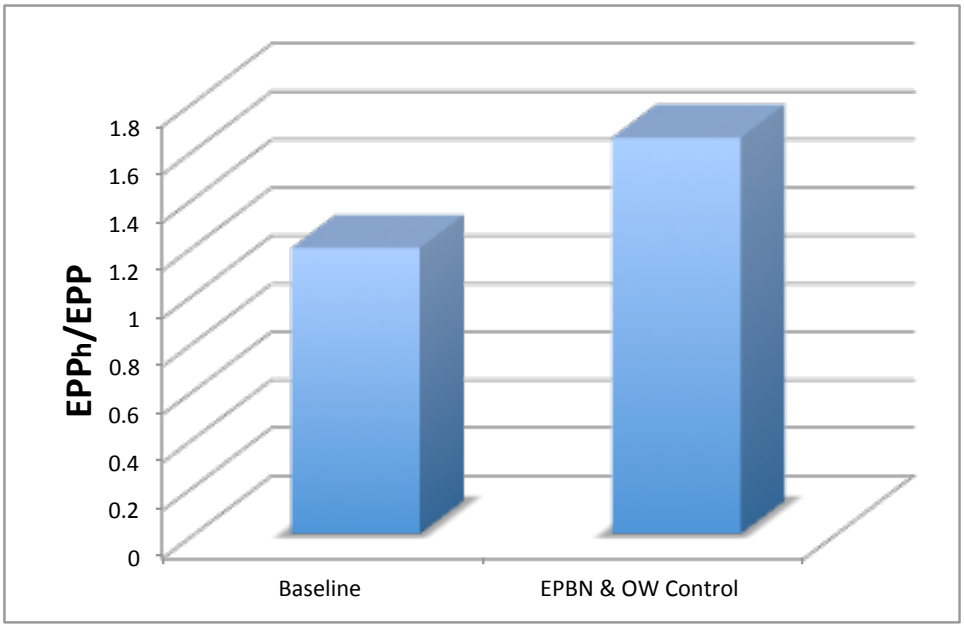

Figure 6.5: $SMPI_{DT}$

Chapter 7

Integrated Heating, Ventilation, and Air Conditioning and Production System Analysis

This chapter explores the energy savings opportunities for a manufacturing facility by combining the two largest energy consumers in a manufacturing plant: the production line and the heating, ventilation, and air conditioning system. The concept of the energy opportunity window (OW) is utilized, which allows each machine to be turned off at set periods of time without any throughput loss. The production system impact on the cooling load is explored and reduced using the opportunity window control methodology. The opportunity window for the production line is then synced with the peak periods of energy demand for the HVAC system to create a heuristic rule to optimize the energy cost savings. This heuristic rule is further developed with a control methodology to reduce overall costs for the manufacturing facility by reducing the energy consumption of both the HVAC system and the production system. An expanded HVAC and production model is built to test an opportunity window control scheme combined with EP-BN mitigation and ROI improvement strategies with variable HVAC set points. By using this methodology, the thermal comfort of the building occupants is studied along with the overall profit of the manufacturing facility.

7.1 Reducing Manufacturing Cooling Load

To study the impact of the manufacturing production line on the HVAC cooling load, we re-introduce the energy consumption equation for the production line (E_{pr}):

$$E_{pr} = \sum_{j=1}^{M} P_{pp,j}\Big[T - \sum_{k=1}^{\eta_j}[d_k - (1+\beta_j)t_{w,j}^k] - (1-\alpha_j)T_{id,j}\Big]. \tag{7.1}$$

It is important to note that each term in Eq. 7.1 can be calculated using readily available sensor data. To investigate the production impact on the cooling load provided by the HVAC system, it is necessary to first analyze the heat gains within the manufacturing facility. The heat gain is the rate at which heat is generated or transferred within the space [70]. The heat gain of the overall system at time t is:

$$\dot{q}(t) = \dot{q}_{env}(t) + \dot{q}_{inf}(t) + \dot{q}_{ihg}(t), \tag{7.2}$$

where $\dot{q}(t)$ is the heat gain of the overall system and $\dot{q}_{env}(t)$ is the heat gain due to the environment, which includes heat gain due to solar radiation, heat gain through the walls and roof, etc. The heat gain from infiltration is $\dot{q}_{inf}(t)$ and $\dot{q}_{ihg}(t)$ is the heat gain from internal sources. The internal heat gain can be further broken down as shown in (7.3):

$$\dot{q}_{ihg}(t) = \dot{q}_{L}(t) + \dot{q}_{P}(t) + \dot{q}_{eqp}(t) + \dot{q}_{M}(t), \tag{7.3}$$

where $\dot{q}_{L}(t)$ is the internal heat gain from lighting and $\dot{q}_{P}(t)$ is the internal heat gain from people within the facility. The $\dot{q}_{eqp}(t)$ represents the internal heat gain from any equipment that is not the machines on the production line and $\dot{q}_{M}(t)$ is the heat gain due to the machines on the production line. Since we are only concerned with the impact of the production system on the overall cooling load, we will focus on $\dot{q}_{M}(t)$. The rate at which a machine generates heat within a space is:

$$\dot{q}_{M}(t) = K(P_{pp}/E_{m})F_{l}F_{u}, \tag{7.4}$$

where:

$$K = \text{constant} = 1.0\ W/W$$

$$P_{pp} = \text{machine power rating while producing parts}$$

$$E_m = \text{motor efficiency, as decimal fraction} < 1.0$$

$$F_l = \text{motor load factor}$$

$$F_u = \text{motor use factor.}$$

The motor use factor is considered to be 1.0 for conventional applications and the motor load factor is dependent on the machine state. If the machine is producing parts then $F_l = 1.0$ and if the machine is off then $F_l = 0.0$. If machine j is idle then $F_l = \alpha_j$ for machine j and if it is warming up then $F_l = \beta_j$. The heat gain from machines must also be broken down into two parts: the convective and the radiative. These can be calculated using percentages provided by the American Society of Heating, Refrigeration and Air Conditioning Engineers (ASHRAE). The percentage of the heat load that is convective is C_M, while the percent of the heat load that is radiative is R_M, where $C_M + R_M = 1$.

After finding the heat gain within the space, it is possible to calculate the HVAC cooling load. The cooling load is the rate at which energy must be removed from the space to maintain the temperature and humidity at design values [70]. The cooling load of the overall facility (Q) is broken down into two portions: the convective (Q^c) and radiative portions (Q^r). The convective portion is the instantaneous cooling load from convection, while the radiative cooling load is the time delayed cooling load from long wave radiation. This is illustrated in (7.5):

$$Q(t) = Q^r(t) + Q^c(t). \tag{7.5}$$

In general, the convective heat load is calculated using the heat balance method, however since we are only concerned with the effect of production on the HVAC system, we can utilize the tables provided by ASHRAE to determine the percentage of the heat load that

is convective. The radiative portion of the cooling load can be calculated using a variety of techniques, however for the purposes of this dissertation the Radiant Time Series Method (RTSM) is applied. This method estimates the cooling load due to the radiative portion of each heat gain by applying a radiant time series, which calculates the cooling load based on the current and past values of radiative heat gains. The RTSM method is shown in (7.6):

$$Q^r(t) = r_o\dot{q}^r(t) + r_1\dot{q}^r(t-\delta) + ... + r_{23}\dot{q}^r(t-23\delta), \tag{7.6}$$

where $\dot{q}^r(t-n\delta)$ is the radiative heat gain n hours ago and r_n is the radiant time factor. The radiant time factors are calculated for a specific zone using a heat balance model as described in [70]. Using this method it is possible to find the radiative component of the cooling load due to the production line:

$$Q^r_M(t) = r_o\dot{q}^r_M(t) + r_1\dot{q}^r_M(t-\delta) + ... + r_{23}\dot{q}^r_M(t-23\delta), \tag{7.7}$$

where $\dot{q}^r_M(t-n\delta)$ is the radiative heat gain due to the production machines n hours ago. This is calculated in (7.8):

$$\dot{q}^r_M(t) = R_M\dot{q}_M(t). \tag{7.8}$$

The convective cooling load of an equipment heat load is calculated by taking the percentage of the heat gain that is convective (C) based on the charts supplied by ASHRAE, where:

$$Q^c_M(t) = C_M\dot{q}_M(t). \tag{7.9}$$

Thus, the cooling load due to the production processes is:

$$Q_M(t) = Q^r_M(t) + Q^c_M(t). \tag{7.10}$$

7.1.1 Case Study: Cooling Load

A portion of a real automotive assembly line is simulated to validate the methodology presented in this research. The simulation model is a 15 machine and 14 buffer serial line. The production characteristics are taken from the real assembly line and mocked up for confidential reasons. The mocked production parameters can be seen in Table 7.1. The Mean Time to Repair (MTTR), Mean Cycle Between Failure (MCBF), and mean time to warmup (ω_j) are assumed to follow an exponential distribution based on the real data. The radiative

Table 7.1: Production Line Parameters: Cooling Load Case Study

	m_1	m_2	m_3	m_4	m_5	m_6	m_7	m_8	m_9	m_{10}	m_{11}	m_{12}	m_{13}	m_{14}	m_{15}
$1/\tau$	2.5	2	3	2.5	2	2.5	1.5	2.5	1	3	2.5	2	2.5	3	2
MTTR	6.7	6.7	6.7	6.7	6.7	6.7	6.7	6.7	6.7	6.7	6.7	6.7	6.7	6.7	6.7
MCBF	450	227	340	200	3960	950	120	4950	1980	540	950	227	450	5940	227
ω	1.0	1.0	1.0	1.0	1.0	1.0	1.0	1.0	1.0	1.0	1.0	1.0	1.0	1.0	1.0
e_j	96	94	94	92	99	98	92	99	99	96	98	94	96	99	94
P_{pp}	80	100	100	120	80	120	100	120	80	120	100	80	100	100	120
P_{id}	64	80	80	96	64	96	80	96	64	96	80	64	80	80	96
P_w	96	120	120	144	96	144	120	144	96	144	120	96	120	120	144
-	-	B2	B3	B4	B5	B6	B7	B8	B9	B10	B11	B12	B13	B14	B15
B_m	-	55	35	35	45	40	50	40	50	40	45	55	30	35	30

portion of the machine heat load is assumed to be $R_M = 0.5$ and the convective portion is $C_M = 0.5$ based on the procedure outlined in [70]. The radiant time factors are based on a heavy weight construction building as described in [70] and they can be seen in Fig. 7.1. To reduce the overall cooling load caused by the production system we employ an opportunity window control scheme that reduces overall energy consumption and cooling load without impacting production. This control methodology is used at each machine j where we allow the buffers between machine j and the slowest machine to reach a certain threshold and then turn off machine j for a set period of time. The buffer level threshold and the amount of time each machine is turned off are found using a greedy search algorithm. The production facility runs two eight hour shifts from 06:00 - 22:00 where the production line either runs with no control methodology, which is our baseline, or with the opportunity window control

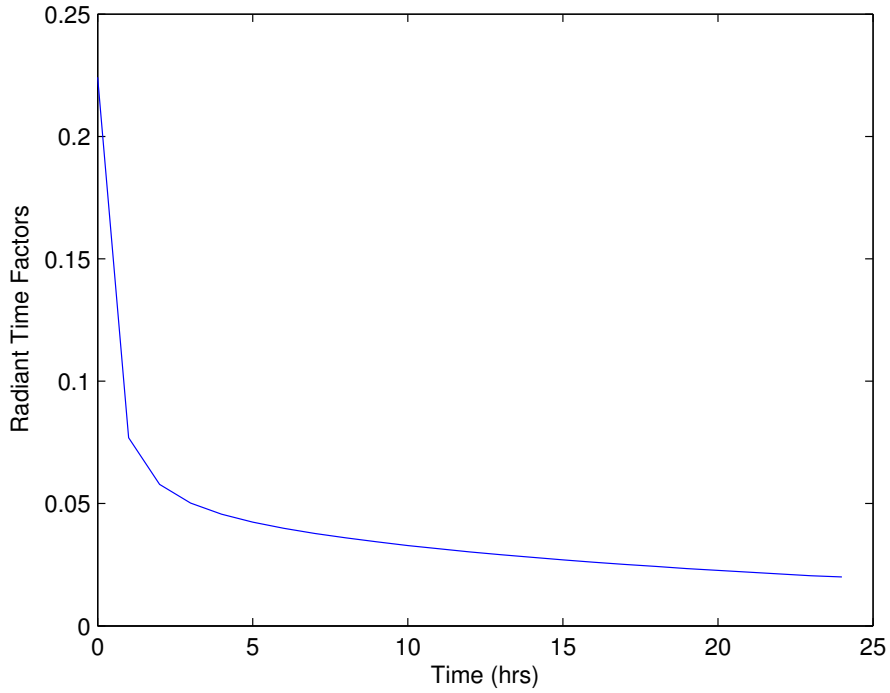

Figure 7.1: Radiant Time Factors

scheme. We compare the two methods to illustrate the energy savings and the cooling load reduction. Since we are only concerned with the impact of production on the cooling load, we will assume all other heat sources will remain unchanged between the control and baseline scenario. The cooling load due to the production system for the baseline and the OW control cases can be seen in Fig. 7.2, while the cooling load savings is displayed in Fig. 7.3 by taking the difference between the baseline and control cases. These figures illustrate the reduction in the cooling load by utilizing a control methodology to reduce the impact of production on the HVAC system. The OW control scenario leads to a maximum of 500 kW cooling load savings, which can reduce overall energy impact of the HVAC system. By using this control methodology, the overall energy consumption of the production system is reduced without any impact on production. This is illustrated in Fig. 7.4. The baseline scenario consumes over 400 kWh more daily than in the OW control scenario, without any difference in production. This shows how the OW control scheme can reduce both the cooling load

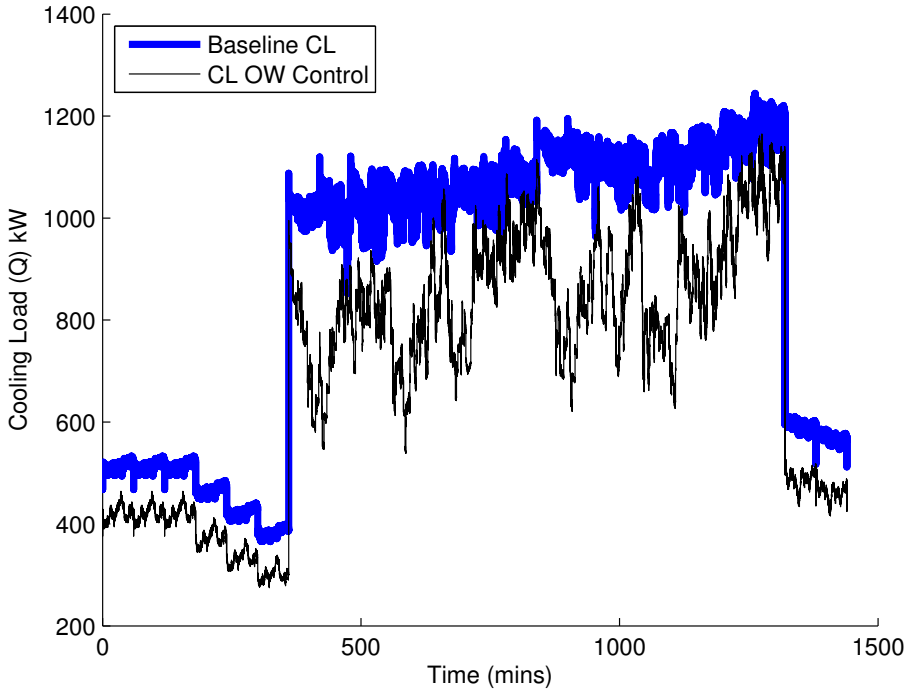

Figure 7.2: Cooling Load: OW Control vs. Baseline

and energy consumption in the manufacturing facility without any impact to production.

7.2 Integrated HVAC and Production Modeling

7.2.1 Initial EnergyPlus Model

The thermal model for this project was built using EnergyPlus, a software developed by the Department of Energy. EnergyPlus evolved from previous DOE programs Building Loads Analysis and System Thermodynamics (BLAST) and DOE-2 as an energy analysis thermal load simulation software [71]. This software utilizes Conduction Transfer Functions (CTF) for the Heat Balance Algorithm for the building. The hot water for the building is supplied through a natural gas boiler. There is a chilled water system, supplied by a chiller connected to a cooling tower on the roof. All heating and cooling is done utilizing an air handler unit with variable air volume boxes with reheat and cooling coils. The system is sized utilizing the

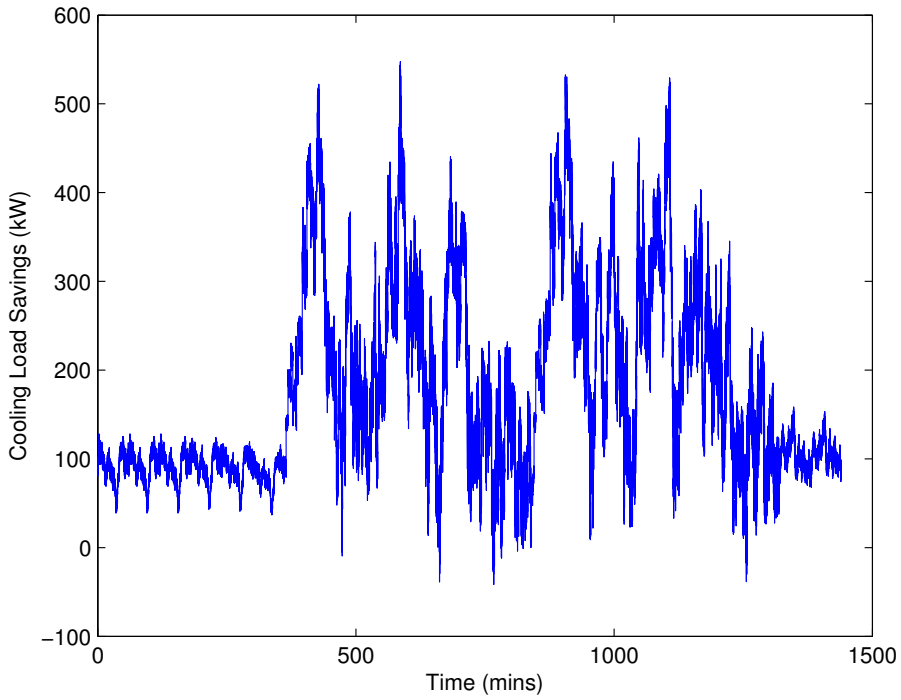

Figure 7.3: Cooling Load Reduction

EnergyPlus design day sizing feature. This feature allows the user to plug in extreme weather conditions in the winter or the summer and the program will auto-calculate the heating and cooling loads necessary for the building. For this research the summer design day is utilized to properly size the HVAC equipment to properly meet the cooling load requirements. Once the equipment is sized, EnergyPlus is capable of responding to any changes in the environment including changes in outside air temperature, internal heat loads, and solar radiation. The program turns on the necessary HVAC equipment to meet the thermostat set points in the facility. The building model that is utilized can be seen in Fig. 7.5.

The production line is modeled as a continuous flow model utilizing Simulink/MATLAB. A serial production line with six machines and five buffers is tested, while taking the opportunity window at various times for different machines. The service time of each machine is modeled using its natural processing time. However, each machine has random downtime

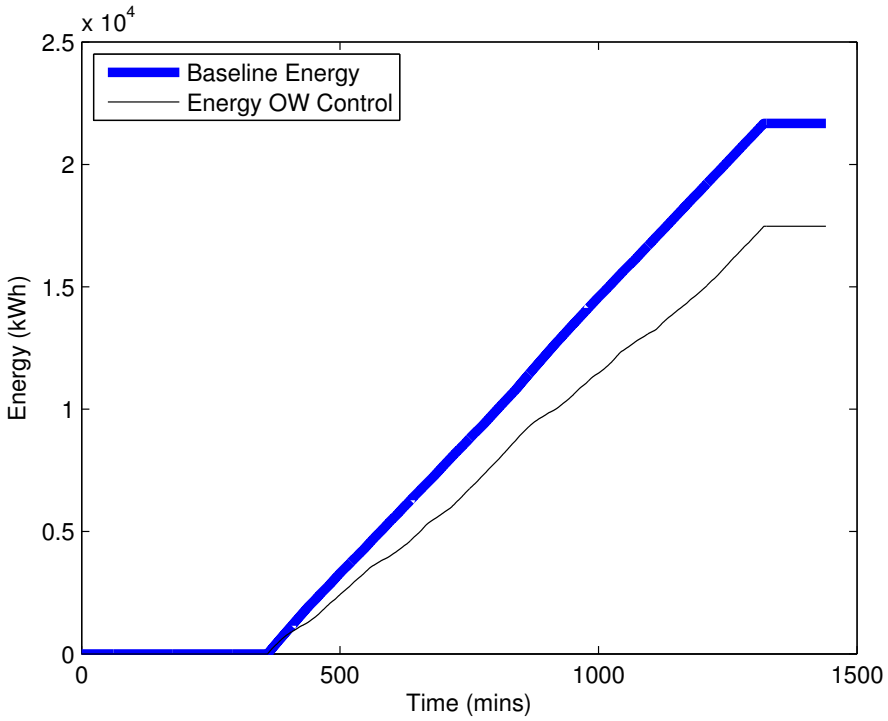

Figure 7.4: Daily Production Line Energy Usage

and uptime leading to a random effective processing time. For a multi-stage production system, a random downtime impact at one stage will propagate to upstream and downstream machines, based on where the event occurs.

The machine up/down times are saved and outputted to EnergyPlus. Within EnergyPlus the production line is simulated as a thermal heat load inside of the building based on the production schedule. The machines are considered to be completely off with no power consumption if the up/downtime status is equal to 0. If the machine status is equal to 1 then the machine will run at its full power consumption, P_{pp}.

The cost due to the power consumption of the integrated facility is calculated based on a time of use basis. This charge is dictated by the energy demand of the grid at the current time. The monetary savings are realized by taking the cost without the inserted opportunity window, and calculating the difference when the energy savings opportunities are realized.

The design day for this project was a summer design day in Chicago. This day was uti-

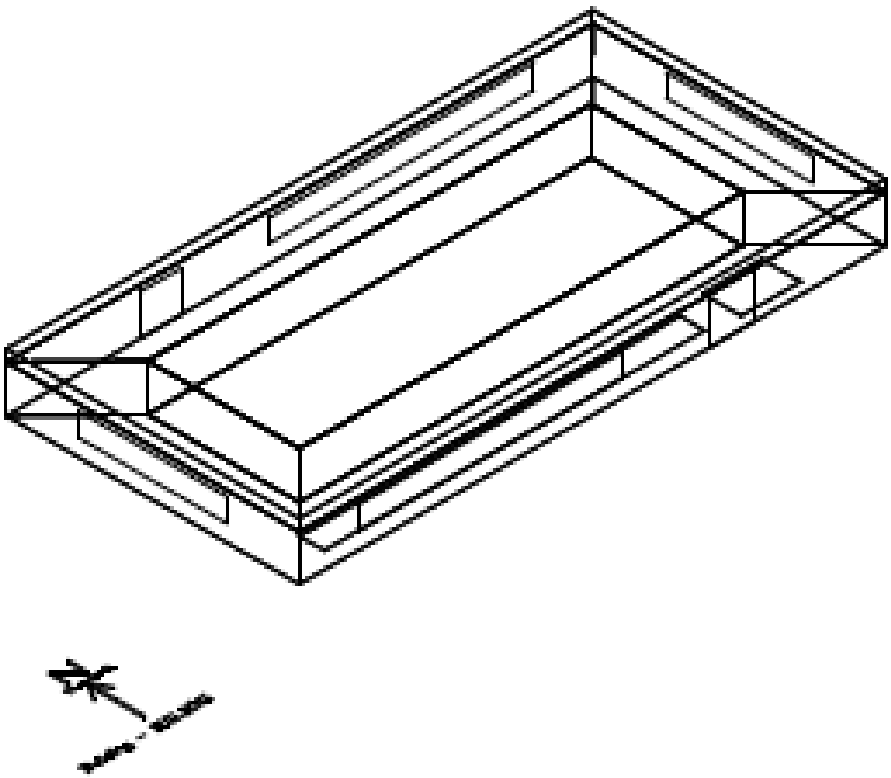

Figure 7.5: Building Model Used For Simulation

lized to size the HVAC equipment to properly deal with ambient temperature as well as the heat load due to the internal equipment and people. The design day outside air temperatures are graphed below in Fig. 7.6.

7.2.2 Case Study: One Opportunity Window

The following is an example of a serial production line with six machines and five 100-capacity buffers with the parameters shown below in Table 7.2. The simulation has a running time of 24 hours with 8 hours of warmup time for each machine. The one story building that is used in the simulation has a floor area of 463.6 m^2 with 3 m ceilings. It has five different zones, however only one zone is analyzed. The machine line is placed in the core of the building, which has a floor area of 184.4 m^2 with 2.43 m ceilings. For the purposes of this project, the other zones are unoccupied and only the core of the building is studied. The internal heat

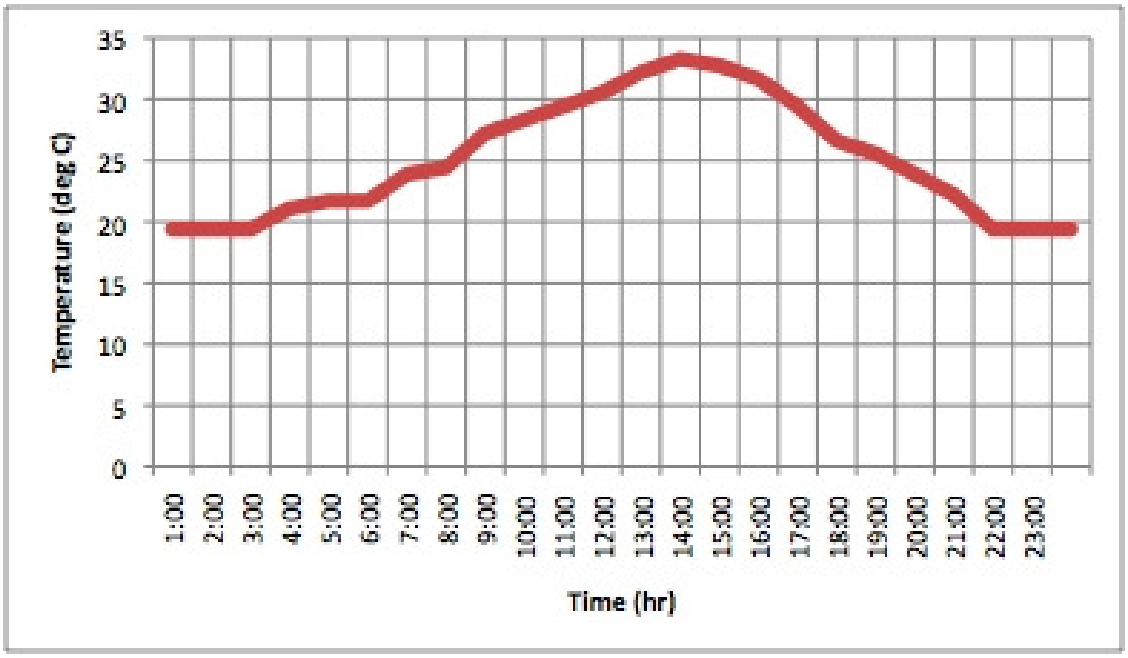

Figure 7.6: Outside Air Temperature

Table 7.2: Production Line Parameters: Initial OW & HVAC Control

Parameter	m_1	m_2	m_3	m_4	m_5	m_6
PR (parts/min)	5	5	5	3	5	5
MTTR (mins)	17.65	17.65	17.65	17.65	17.65	17.65
MCBF (cycles)	500	500	500	300	500	500
Efficiency (%)	85%	85%	85%	85%	85%	85%

loads are in Table 7.3:

The schedules for the people and the lighting are constantly on to simulate having multiple shifts throughout the day assuming that this will be a 24 hr shift. The schedule for the machines is dependent on when the opportunity window is taken. The different opportunity windows for each machine are calculated and run at the odd hours of the day from 01:00 to 15:00.

The first study utilizes only one inserted opportunity window, which is taken based on the above schedule. There was less than a five percent production count loss in each case. The algorithm calculates the optimal time to take the opportunity window for the production

Table 7.3: Internal Heat Loads

Heat Source	Amount	Power Consumption (W)	% Radiant
People	10	20	30%
Lighting	1	2,964	59%
Machines	6	150,000	30%

line based on the time of use charge. The energy saving opportunities are calculated utilizing the various production data and taken during times of high energy demand. The HVAC set points are changed with each scenario to allow for further energy savings.

The energy cost for the factory is calculated using a time of use charge where the energy usage is priced differently depending on the time of day. The energy cost per kilowatt-hour is displayed in Fig. 7.7.

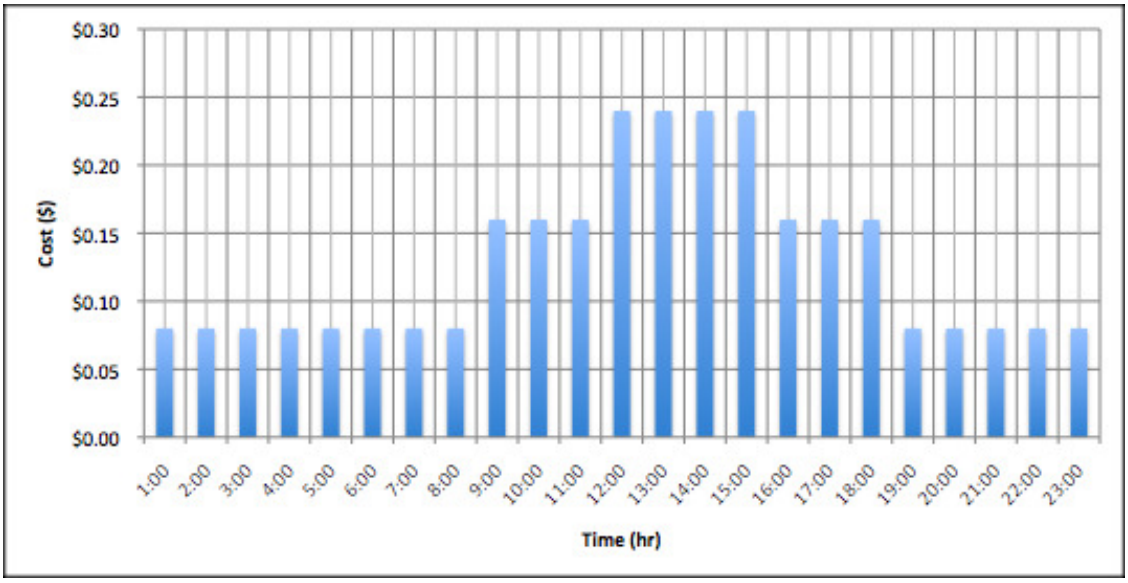

Figure 7.7: Time of Use Charge

The time of use charge is highest during the hottest points during the day, which corresponds to the most energy usage on the grid. While the algorithm does not explicitly consider the environment, it does take it into account through this charge. The opportunity window will be taken when the time of use charge is highest (i.e. when the temperature is

hottest during the day). Obviously, this is not always as the case since the environment is random by nature and the hottest temperature might not correspond to the largest time of use charge. However, probabilities suggest that this is normally the situation. Also, changes to the environment take place over a much longer period of time compared to the randomness of the production line, which allows for the ability to plan in the short term around predicted weather patterns, such as the outside air temperature for the day. This suggests that set points and opportunity windows can be adjusted based on the predicted temperatures for the day, while still taking into account the time of use charge.

Utilizing the differential pricing the set points for the HVAC system can be changed to allow for the maximum energy cost savings for the system. These different scenarios are seen in Table 7.4.

Table 7.4: HVAC Schedule

Scenario	Time	Set Point ($°C$)
1	Until 06:00	25.5
	Until 11:00	24.4
	Until 18:00	23.3
	Until 22:00	24.4
	Until 24:00	25.5
2	Non OW Periods	24.4
	OW Periods	23.3
3	Non OW Periods	23.3
	OW Periods	24.4
4	All Times	24.4
5	All Times	23.3

These scenarios are run through EnergyPlus and MATLAB utilizing the different opportunity windows for each machine. The energy cost savings is then calculated by comparing each scenario with various energy opportunity windows to the scenarios with no opportunity window and the results are then plotted in Fig. 7.8.

It is evident that scenario 3 at the 15^{th} hour is the largest cost savings, which corresponds to the highest time of use charge as seen in Fig. 7.7.

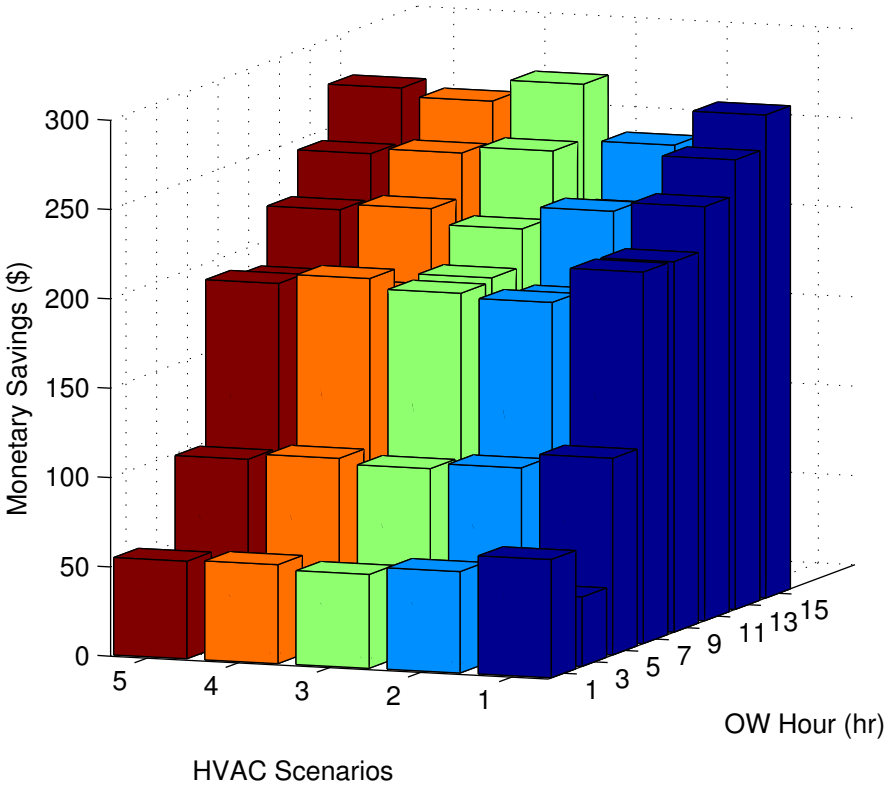

Figure 7.8: Daily Savings: One OW ($)

7.2.3 Case Study: Two Opportunity Windows

The second simulation study utilizes the same parameters as above, except it utilizes multiple inserted opportunity windows. As in the case with one opportunity window, the production count loss was less than five percent for each simulation. Two opportunity windows are taken for each machine: one at the 15^{th} hour since this was the optimal time from the first simulation study and the second is paired at the other odd hours of the day. They are taken after the minimum recovery time for the maximum cost savings. The various energy saving opportunities can be seen with the average savings from each opportunity window combination in Table 7.5. There is no simulation with the opportunity window at the 13^{th}

hour since there is not enough recovery time to allow for no production loss. It is evident that taking the opportunity windows in the middle of the day leads to the most cost savings as seen by the 11^{th} and 15^{th} hours in Table 7.5.

Table 7.5: Average Energy Cost Daily Savings

Opportunity Window	Average Savings ($)
1 & 15	$337.95
3 & 15	$331.20
5 & 15	$362.85
7 & 15	$422.55
9 & 15	$439.65
11 & 15	$513.15

The different scenarios in Table 7.4 are simulated and plotted in Fig. 7.9. The OW hours are all taken with the 15^{th} hour as indicated above.

The best option is scenario 3 with opportunity windows taken at the 11^{th} and the 15^{th} hours, which shows a strong correlation between changing set points with the various opportunity windows for maximum cost savings. The average daily savings per HVAC scenario can be seen in Table 7.6 below.

Table 7.6: Average Daily Savings per HVAC Scenario

Scenario	Savings: One OW ($)	Savings: Two OWs ($)
1	$172.97	$396.56
2	$157.14	$362.33
3	$163.05	$408.35
4	$162.91	$391.86
5	$161.81	$388.69

This illustrates that for multiple opportunity windows, scenario 3 is the optimal strategy, while with one opportunity window, scenario 1 resulted in the highest cost savings. However, when there is only one opportunity window there is only an insignificant difference between scenario 1 and scenario 3. This suggests that as there are more opportunity windows the

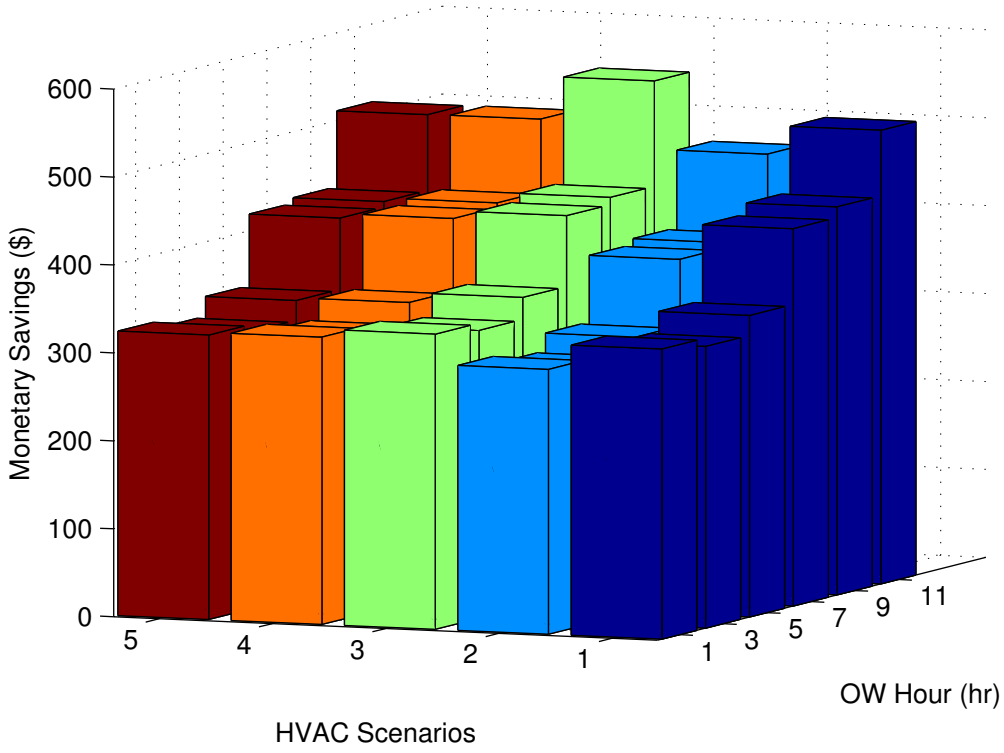

Figure 7.9: Daily Savings: Two OWs ($)

most cost savings will be realized when the HVAC set points are coupled with the production system. The highest cost savings for the multiple opportunity window simulation is the 15^{th} hour paired with the 11^{th} hr during the 3^{rd} scenario. This demonstrates that proper coordination through taking the opportunity window and changing the set points based on the maximum time of use charge, which is in the middle of the afternoon, leads to the optimal cost saving strategy.

7.2.4 Expanded HVAC and Production Model

This section builds upon the work in Section 7.2.1 by expanding the HVAC and production model in EnergyPlus. The building used for this integrated thermal and production model is shown in Fig. 7.10. The building has a total floor area of 24,695 square feet, with

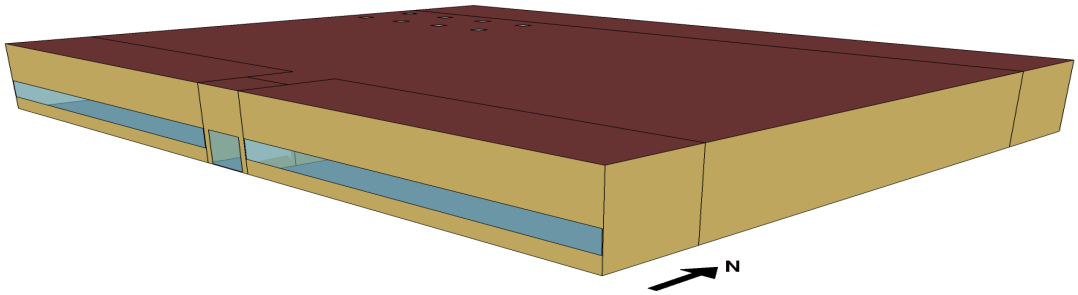

Figure 7.10: Building Model Used For Expanded HVAC Model

dimensions of 178 ft x 139 ft x 20 ft. The outer walls are concrete block wall consisting of 8 in concrete masonry units, wall insulation and 0.5 in gypsum board. The roof is a built up roof consisting of a roof membrane, roof insulation, and metal decking. There are five thermal zones for HVAC purposes, which are shown in Fig. 7.11. Cooling within the

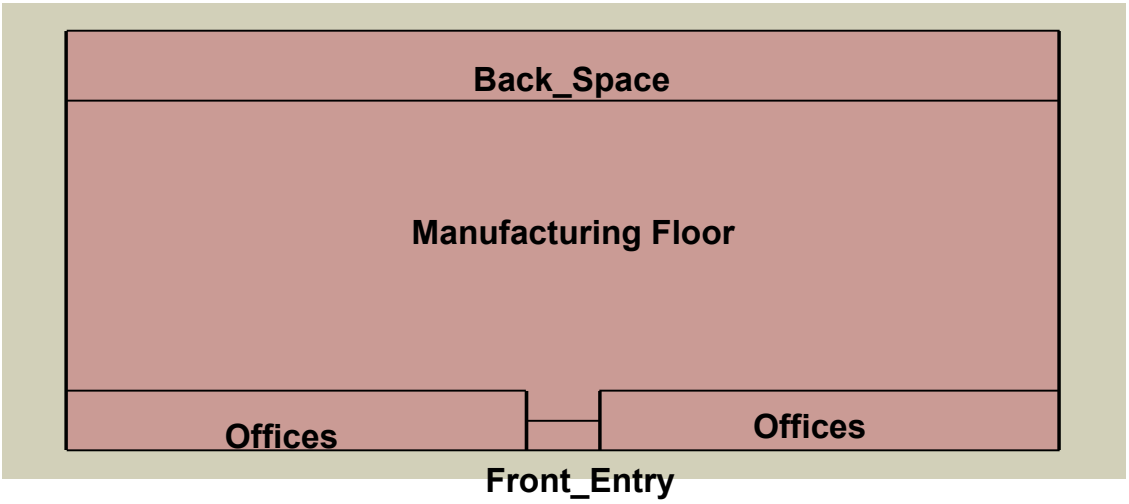

Figure 7.11: Building Zones

building is provided by a packaged air conditioning unit that is sized based on the EnergyPlus autosizing feature. Heating in the space is provided by a gas furnace inside the packaged air conditioning unit. The air distribution is constant air volume with one roof top unit per zone, with the exception of the front entry. The lighting in each zone has a 70% radiant portion and 20% visible light. The back space has 7.56 W/m^2 of lighting, the front offices each have

15.5 W/m^2 of lighting, the front entry has 9.69 W/m^2 of lighting and the manufacturing floor has 17.11 W/m^2 of lighting. The manufacturing production line is located in the zone "Manufacturing Floor," while all other zones have no manufacturing equipment within them. The manufacturing equipment will follow a set production schedule. In the previous section, we set the machines to either "On" or "Off" depending on the average up time during a one minute period. In this expanded model, the average machine energy consumption over each one minute period is calculated and set as the heat load for the machine during that period. The front offices have miscellaneous equipment (such as computers) that consume 487 W and 3,245 W of electricity respectively. The manufacturing floor has miscellaneous equipment, which excludes the manufacturing line, that consumes 5,169 W of electricity. This miscellaneous equipment is on throughout the production shifts and off when there is no production. Each piece of miscellaneous equipment and each machine has a radiant fraction of 0.5. For each hour there is approximately 400 people within the facility, with each person having a radiant fraction of 0.3.

7.2.5 Case Study: Control Methodology

In this section, we provide a control methodology that merges opportunity window control, the EP-BN mitigation, and ROI analysis. The control methodology that is utilized is modified from Chapter 5 to include thermal comfort (TC) since we are evaluating the merged production and HVAC system.

$$\max_{\substack{t_{OW} \\ \eta_{OW}}} Profit, \quad s.t.\ PC \geq PC_0 \ \ \& \ \ -1.0 < TC < 1.0 \tag{7.11}$$

To check overall profit, the profit equation is expanded to include the HVAC energy consumption. We are interested in looking at the tradeoff of production throughput versus the energy consumption of the production and HVAC systems. The thermal comfort is measured using the Fanger Comfort Analysis [72], where thermal comfort is measured on a scale from

-3.0 to 3.0. This is measured based on outdoor temperature, indoor temperature, relative humidity, etc. and then equated by Predicted Mean Vote (PMV) to the proper scale. The meaning of PMV is shown in Fig. 7.12. The control methodology ensures that the people

Value	Sensation
+3	Hot
+2	Warm
+1	Slightly warm
0	Neutral
-1	Slightly cool
-2	Cool
-3	Cold

Figure 7.12: Predicted Mean Vote

within the facility only feel slightly warm or slightly cool. Figure 7.13 illustrates how PMV relates to the number of people that are dissatisfied with their current thermal comfort level through the Predicted Percentage Dissatisfied (PPD). By controlling the thermal comfort level between -1.0 and 1.0, we ensure that approximately only 20% of people are dissatisfied with their current thermal comfort state. To achieve this goal, we will study seven different scenarios for the production line as well as five different set point schedules for the HVAC system. The seven options for the production line are: 1) no control methodology (baseline scenario), 2) an opportunity window control scheme, 3) EP-BN mitigation, 4) Replacing a

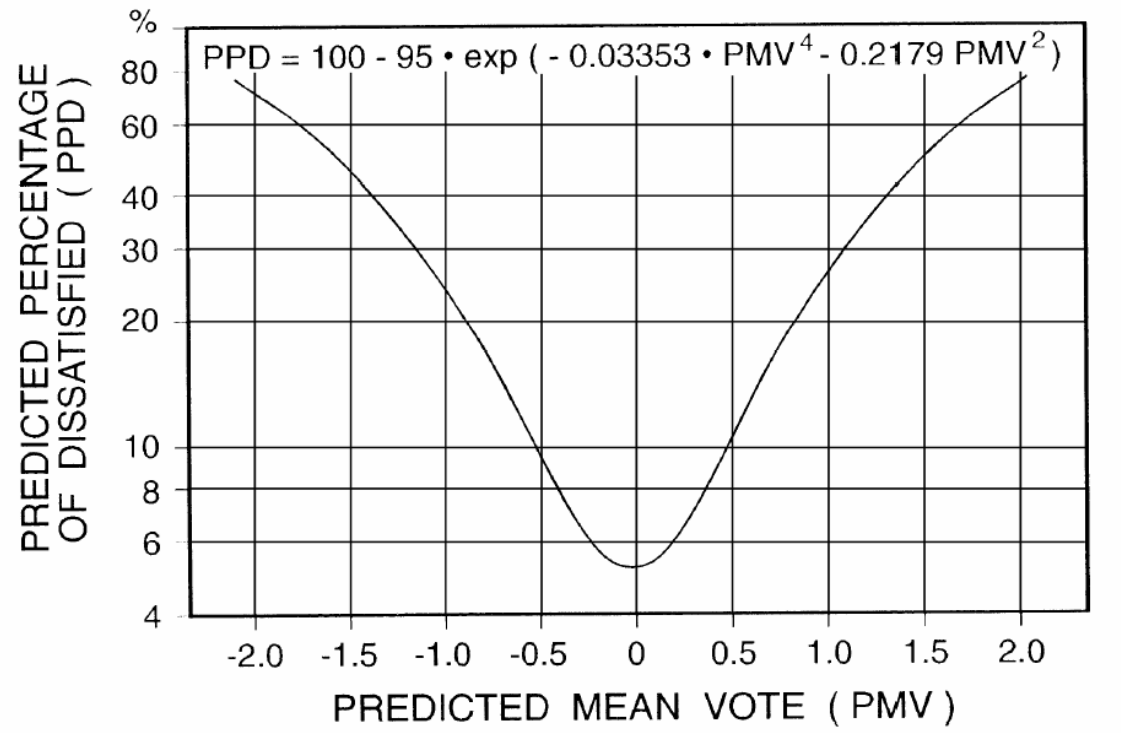

Figure 7.13: Predicted Percentage Dissatisfied

part/machine based on ROI analysis, 5) Combination of OW control and EP-BN mitigation, 6) Combination of OW control and ROI replacement, and 7) Combination of OW control, EP-BN mitigation, and ROI replacement. The opportunity window control methodology for the production line is presented as follows from the return on investment case study:

1. *Begin shift*
2. *Collect pertinent data from buffer levels and machine states*
3. *If* $b_j = B_{0,j}$, $\forall j < M^*$ *turn off machine* $j-1$ *for* $t_{OW,j-1}$.
   (a) *After* $t_{OW,j-1}$ *turn on machine* $j-1$
4. *If* $b_j \neq B_{0,j}$, $\forall j < M^*$, *go to step 5*

5. *If* $b_j = B_{0,j}$, $\forall j > M^*$ *turn off machine* j *for* $t_{OW,j}$.

   (a) *After* $t_{OW,j}$ *turn on machine* j

6. *If* $b_j \neq B_{0,j}$, $\forall j > M^*$ *return to step 2.*

The EP-BN is selected based on the methodology presented in Chapter 5 by reducing the MTTR of the EP-BN machine by 10%. The ROI machine is selected based on the analysis from Chapter 5. For this case study we utilize a real automotive production line. The production line parameters are taken from real data and mocked up for confidential reasons in Table 7.7. The profit of each part, is assumed to be c_p is \$100 per part based on the real

Table 7.7: Production Line Parameters: HVAC Expanded Model Case Study

	m_1	m_2	m_3	m_4	m_5	m_6	m_7	m_8	m_9	m_{10}	m_{11}	m_{12}	m_{13}	m_{14}	m_{15}
$1/\tau$	2.5	1.3	1.7	1.2	1.8	1.5	2.1	0.9	0.5	1.2	2.3	1.6	1.9	2.4	1.7
MTTR	13	11	13	14	18	11	13	11	12	12	18	11	13	11	13
MCBF	250	270	300	350	325	205	245	250	200	265	350	200	280	275	400
ω_j	1.0	1.0	1.0	1.0	1.0	1.0	1.0	1.0	1.0	1.0	1.0	1.0	1.0	1.0	1.0
e_j	89	95	93	95	91	93	90	96	97	95	89	92	92	91	95
P_{pp}	80	100	100	120	80	120	100	120	80	120	100	80	100	100	120
P_{id}	64	80	80	96	64	96	80	96	64	96	80	64	80	80	96
P_w	72	90	90	108	72	108	90	108	72	108	90	72	90	90	108
-	-	B2	B3	B4	B5	B6	B7	B8	B9	B10	B11	B12	B13	B14	B15
B_m	-	40	60	30	40	50	40	50	35	30	25	60	50	40	30

value after it is mocked up for confidential reasons and the cost of energy, c_e^l is assumed to be [67]:

$$c_e^l(t) = \begin{cases} \$0.08, & 00:00 \leq t < 06:00, \\ \$0.14, & 06:00 \leq t < 11:00, \\ \$0.24, & 11:00 \leq t < 19:00, \\ \$0.14, & 19:00 \leq t \leq 23:59. \end{cases}$$

The return on investment analysis for the production line is shown in Table 7.8, where: option 1 involves replacing a part of the machine during a regular shift, option 2 is replacing that part during an overtime period, and option 3 is replacing the entire machine. The CTR

Table 7.8: Economic Analysis

Option 1	m_1	m_2	m_3	m_4	m_5	m_6	m_7	m_8	m_9	m_{10}	m_{11}	m_{12}	m_{13}	m_{14}	m_{15}
ΔP_{pp} (kW)	5	2	3	4	5	4	2	3	3	4	5	6	4	5	5
CTR (\$)	5.2k	4.2k	3.1k	4.4k	5.1k	3.2k	4.1k	3.1k	8.6k	4.4k	5.1k	3.2k	3.2k	4.2k	5.3k
Option 2	m_1	m_2	m_3	m_4	m_5	m_6	m_7	m_8	m_9	m_{10}	m_{11}	m_{12}	m_{13}	m_{14}	m_{15}
ΔP_{pp} (kW)	5	2	3	4	5	4	2	3	3	4	5	6	4	5	5
CTR (\$)	5.5k	4.5k	3.3k	4.7k	5.2k	3.4k	4.2k	3.2k	6.2k	4.3k	5.3k	3.3k	3.2k	4.5k	5.6k
Option 3	m_1	m_2	m_3	m_4	m_5	m_6	m_7	m_8	m_9	m_{10}	m_{11}	m_{12}	m_{13}	m_{14}	m_{15}
ΔP_{pp} (kW)	20	15	10	9	10	17	20	15	17	16	15	21	20	15	17
CTR (\$)	23k	35k	21k	37k	23k	37k	49k	34k	20k	60k	23k	36k	25k	28k	35k

is in thousands of dollar, i.e. 5k = \$5,000. We assume that $C_{Reg,j}$ is \$70 per hour and $C_{OT,j}$ is \$140 per hour for each machine. We also manage the replacement of the part during a regular shift when the machine has its maximum opportunity window therefore limiting production loss. The ROI analysis illustrates that machine 12 should be replaced during a regular shift, which leads to a break even point of 583 days.

The HVAC schedule for the Manufacturing Floor consists of five different schedules: 1) set schedule (not based on production energy consumption or time of day), 2) lower production energy consumption = lower set point, 3) lower production energy consumption = higher set point, 4) higher time of use cost = lower set point, 5) higher time of use cost = higher set point. The second and third schedule are based on the maximum energy consumption of the line, which is the scenario when each machine is producing parts:

$$E_{pr}^{max}(t) = \sum_{j=1}^{M} P_{pp,j} \times t$$

The HVAC schedules are shown below:

Schedule 1:

$$Set\ Point(t) = \begin{cases} 29.44°C, & 00:00 \leq t < 05:00, \\ 27.80°C, & 05:00 \leq t < 06:00, \\ 25.60°C, & 06:00 \leq t < 07:00, \\ 23.89°C, & 07:00 \leq t < 21:00, \\ 29.44°C, & 21:00 \leq t \leq 23:59. \end{cases}$$

Schedule 2:

$$Set\ Point(E_{pr}, t) = \begin{cases} 24.44°C, & E_{pr}(t) = E_{pr}^{max}, \\ 23.89°C, & 0.9E_{pr}^{max} \leq E_{pr}(t) < E_{pr}^{max}, \\ 23.33°C, & 0.8E_{pr}^{max} \leq E_{pr}(t) < 0.9E_{pr}^{max}, \\ 22.77°C, & 0.7E_{pr}^{max} \leq E_{pr}(t) < 0.8E_{pr}^{max}, \\ 22.22°C, & 0.6E_{pr}^{max} \leq E_{pr}(t) < 0.7E_{pr}^{max}, \\ 21.67°C, & 0.5E_{pr}^{max} \leq E_{pr}(t) < 0.6E_{pr}^{max}, \\ 21.22°C, & E_{pr}(t) < 0.5E_{pr}^{max}. \end{cases}$$

Schedule 3:

$$Set\ Point(E_{pr}, t) = \begin{cases} 21.22°C, & E_{pr}(t) = E_{pr}^{max}, \\ 21.67°C, & 0.9E_{pr}^{max} \leq E_{pr}(t) < E_{pr}^{max}, \\ 22.22°C, & 0.8E_{pr}^{max} \leq E_{pr}(t) < 0.9E_{pr}^{max}, \\ 22.77°C, & 0.7E_{pr}^{max} \leq E_{pr}(t) < 0.8E_{pr}^{max}, \\ 23.33°C, & 0.6E_{pr}^{max} \leq E_{pr}(t) < 0.7E_{pr}^{max}, \\ 23.89°C, & 0.5E_{pr}^{max} \leq E_{pr}(t) < 0.6E_{pr}^{max}, \\ 24.44°C, & E_{pr}(t) < 0.5E_{pr}^{max}. \end{cases}$$

Schedule 4:

$$Set\ Point(t) = \begin{cases} 24.44°C, & 00:00 \leq t < 06:00, \\ 23.33°C, & 06:00 \leq t < 11:00, \\ 22.22°C, & 11:00 \leq t < 18:00, \\ 21.12°C, & 18:00 \leq t \leq 23:59. \end{cases}$$

Schedule 5:

$$Set\ Point(t) = \begin{cases} 21.12°C, & 00:00 \leq t < 06:00, \\ 22.22°C, & 06:00 \leq t < 11:00, \\ 23.33°C, & 11:00 \leq t < 18:00, \\ 24.44°C, & 18:00 \leq t \leq 23:59. \end{cases}$$

The production line runs from 06:00-22:00 (two 8 hour shifts) each week day for a five year period, while the HVAC system follows Schedules 1-5. Since the production system does not depend on the HVAC schedule, we present one set of data that is utilized for each schedule. The average daily parameters are shown in Table 7.9. The results show that the

Table 7.9: Average Daily Production Line Results

-	No OW	OW	EPBN	ROI	OW + EPBN	OW + ROI	OW + EPBN + ROI
TH	463	452	470	463	465	459	465
E (kWh)	19,660	13,108	19,698	19,584	13,352	13,192	13,315
EPP	42.4	29.0	41.9	42.2	28.7	28.8	28.6
$SMPI_{SA}$	0.429	0.627	0.434	0.431	0.633	0.632	0.634
$SMPI_{DT}$	1.19	1.75	1.21	1.20	1.76	1.76	1.78

EP-BN scenario leads to the largest throughput and energy consumption per day. However, this is not necessarily the optimal case since the scenario with the combined OW control methodology, the EP-BN mitigation, and the ROI improvement leads to the least amount of waste as shown with the $SMPI_{DT}$ and $SMPI_{SA}$. To study the profit, we need to show the overall energy cost for each schedule as presented above. The average daily HVAC cost is shown in Fig. 7.14, the monthly HVAC cost is shown in Fig. 7.15, the yearly HVAC cost

is shown in 7.16, and lastly, the five year HVAC cost is shown in Fig. 7.17. We select these time horizons to show the difference in the short term versus the long term for each case.

The results show that the largest cost for the HVAC is Schedule 3 with the EP-BN

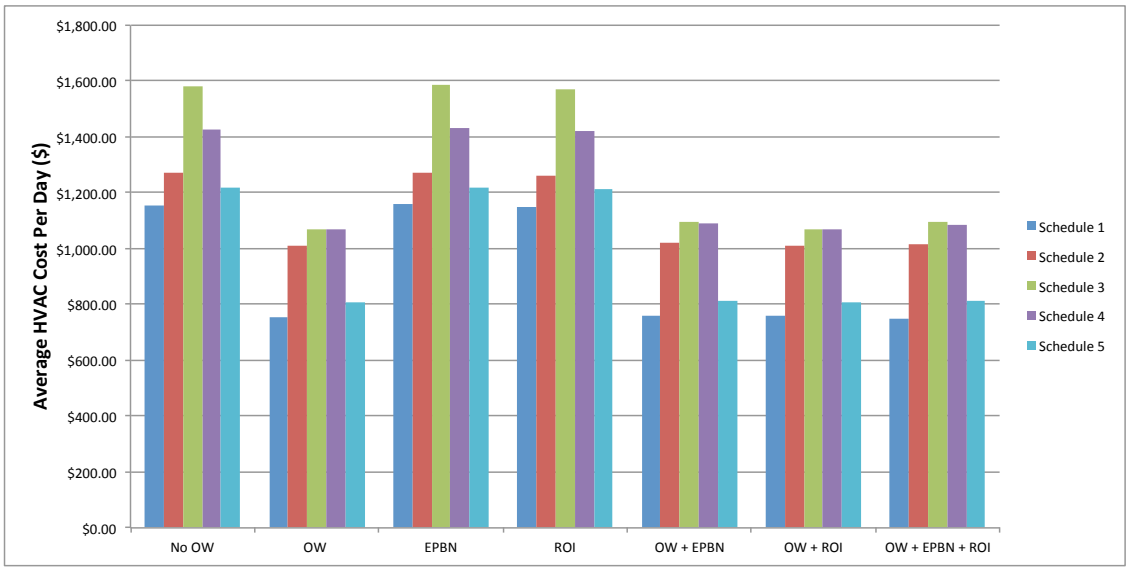

Figure 7.14: Average Daily HVAC Cost ($)

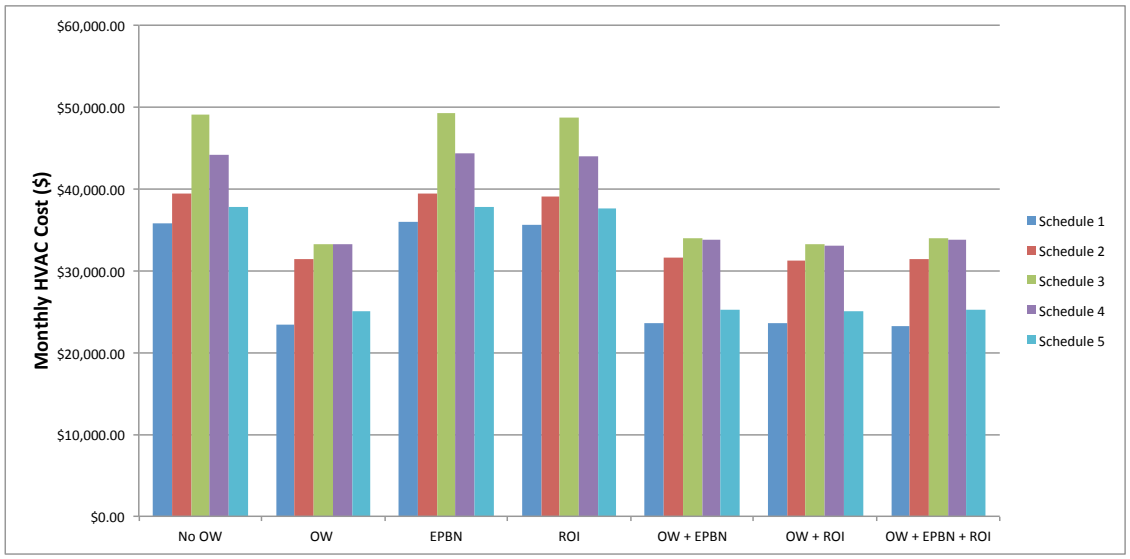

Figure 7.15: Monthly HVAC Cost ($)

mitigation. This leads to a daily HVAC energy cost of $1,573.01. The EP-BN mitigation

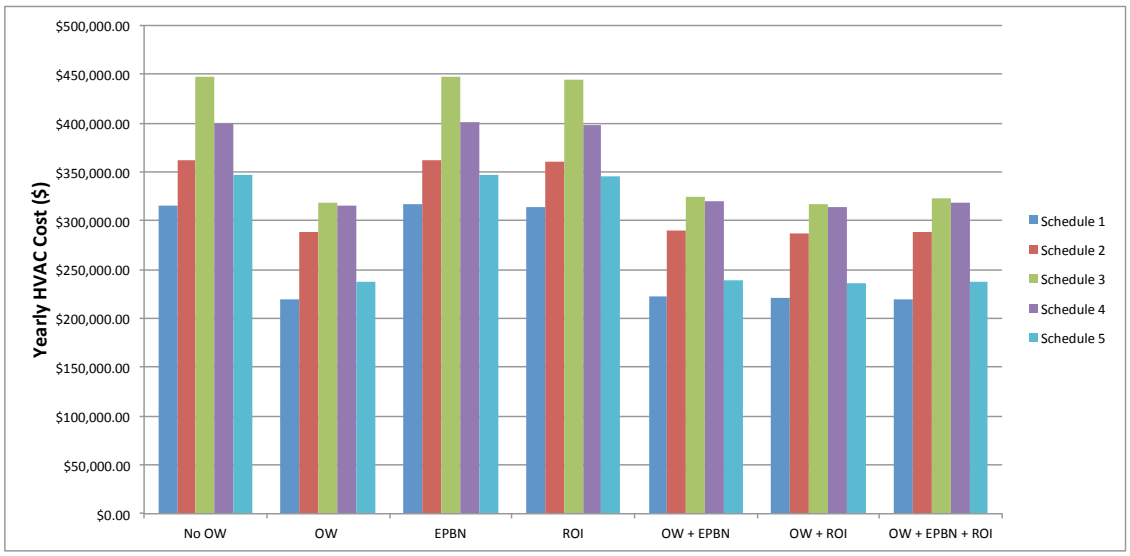

Figure 7.16: Yearly HVAC Cost ($)

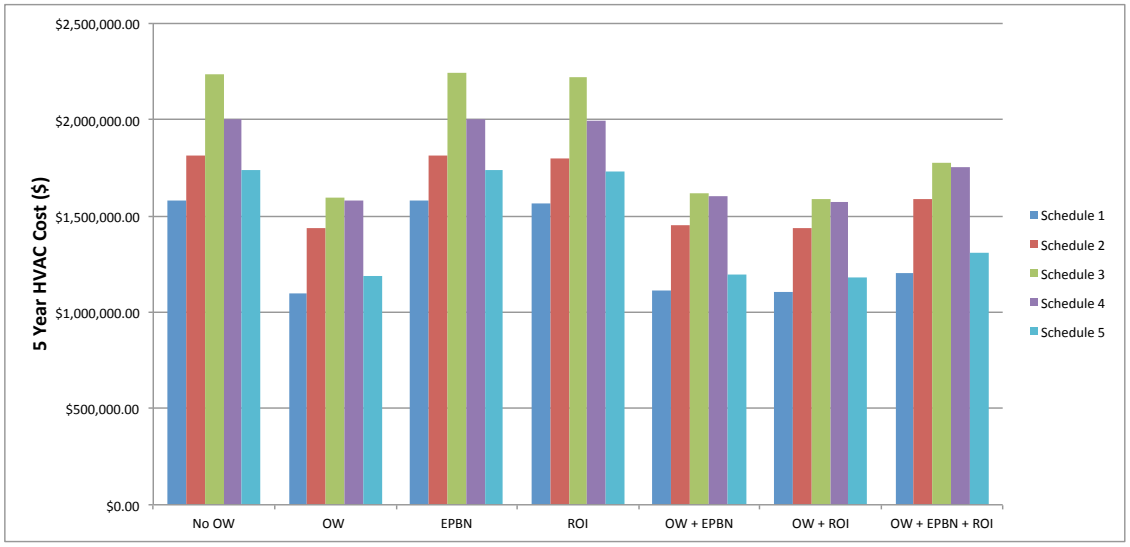

Figure 7.17: 5 Year HVAC Cost ($)

leads to more energy consumption because of the reduced MTTR, meaning that the EP-BN machine will be down less often. However, this leads to an increased throughput as seen in Table 7.9. Schedule 3 is the scenario when the HVAC set point is turned to a lower temperature during periods of higher production energy consumption, which means an increased HVAC energy consumption during these time periods. The smallest HVAC cost

is during Schedule 1 with the OW control, EP-BN mitigation, and ROI improvement, which has a cost of $750.58 per day. Using the HVAC energy cost, the production energy cost, and the production throughput leads to the overall profit as shown in Fig. 7.18 for the average daily profit, Fig. 7.19 for the monthly profit, Fig. 7.20 for the yearly profit, Fig. 7.21 for the five year profit, and Fig. 7.22 for the 5 year profit difference between each scenario and the baseline production case.

The profit results illustrate that the best daily scenario is the OW control and EP-BN

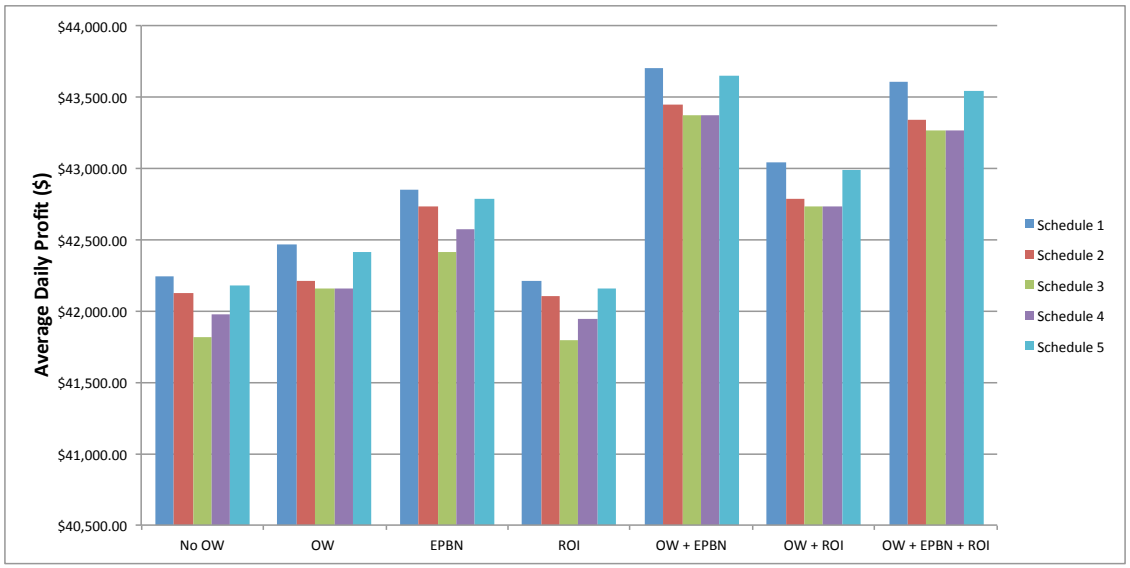

Figure 7.18: Average Daily Profit ($)

mitigation with Schedule 1: a profit of $43,705.99 per day. However, this is a larger profit than the OW control, EP-BN mitigation, and ROI strategy because of the initial cost of the return on investment improvement at machine 12. At the five year mark for Schedule 1, the OW control, EP-BN mitigation, and ROI improvement leads to a profit of $27,102,647.71 versus $26,841,925.77 for the OW control and EP-BN mitigation. Next, we check each schedule for the occupant comfort level using the PMV model in Fig. 7.23. If the PMV is greater than 1.0 or less than -1.0 then the HVAC schedule cannot be utilized. Figure 7.23 illustrates that Schedule 1 and Schedule 5 cannot be utilized since the average comfort level is well above 1.0 for each production scenario. While Schedule 1 leads to the highest

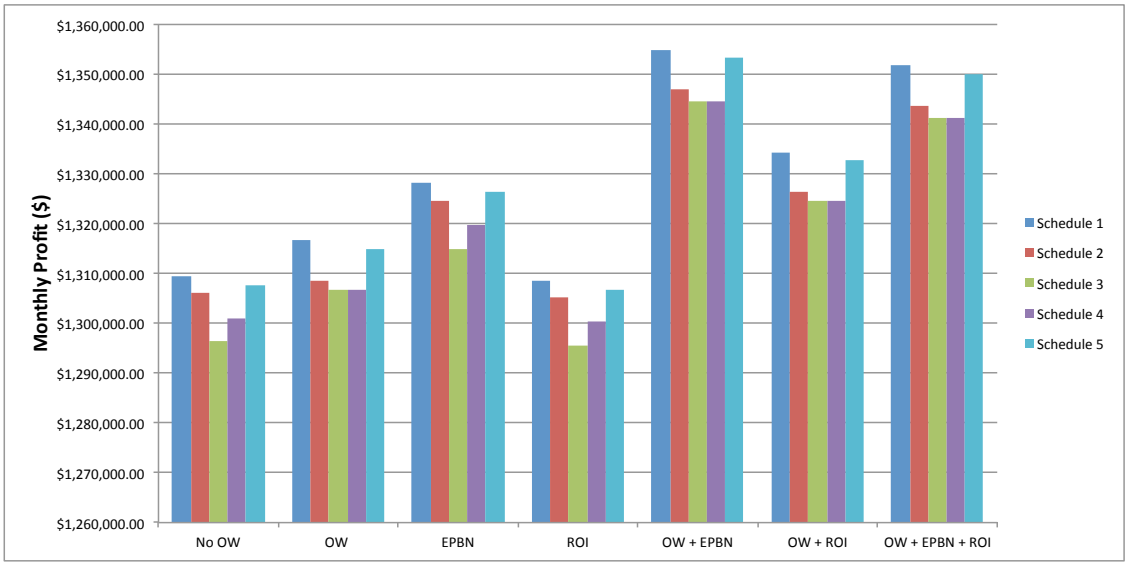

Figure 7.19: Monthly Profit ($)

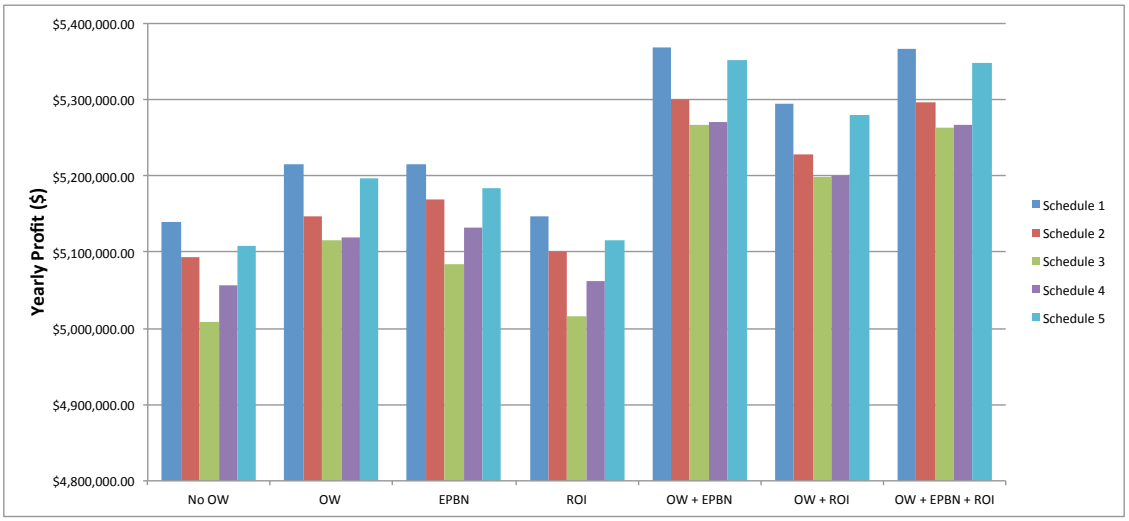

Figure 7.20: Yearly Profit ($)

profit, this HVAC schedule will lead to over 50% of people in the facility feeling discomfort with the overall thermal comfort level. This leaves Schedule 2, Schedule 3, or Schedule 4 as the best scenario for thermal comfort. By studying the five year profits, Schedule 2 with the OW control, EP-BN mitigation and the ROI improvement is the best case for the long term: leading to a profit of $26,747,346.12 over the five year period. The average comfort level with this scenario is 0.831, which is below the 1.0 threshold. For the short term time

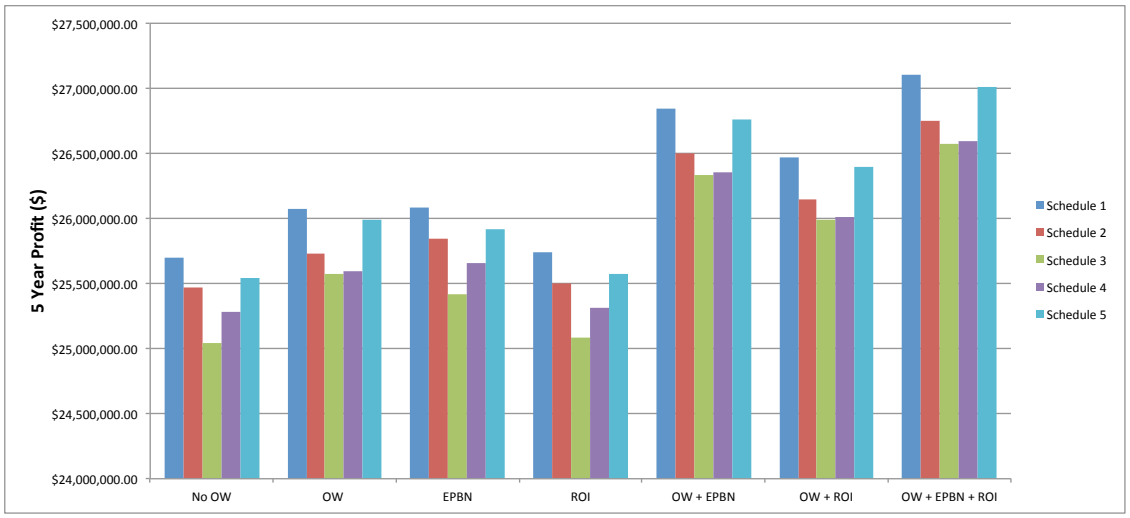

Figure 7.21: 5 Year Profit ($)

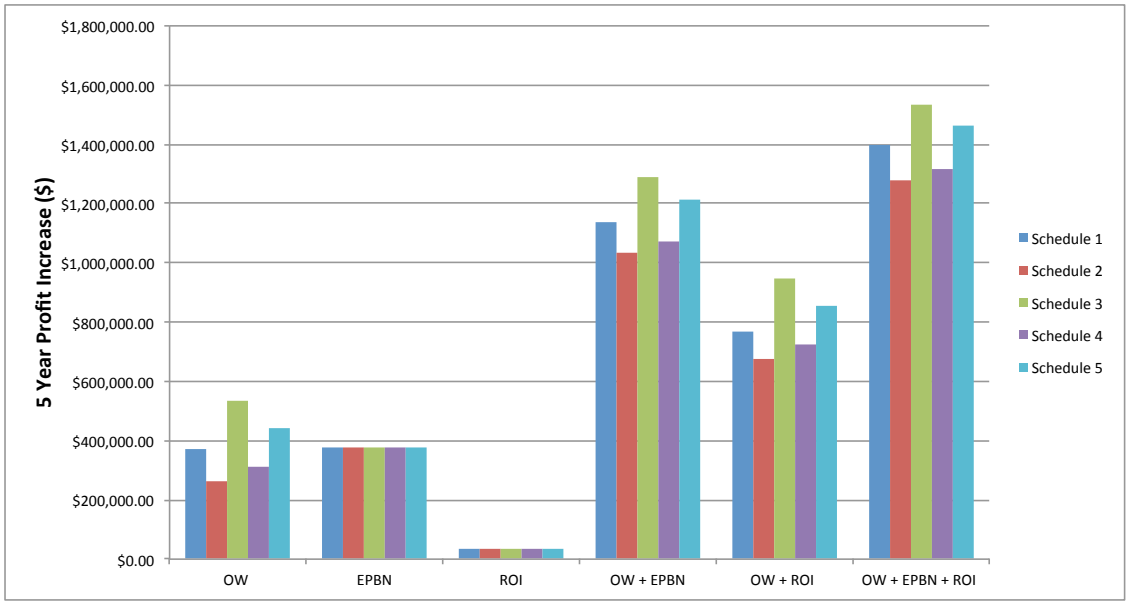

Figure 7.22: 5 Year Profit Increase from Baseline ($)

horizon, the OW control and EP-BN mitigation with Schedule 2 is the best solution. The average daily profit is $43,449.05 with an average comfort level of 0.835. These results show that by scheduling the HVAC set points with overall production energy consumption leads to the optimal thermal comfort according to the PMV scale. By merging the production with the HVAC, it is possible to minimize overall energy consumption of both systems without

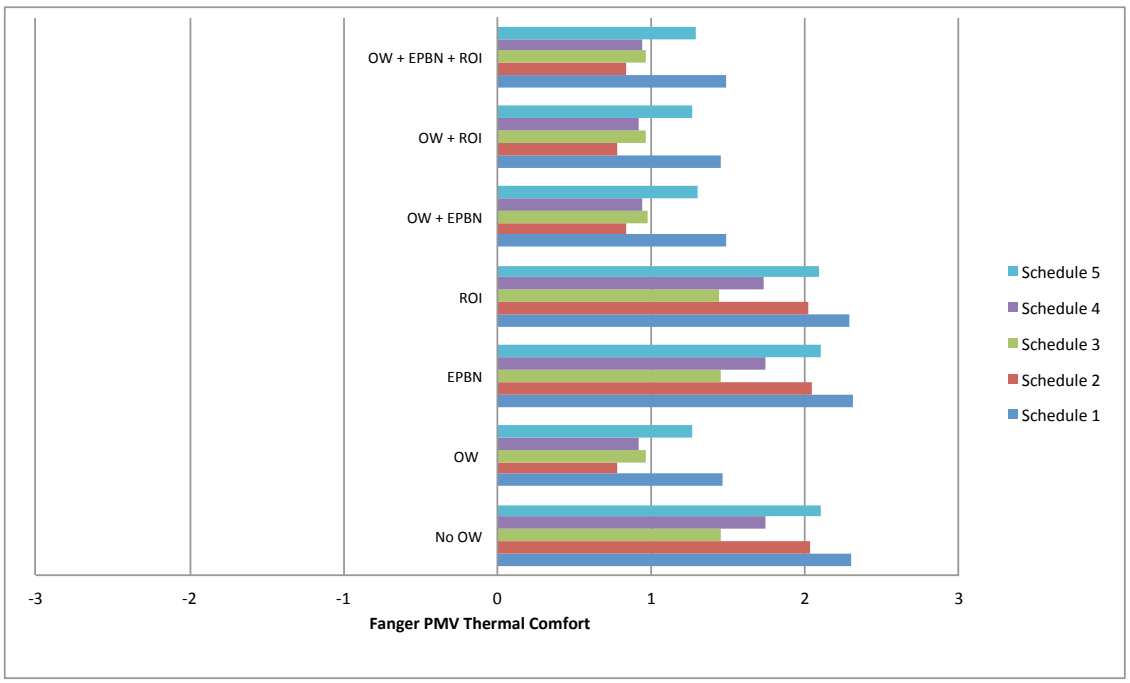

Figure 7.23: Average Comfort Level

any throughput loss through a combination of an opportunity window control methodology, energy profit bottleneck mitigation, and return on investment improvement strategies.

7.3 Conclusions

This chapter investigates the effect of the energy consumption of the production line on the facility HVAC system. The HVAC cooling load impact due the production line is analyzed using a Radiant Time Series Method and reduced using an opportunity window control methodology. A simple integrated thermal model that merges the production and HVAC systems is built using EnergyPlus to study the effect of changing set points with multiple opportunity windows. This model is expanded to include a larger production and HVAC system to test the effects of an opportunity window control scheme, EP-BN mitigation, and ROI improvement strategies on the overall profit and the thermal comfort of occupants within the building. The results indicate that changing the set points of the HVAC system in conjunction with an opportunity window control scheme, EP-BN mitigation, and ROI

improvement lead to an increase in profit without sacrificing throughput or the thermal comfort of the building occupants.

Chapter 8

Conclusions and Future Work

8.1 Conclusions

This dissertation focuses on energy analytics with the intent of increasing profits by decreasing energy waste within the manufacturing industry. The major contributions of this dissertation can be summarized as follows:

1. The impact of disruption events on system productivity is addressed to provide a quantifiable method to measure energy waste. It is discovered that not every disruption event leads to permanent production loss. If a disruption event causes the slowest machine on the line to become blocked, starved, or broken down this will lead to permanent production loss, which is considered an effective downtime event. This directly leads to the concept of the opportunity window, which is the longest amount of time a machine can be down without leading to permanent production loss. If a disruption event is less than the opportunity window than this is referred to as a non-effective downtime event. The opportunity window is proven to be constant if there are no random downtime events on the production line. The recovery time is introduced, which is the amount of time it takes the buffers to recover back to their original state after a downtime event. These concepts are then used in the control methodology to increase profits by inserting non-effective downtime events into the system, which lowers overall energy consumption with minimal loss in productivity.

2. Building on the study of disruption events leads to the analysis of the dynamic energy structure of the production line. The energy consumption is categorized into two portions: the static component, which is the energy utilized in the production of parts

and the dynamic component, which is the energy wasted due to disruption events on the line. The static component is further analyzed to diagnose energy inefficiencies due to the unsynchronous nature of the production line. This leads to the optimal minimum energy consumption per part that can be achieved if each machine were to run standalone. The dynamic energy structure is used to create accurate sustainable manufacturing performance indicators that properly identify system performance for the production line. Two bottlenecks are created to further diagnose inefficiencies at the machine level. The downtime energy bottleneck allows the production manager to allocate maintenance workers to the machine which will lead to the largest decrease in energy waste. The rated power bottleneck provides the machine, which when replaced, leads to the biggest decrease in energy waste.

3. Energy economic analytics are developed to improve profits for the manufacturing line. The energy profit bottleneck is created using readily available sensor information to provide the plant manager with a method to identify the machine, which when prioritized for reactive maintenance, provides the largest increase in profit. A return on investment analysis is introduced that allows the plant manager to replace a machine with a more energy efficient version leading to the largest return on investment. This strategy is combined with an opportunity window control methodology to improve the overall profit of the production facility.

4. A control methodology is developed to combine opportunity window control with EP-BN bottleneck mitigation. This leads to increased profits for the production line by reducing energy consumption with minimal throughput impact. A numerical study is performed to find a general rule for selecting the length and frequency of inserted opportunity windows as well as for determining the correct amount of recovery time to reduce production loss.

5. An integrated production and facility model is developed using EnergyPlus and MATLAB/Simulink. This model merges the production dynamics with the HVAC energy dynamics to reduce the overall energy consumption of the facility, while maintaining production throughput. An analytical method is developed to measure the production impact on the HVAC cooling load. An energy opportunity window control methodology is created to reduce the energy consumption of the production line and the HVAC system. This control methodology is used in conjunction with the EP-BN and the return on investment strategy to increase the overall profits of the facility while maintaining the thermal comfort of the building occupants.

8.2 Future Work

8.2.1 Optimal Control Algorithm

An optimal control algorithm will be developed that will further improve upon the control methodologies presented in this dissertation. Using the combined HVAC and production system a Markov Decision Process (MDP) control methodology will be developed. This control scheme will maximize profits without sacrificing production targets and while maintaining a desired comfort level on the manufacturing floor. The HVAC and production system will be integrated to reduce loads during peak hours of demand. By utilizing the opportunity window control methodology the controlled shut downs of certain machines will not impact overall production. This will further reduce the overall heat load, which will in turn reduce the amount of power consumed by the HVAC system and increases profits for the overall manufacturing facility by reducing energy costs.

8.2.2 Data Uncertainty

The issue of data uncertainty from sensors within the facility will be addressed in future work. Both operational data from the facilities and sophisticated mathematical algorithms

will be utilized to estimate parameters in the integrated models. For example, the prediction error method or the Viterbi algorithm and Baum-Welch approach can be applied to find an optimal parameter based on measurements taken from the facility during normal operation. The Extended Kalman Filter will be investigated for performing real-time estimation of unmeasured variables and energy performance metrics in the manufacturing processes and HVAC systems.

Bibliography

[1] U.S. Energy Information Administration. (2011). *Annual Energy Review 2011* [Online] Available: http://www.eia.gov/totalenergy /data/annual/pdf/sec2_4.pdf

[2] U.S. Energy Information Administration. (2014). *Energy Consumption by Sector and Source* http://www.eia.gov/forecasts/aeo/pdf/tbla2.pdf

[3] U.S. Energy Information Administration. (2014). *Consumption & Efficiency* http://www.eia.gov/consumption/

[4] U.S. Energy Information Administration. (2014). *Manufacturing Energy Consumption Survey* http://www.eia.gov/consumption/manufacturing/

[5] U.S. Energy Information Administration. (2011). *Annual Energy Review 2011* [Online] Available: http://www.eia.gov/totalenergy /data/annual/pdf/sec2_14.pdf

[6] C.W. Gellings, "The concept of demand-side management for electric utilities", *Proceedings of the IEEE*, Vol. 73, Issue 10, pp 1468-1470, Oct. 1985, DOI: 10.1109/PROC.1985.13318.

[7] G. Boyd. (2009). Development of a performance-based industrial energy efficiency indicator for glass manufacturing plants, [Online] Available: http://www.energystar.gov/buildings/tools-and-resources/development-performance-based-industrial-energy-efficiency-indicator-glass

[8] A. Vijayaraghavan, D. Dornfeld, "Automated energy monitoring of machine tools", *CIRP Annals - Manufacturing Technology* Vol. 59, Issue 1, pp. 21-24, 2010, ISSN 0007-8506, http://dx.doi.org/10.1016/j.cirp.2010.03.042.

[9] C. Gutowski, C. Murphy, D. Allen, et al., "Environmentally benign manufacturing: observations from Japan, Europe and the United States," *Journal of Cleaner Production, 13, 1-17,* 2005.

[10] S. Gershwin and I. Schick, "Continuous model of an unreliable two-stage material flow system with a finite inter–stage buffer," *Technical Report 1039,* Massachusetts Institute of Technology, MA, 1980.

[11] S. Gershwin, *Manufacturing Systems Engineering,* Prentice-Hall, Englewood Cliffs, NJ., 1994.

[12] B.A. Sevast'yanov, "Influence of storage bin capacity on the average standstill time of a production line," *Theory of Probability and its Applications,* 7(4):429–438, 1962.

[13] J. Wijngaard,"The effect of interstage buffer storage on output of two unreliable production units in series with different production rates," *AIIE Transactions,* 11(1):42–47, 1979.

[14] Q. Chang, S. Biller, G. Xiao, "Transient analysis of downtimes and bottleneck dynamics in serial manufacturing systems," *ASME Transaction, Journal of Manufacturing Science and Engineering*, Vol 132, Iss. 5, 051015, Oct. 2010.

[15] X. Gu, X. Jin, and J. Ni, "Resilience Measures of Manufacturing Systems Under Disruptions," *Proceedings of the 2014 International Conference on Manufacturing Science and Engineering*, Detroit, Michigan, USA, 2014.

[16] H. Hishamuddin, R. A. Sarker, and D. Essam, "A disruption recovery model for a single stage production-inventory system," *European Journal of Operational Research*, vol. 222, pp. 464-473, Nov 1 2012.

[17] T. Wu, J. Blackhurst, and P. Ogrady., "Methodology for supply chain disruption analysis," *International Journal of Production Research*, vol. 45, pp. 1665-1682, 2007.

[18] Q. Chang, J. Ni, P. Bandyopadhyay, et. al, "Supervisory Factory Control Based on Real-time Production Feedback," *Transactions of the ASME, Journal of Manufacturing Science and Engineering*, vol. 129, pp. 653-660, Jun 2007.

[19] J. Liu, Q. Chang, G. Xiao, S. Biller, "The costs of downtime incidents in serial multi-stage manufacturing systems," *ASME Transaction, Journal of Manufacturing Science and Engineering*, Vol 134, Issue 2, 02101, April 2012.

[20] R. Langer, J. Li, S. Biller, Q. Chang, N. Huang, and G. Xiao, "Simulation Study of a Bottleneck-Based Dispatching Policy for a Maintenance Workforce," *International Journal of Production Research*, vol. 48, pp. 1745-1763, 2010.

[21] C.A. Guerrero, J. Wang, J. Li, et al., "Production system design to achieve energy savings in an automotive paint shop" *International Journal of Production Research* Volume 49, No. 22, 6679–6785, 2011.

[22] K. Fang, N. Uhan, F. Zhao, J. Sutherland, "A new approach to scheduling in manufacturing for power consumption and carbon footprint reduction", *Journal of Manufacturing Systems*, Vol. 30, Issue 4, pp 234-240, Oct. 2011,ISSN 0278-6125, http://dx.doi.org/10.1016/j.jmsy.2011.08.004.

[23] Bohringer, C., Moslener, U., Oberndorfer, U., and Ziegler, A., (2012.) "Clean and productive? Empirical evidence from the German manufacturing industry," *Research Policy,* 41(2): 442–451, DOI: 10.1016/j.respol.2011.10.004.

[24] Haapala, K.R., Zhao, F., Camelio, J., Sutherland, J.W., Skerlos, S.J., Dornfeld, D.A., Jawahir, I.S., Clarens, A.F., and Rickli, J.L. (2013). "A Review of Engineering Research in Sustainable Manufacturing" *Journal of Manufacturing Science and Engineering* 135(4), DOI: 10.1115/1.4024040.

[25] Singh, S., Olugu, E.U., and Fallahpour, A. (2014). "Fuzzy-based sustainable manufacturing assessment model for SMEs, " *Clean Technologies and Envinronmental Policy,* 16(5): 847-860. DOI: 10.1007/s10098-013-0676-5.

[26] Despeisse, M., Ball, P.D., and Evans, S. (2012). "Modelling and Tactics for Sustainable Manufacturing: An Improvement Methodology," *Sustainable Manufacturing,* pp. 9-16. DOI: 10.1007/978-3-642-27290-5_2.

[27] U.S. Environmental Protection Agency (EPA), "Chapter 3: Energy Assessment Strategies", *Lean and Energy Toolkit*, 2009.

[28] "Rockwell Software Enterprise Energy Management", Nov. 2009, Publication RSEEM-PP001A-En-P

[29] "Optimized energy system management with B.Data" [Online], Siemens.com/bdata

[30] LA. Greening, G. Boyd, J.M. Roop, "Modeling of industrial energy consumption: An introduction and context", *Energy Economics*, Vol 29, Issue 4, pp 599-608, July 2007, ISSN 0140-9883, http://dx.doi.org/10.1016/j.eneco.2007.02.011.

[31] C.B, Joung, J. Carrell, P. Sarkar, S. Feng, "Categorization of indicators for sustainable manufacturing", *Ecological Indicators*, Vol 24, pp 148-157, Jan 2013, DOI: 10.1016/j.ecolind.2012.05.030.

[32] P. Bertoldi and S. Kromer, "Efficiency valuation-concepts and practice", *Proceedings of the 2005 ECEEE, Panel 5, European Council for an Energy Efficient Economy*, 2005.

[33] A. Dietmair., A. Verl, "Energy consumption modeling and optimization for production machines," *Sustainable Energy Technologies, 2008.* IEEE International Sustainable Energy Technologies Conference, pp.574-579, 24-27 Nov. 2008, DOI: 10.1109/ICSET.2008.4747073.

[34] F. Zammori, M. Braglia, M. Frosolini, "Stochastic overall equipment effectiveness," *International Journal of Production Research*. Vol. 49, Issue 21, pp 6469-6490, 2011, DOI: 10.1080/00207543.2010.519358.

[35] J.K. Berguland, J.L. Michaloski, S.K. Leong, G. Shao, F.H. Riddick, J. Arinez, S. Biller, "Energy efficiency analysis for a casting production system," *Proceedings of the Winter Simulation Conference, 2011*. Dec. 2011.

[36] M. Colledani, S. Gershwin, "A decomposition method for approximate evaluation of continuous flow multi-stage lines with general Markovian machines", *Annals of Operations Research*, Vol. 209, Issue 1, pp. 5-40, Sep 2011, ISSN 0254-5330, DOI:10.1007/s10479-011-0961-9.

[37] R.S.J Tol, J.P. Weyant, "Energy economics' most influential papers," *Energy Economics 28* (3), pp 405-409, 2006.

[38] N. Liu, B.W. Ang, "Factors shaping aggregate energy intensity trend for industry: Energy intensity versus product mix", *Energy Economics*, Vol. 29, Issue 4, pp. 609-635, July 2007, ISSN 0140-9883, http://dx.doi.org/10.1016/j.eneco.2006.12.004.

[39] G.P. Hammond, J.P. Norman, "Decomposition analysis of energy-related carbon emissions from UK manufacturing", *Energy*, Vol 41, pp 220-27, May 2012, DOI: 10.1016/j.energy.2011.06.035.

[40] S.M. Miranda-da-Cruz, "A model approach for analyzing trends in energy supply and demand at country level: Case study of industrial development in China," *Energy Economics*, Vol 29, Issue 4, pp 913-933, , July 2007, ISSN 0140-9883, http://dx.doi.org/10.1016/j.eneco.2007.01.012.

[41] Bunse, K., Vodicka, M., Schonsleben, P., Brulhart, M., and Ernst, F.O., (2011). "Integrating energy efficiency performance in production management - gap analysis between

industrial needs and scientific literature," *Journal of Cleaner Production,* 19(6-7): 667–679. DOI: 10.1016/j.jclepro.2010.11.011.

[42] Decanio, S.J. and Watkins, W.E. (1998.) "Investment in energy efficiency: do the characteristics of firms matter?", *The Review of Economics and Statistics* 80:95–107.

[43] G. Caifen and L. Shao-kun "Machine Utilization Optimization in Manufacturing Systems," *International Conference on Information Technology and Computer Science, 2009* , vol. 1, pp.11,14,25-26, July 2009, DOI: 10.1109/ITCS.2009.11.

[44] P. Georgiadis and C. Michaloudis "Real-time production planning and control system for job-shop manufacturing: A system dynamics analysis," *European Journal of Operational Research.* Vol. 216, Issue 1, pp 94-104, Jan. 2012, DOI: 10.1016/j.ejor.2011.07.022.

[45] G. Chen, L. Zhang, J. Arinez, et al., "Energy-Efficient Production Systems Through Schedule-Based Operations," *IEEE Transaction on Automation Science and Engineering.* Vol. 10, No. 1, pp 27,37, Jan 2013, DOI: 10.1109/TASE.2012.2202226

[46] Z. Li and M. Zhou, "Elementary siphons of Petri nets and their application to deadlock prevention in flexible manufacturing systems," *IEEE Transactions on Systems, Man and Cybernetics, Part A: Systems and Humans,* vol. 34, pp. 38-51, 2004.

[47] S.-H. Liao and C.-H. Wen, "Mining demand chain knowledge for new product development and marketing," *IEEE Transactions on Systems, Man and Cybernetics, Part C: Applications and Reviews,* vol. 39, pp. 223-227, 2009.

[48] C.-H. Chiu and T.-M. Choi, "Optimal pricing and stocking decisions for news vendor problem with value-at-risk consideration," *IEEE Transactions on Systems, Man and Cybernetics, Part A: Systems and Humans,* vol. 40, pp. 1116-1119, 2010.

[49] W. Jerbi, J. Gaudreault, S. D'Amours, et al., "Optimization/simulation-based framework for the evaluation of supply chain management policies in the forest product

industry," *2012 IEEE International Conference on the Systems, Man, and Cybernetics* 2012.

[50] B. Shen, T.-M. Choi, Y. Wang, et al. "The coordination of fashion supply chains with a risk-averse supplier under the markdown money policy," *IEEE Transactions on Systems, Man and Cybernetics: Systems,* vol. 43, pp. 266-276, 2013.

[51] N. Liu, T.-M. Choi, C. M. Yuen, et al. "Optimal pricing, modularity, and return policy under mass customization," *IEEE Transactions on Systems, Man and Cybernetics, Part A: Systems and Humans,* vol. 42, pp. 604-614, 2012.

[52] Y. Hu, J. Li, and L. E. Holloway, "Resilient Control for Serial Manufacturing Networks With Advance Notice of Disruptions," *IEEE Transactions on Systems, Man and Cybernetics: Systems,* vol. 43, pp. 98-114, 2013.

[53] T. Xiao and T.-M. Choi, "Competitive capacity and price decisions for two build-to-order manufacturers facing time-dependent demands,' *IEEE Transactions on Systems, Man and Cybernetics, Part A: Systems and Humans,* vol. 40, pp. 583-595, 2010.

[54] W. Shen, L. Wang, and Q. Hao, "Agent-based distributed manufacturing process planning and scheduling: a state-of-the-art survey," *IEEE Transactions on Systems, Man and Cybernetics, Part C: Applications and Reviews,* vol. 36, pp. 563-577, 2006.

[55] S. Ioannidis, N. Tsourveloudis, and K. Valavanis, "Fuzzy supervisory control of manufacturing systems," *IEEE Transactions on Robotics and Automation,* , vol. 20, pp. 379-389, 2004.

[56] S. Moujaes and N. Nassif, "A cost-effective operating strategy to reduce energy consumption in a HVAC system," *International Journal of Energy Research* 32: 543-558, 2008.

[57] R. Dazai, T. Kondam, and J. Nishiguchi,"Adaptive optimization method for energy conservation in HVAC systems," *American Society of Heating, Refrigerating and Air-conditioning Engineers, Inc. (ASHRAE) Transactions, Vol. 117 pt. 1, LV-11-C068* Jan 2011.

[58] X. Xu, S. Wang, G. Huang, "Robust MPC for temperature control of air-conditioning systems concerning on constraints and multitype uncertainties," *Building Serv. Eng. Res. Technol.* 31, 1, pp. 39-55, 2010.

[59] K.C. McKinstry, J. Arinez, S. Biller, et. al, "Decision Making Methodology to Reduce Energy in Automobile Manufacturing" *19th CIRP International Conference on Life Cycle Engineering 67-71*, Berkeley, 2012.

[60] S. Wang and Z. Ma, "Supervisory and Optimal Control of Building HVAC Systems: A Review, " *HVAC&R Research,* Volume 14, No. 1, pp 3-32 2008.

[61] J.C. Ghislain and A.T. Mckane, "Energy efficiency as industrial management practice: The Ford production system and institutionalizing energy efficiency," *SAE International* 01-0829, 2006.

[62] H. Liu, Q. Zhao, N. Huang, et al. "A Simulation-Based Tool for Energy Efficient Building Design for a Class of Manufacturing Plants" *IEEE Transactions of Automation Science and Engineering* DOI: 10.1109/TASE.2012.2203595, 2012.

[63] G.P. Moynihan and D. Triantafillu"Energy Savings for a Manufacturing Facility Using Building Simulation Modeling: A Case Study" *Engineering Management Journal*, Vol 24, No. 4, Dec 2012.

[64] Q. Chang, G. Xiao, S. Biller, L. Li, "Energy saving opportunity analysis of automotive serial production systems," *IEEE Transaction on Automation Science and Engineering.* DOI: 10.1109/TASE.2012.2210874, 2012.

[65] Y. Li, Q. Chang, G. Xiao, S. Biller, "Event-based modelling of distributed sensor networks in battery manufacturing," *International Journal of Production Research*, Manuscript ID: TPRS-2013-IJPR-1174, Accepted.

[66] Y. Li, Q. Chang, M.P. Brundage, et. al, "Market Demand Oriented Data-Driven Modeling for Dynamic Manufacturing System Control," *IEEE Transactions on Systems, Man and Cybernetics: Systems,* vol. 45, pp. 109-121, 2015.

[67] U.S. Energy Information Administration. (2011). *Electric Power Monthly* [Online] Available: http://www.eia.gov/electricity/monthly/epm_table_grapher.cfm?t= epmt_5_6_a

[68] Investopedia (2014). *Return on Investment (ROI)* http://www.investopedia.com/terms/r/returnoninvestment.asp

[69] T. T. Tay , I. M. Y. Mareels , J. B. Moore *High Performance Control,* 1997.

[70] F. C. McQuiston, J.D. Parker, J.D. Spitler *Heating, Ventilation and Air Conditioning Analysis and Design,* John Wiley & Sons, 2004.

[71] DOE, "Basic Concepts Manual–Essential Information You Need about Running Energy Plus" *Getting Started with Energy Plus,* 2012.

[72] K.E. Charles "Fanger's Thermal Comfort and Draught Models" *IRC Research Report RR-162*, 2003.

[73] J. Li, S. Meerkov, *Production Systems Engineering,* Springer, 2008.

Appendix A

DE-BN and RP-BN Industry Scenarios

To further show the effectiveness of the DE-BN and RP-BN versus other common industry standards, we randomly pull out the results for 10 combinations. These combinations are seen in Tables A.1 - A.10. Each line combination has an $\alpha_j = 0.8$, which means that the idle power is 80% of the power for producing parts. The mean time to warm up, ω_j is assumed to be 1 min and β_j is assumed to be 0.9. The MTTR for each machine is 10 minutes. The rated speed, 1 / τ, is in parts/min, the MCBF is in minutes. These line combinations represent line configurations commonly found in industry [73].

Line 1 represents a scenario when the efficiency and the buffer capacities are the same. Line 2 is the scenario where the efficiency increases down the line. Lines 3 and 4 are where the efficiency is allocated based on a bowl and inverted bowl pattern respectively. Line 5 is the case where the efficiency decreases across the line. Lines 6 and 7 represents the cases where the buffer capacities are arranged in a bowl and inverted bowl pattern respectively. Lines 8 and 9 are the cases where the buffer capacities are arranged in an increasing and decreasing pattern respectively. Line 10 represents a random case where the machine efficiencies and buffer capacities are arranged randomly. To compare these scenarios, we look at the decrease in $SMPI_{DT}$ for each common industry indicator as compared with the baseline case. This represents the percent decrease in energy waste on the production line. These results are seen in Table A.11 for the DE-BN and Table A.12 for the RP-BN.

The results show that in all scenarios the DE-BN and RP-BN always provide the best results. The other indicators may result in similar performance as with the DE-BN and

RP-BN, but only in certain conditions and they never provide better results. As for these 10 lines shown, only line 3 and line 6 result in a close energy waste reduction percentage as the DE-BN with "Min e_j" and "Max EC_j". However, they still result in less reduction of energy waste. For the RP-BN, line 1 results in a close energy waste reduction with the "Max EC_j", however it does not result in more energy waste reduction. The RP-BN leads to the most energy waste reduction for all 1000 scenarios.

Table A.1: Line 1: Same Efficiency & Buffer Parameters

	m_1	m_2	m_3	m_4	m_5	m_6	m_7	m_8	m_9	m_{10}	m_{11}	m_{12}	m_{13}	m_{14}	m_{15}
$1/\tau$	3	3	3	3	3	3	3	3	2	3	3	3	3	3	3
MCBF	120	120	120	120	120	120	120	120	80	120	120	120	120	120	120
e_j	80	80	80	80	80	80	80	80	80	80	80	80	80	80	80
P_{pp}	100	100	100	100	100	100	100	100	100	100	100	100	100	100	100
Buffer	-	B2	B3	B4	B5	B6	B7	B8	B9	B10	B11	B12	B13	B14	B15
B_m	-	30	30	30	30	30	30	30	30	30	30	30	30	30	30

Table A.2: Line 2: Increasing Efficiency

	m_1	m_2	m_3	m_4	m_5	m_6	m_7	m_8	m_9	m_{10}	m_{11}	m_{12}	m_{13}	m_{14}	m_{15}
$1/\tau$	3	3	2	2.5	2.5	3	2.5	2	1.5	2	3	2.5	3	2.5	3
MCBF	120	120	80	142	142	170	225	180	135	380	570	475	2970	2475	2970
e_j	80	80	80	85	85	85	90	90	90	95	95	95	99	99	99
P_{pp}	100	120	80	80	100	120	100	80	80	100	120	80	100	80	100
Buffer	-	B2	B3	B4	B5	B6	B7	B8	B9	B10	B11	B12	B13	B14	B15
B_m	-	30	30	30	30	30	30	30	30	30	30	30	30	30	30

Table A.3: Line 3: Efficiency Inverted Bowl

	m_1	m_2	m_3	m_4	m_5	m_6	m_7	m_8	m_9	m_{10}	m_{11}	m_{12}	m_{13}	m_{14}	m_{15}
$1/\tau$	2.5	2	2.5	2	3	3	2.5	3	1.5	3	2.5	2	2.5	3	2
MCBF	2475	1980	475	380	270	270	142	170	60	170	142	180	475	570	1980
e_j	99	99	95	95	90	90	85	85	80	85	85	90	95	95	99
P_{pp}	80	100	80	120	80	120	100	120	80	120	100	120	100	120	80
Buffer	-	B2	B3	B4	B5	B6	B7	B8	B9	B10	B11	B12	B13	B14	B15
B_m	-	10	30	50	50	10	30	50	10	10	30	50	30	10	50

Table A.4: Line 4: Efficiency Bowl

	m_1	m_2	m_3	m_4	m_5	m_6	m_7	m_8	m_9	m_{10}	m_{11}	m_{12}	m_{13}	m_{14}	m_{15}
$1/\tau$	2.5	2	2.5	2	3	3	2.5	3	1.5	3	2.5	2	2.5	3	2
MCBF	2475	1980	475	380	270	270	142	170	60	170	142	180	475	570	1980
e_j	80	80	85	85	90	90	95	95	90	90	85	85	80	80	80
P_{pp}	80	100	80	120	80	120	100	120	80	120	100	120	100	120	80
Buffer	-	B2	B3	B4	B5	B6	B7	B8	B9	B10	B11	B12	B13	B14	B15
B_m	-	10	30	50	50	10	30	50	10	10	30	50	30	10	50

Table A.5: Line 5: Efficiency Decreasing

	m_1	m_2	m_3	m_4	m_5	m_6	m_7	m_8	m_9	m_{10}	m_{11}	m_{12}	m_{13}	m_{14}	m_{15}
$1/\tau$	3	2	3	2	2	2.5	3	2.5	1.5	2	2.5	3	2	3	2.5
MCBF	2970	1980	2970	380	380	475	270	225	135	113	142	170	80	120	100
e_j	99	99	99	95	95	95	90	90	90	85	85	85	80	80	80
P_{pp}	80	100	120	100	120	120	100	100	80	100	80	80	120	80	100
Buffer	-	B2	B3	B4	B5	B6	B7	B8	B9	B10	B11	B12	B13	B14	B15
B_m	-	30	50	10	10	50	30	10	50	30	10	50	30	50	10

Table A.6: Line 6: Buffer Bowl

	m_1	m_2	m_3	m_4	m_5	m_6	m_7	m_8	m_9	m_{10}	m_{11}	m_{12}	m_{13}	m_{14}	m_{15}
$1/\tau$	3	3	2	2.5	2.5	3	2.5	3	1.5	3	3	2.5	3	2.5	3
MCBF	2970	120	80	142	225	170	100	120	1485	120	570	100	2970	2475	2970
e_j	99	80	80	85	90	85	80	80	99	80	95	80	99	99	99
P_{pp}	100	120	80	80	100	120	100	120	80	120	100	80	100	80	100
Buffer	-	B2	B3	B4	B5	B6	B7	B8	B9	B10	B11	B12	B13	B14	B15
B_m	-	10	10	10	30	30	30	50	50	50	30	30	10	10	10

Table A.7: Line 7: Buffer Inverted Bowl

	m_1	m_2	m_3	m_4	m_5	m_6	m_7	m_8	m_9	m_{10}	m_{11}	m_{12}	m_{13}	m_{14}	m_{15}
$1/\tau$	3	3	2	2.5	2.5	3	2.5	3	1.5	3	3	2.5	3	2.5	3
MCBF	2970	120	80	142	225	170	100	120	1485	120	570	100	2970	2475	2970
e_j	99	80	80	85	90	85	80	80	99	80	95	80	99	99	99
P_{pp}	100	120	80	80	100	120	100	120	80	120	100	80	100	80	100
Buffer	-	B2	B3	B4	B5	B6	B7	B8	B9	B10	B11	B12	B13	B14	B15
B_m	-	50	50	50	30	30	30	10	10	10	30	30	50	50	50

Table A.8: Line 8: Buffer Increasing

	m_1	m_2	m_3	m_4	m_5	m_6	m_7	m_8	m_9	m_{10}	m_{11}	m_{12}	m_{13}	m_{14}	m_{15}
$1/\tau$	3	2	2.5	2.5	3	2.5	3	3	1	1.5	3	1.5	2.5	3	2.5
MCBF	5940	760	4950	950	540	200	340	5940	180	170	240	2970	950	5940	200
e_j	99	95	99	95	90	80	85	99	90	85	80	99	95	99	80
P_{pp}	120	80	100	100	120	80	80	120	80	120	80	100	80	100	80
Buffer	-	B2	B3	B4	B5	B6	B7	B8	B9	B10	B11	B12	B13	B14	B15
B_m	-	10	10	10	10	30	30	30	30	30	30	50	50	50	50

Table A.9: Line 9: Buffer Decreasing

	m_1	m_2	m_3	m_4	m_5	m_6	m_7	m_8	m_9	m_{10}	m_{11}	m_{12}	m_{13}	m_{14}	m_{15}
$1/\tau$	3	2	3	2.5	2.5	2	2	2.5	1.5	3	2.5	2	3	2.5	3
MCBF	2970	80	120	142	225	113	80	100	1485	120	475	80	2970	2475	2970
e_j	99	80	80	85	90	85	80	80	99	80	95	80	99	99	99
P_{pp}	120	80	100	100	120	80	80	120	80	120	80	100	80	100	80
Buffer	-	B2	B3	B4	B5	B6	B7	B8	B9	B10	B11	B12	B13	B14	B15
B_m	-	50	50	50	50	30	30	30	30	10	10	10	10	10	10

Table A.10: Line 10: Random Parameters

	m_1	m_2	m_3	m_4	m_5	m_6	m_7	m_8	m_9	m_{10}	m_{11}	m_{12}	m_{13}	m_{14}	m_{15}
$1/\tau$	2	3	2	3	2.5	2	2	2.5	1	2.5	1.5	2	3	2	2.5
MCBF	113	120	180	2970	100	113	80	2475	90	475	85	180	2970	113	100
e_j	85	80	90	99	80	85	80	99	90	95	85	90	99	85	80
P_{pp}	100	120	120	80	100	80	80	120	100	120	100	100	120	80	80
Buffer	-	B2	B3	B4	B5	B6	B7	B8	B9	B10	B11	B12	B13	B14	B15
B_m	-	50	50	50	50	30	30	30	30	10	10	10	10	10	10

Table A.11: Downtime Energy Bottleneck Lines 1-10: Percent Decrease in Energy Waste

Lines	1	2	3	4	5	6	7	8	9	10
DE-BN	7.2 %	3.4 %	5.1 %	3.3 %	4.2 %	4.8 %	4.3 %	4.6 %	5.7 %	5.9 %
Max EPP_j	1.3 %	-0.1 %	1.9%	.03 %	-.02 %	-.90 %	1.8 %	.04%	1.5 %	1.8 %
Min e_j	.06 %	.05 %	5.10%	-0.2 %	.01 %	-.89 %	.03 %	3.0 %	.02 %	.01 %
Max $P_{pp,j}$	.05 %	.08 %	-.05%	.03 %	.03 %	-.9 %	.04 %	0.0 %	0.0 %	.00 %
Max EC_j	1.3 %	.07 %	-.03	.04 %	.04 %	4.7 %	.03 %	.05 %	1.50 %	1.8 %

Table A.12: Rated Power Bottleneck Lines 1-10: Percent Decrease in Energy Waste

	Line 1	Line 2	Line 3	Line 4	Line 5	Line 6	Line 7	Line 8	Line 9	Line 10
RP-BN	2.0 %	2.4 %	1.8 %	2.3 %	2.2 %	2.5 %	1.9 %	2.3 %	2.4 %	2.4 %
Max EPP_j	1.9 %	2.3 %	1.6 %	2.2 %	2.0 %	2.2 %	1.8 %	2.2 %	2.2 %	2.1 %
Min e_j	1.8 %	2.1 %	1.3 %	1.9 %	1.9 %	1.9 %	1.7 %	1.8 %	2.0 %	2.0 %
Max $P_{pp,j}$	1.8 %	2.1 %	1.6 %	2.1 %	1.8 %	1.9 %	1.7 %	1.8 %	2.1 %	2.0 %
Max EC_j	1.9 %	2.3 %	1.6 %	2.2 %	2.0 %	2.2 %	1.8 %	2.2 %	2.2 %	2.2 %

Appendix B

Scenarios for Recovery Time Numerical Studies

The numerical studies are used to provide guidance for the control methodology presented in Chapter 6. The amount of time each machine is turned off is t_{OW} and the recovery time is t_r. The recovery time simulation results can be seen for Lines 2A-2E in Fig. B.1, Lines 3A-3E in Fig. B.2, Lines 4A-4E in Fig. B.3, and Lines 5A-5E in Fig. B.4.

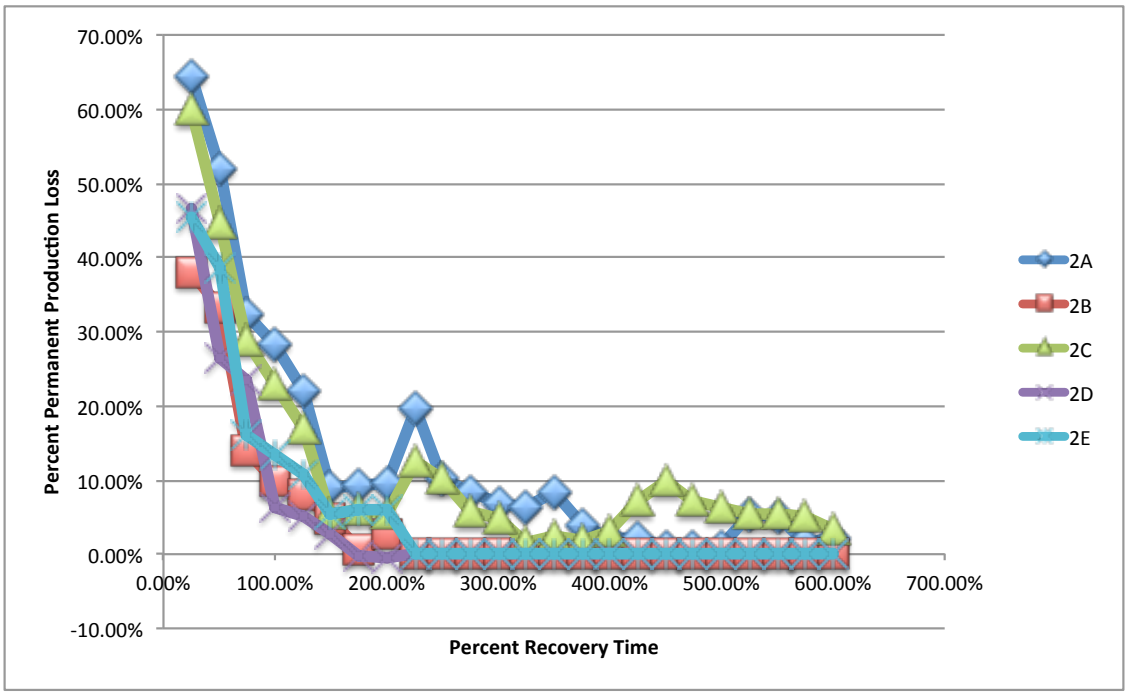

Figure B.1: Recovery Time Lines 2A-2E

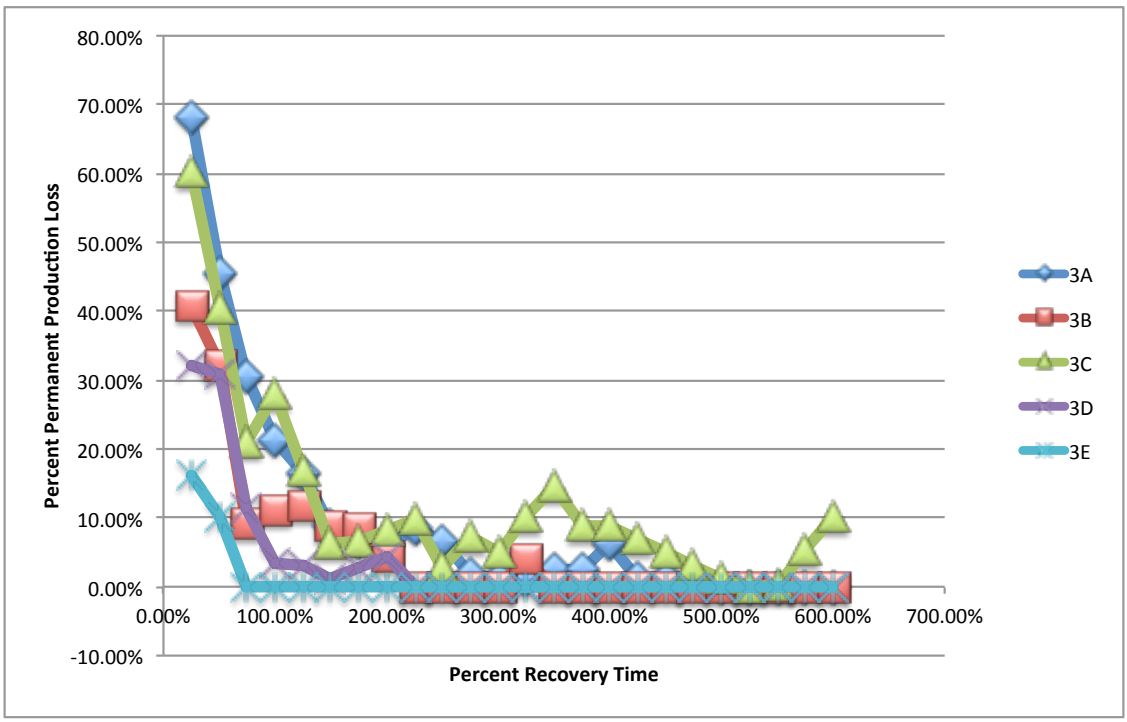

Figure B.2: Recovery Time Lines 3A-3E

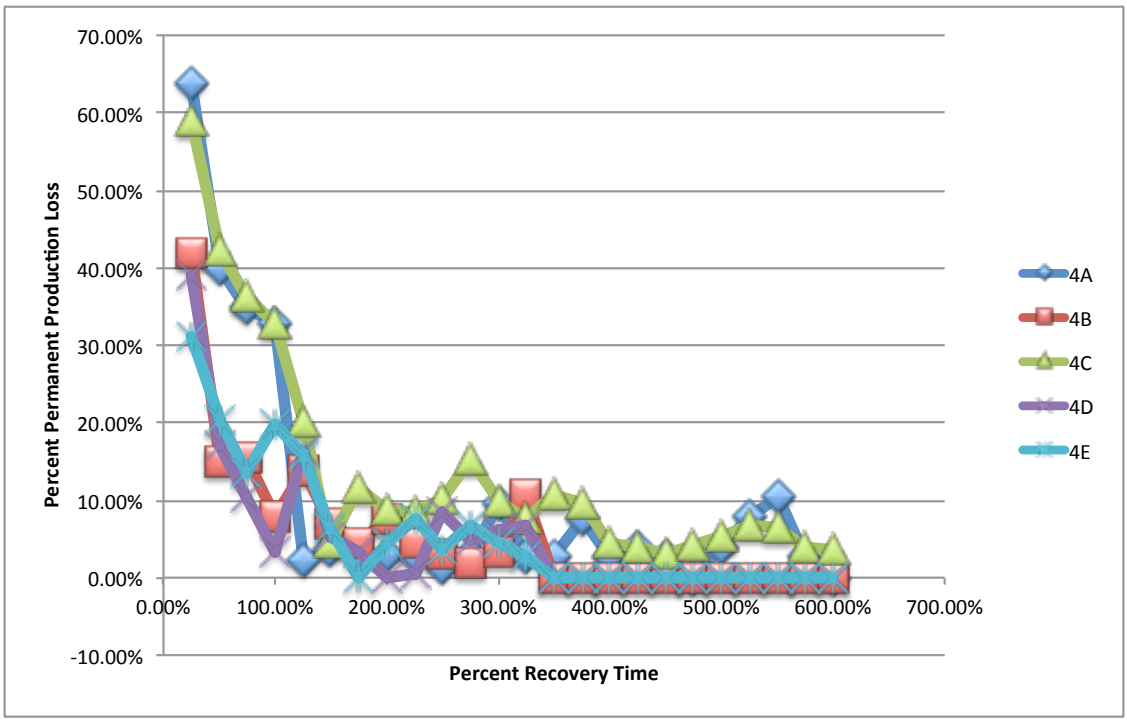

Figure B.3: Recovery Time Lines 4A-4E

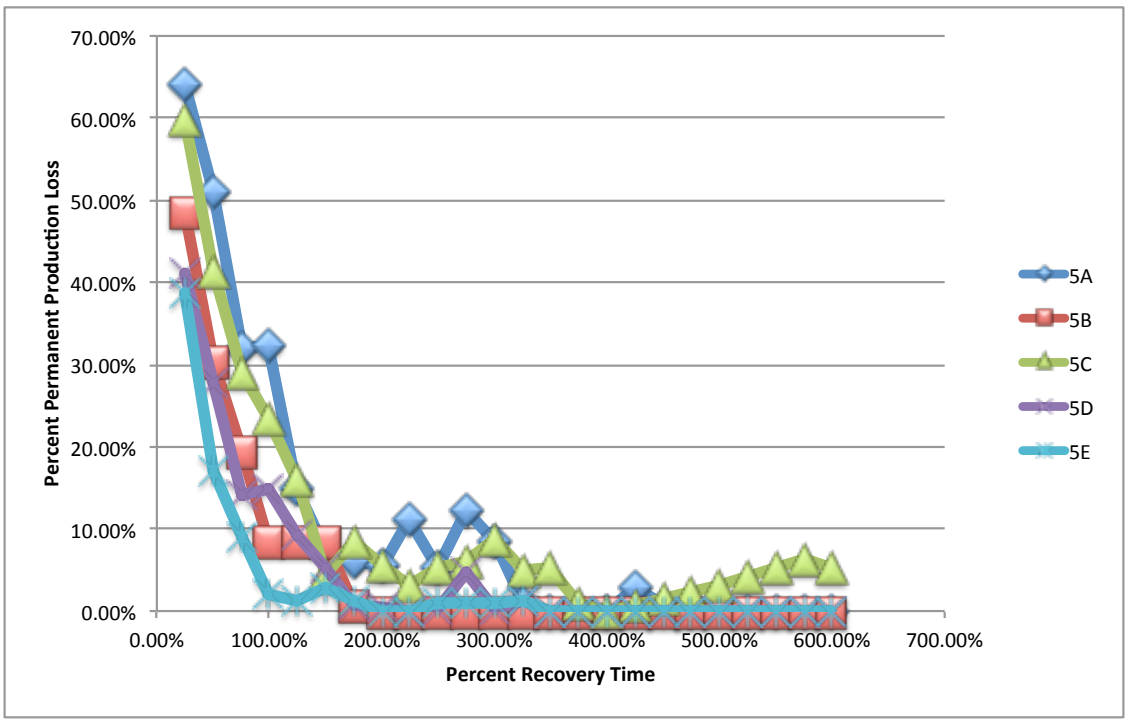

Figure B.4: Recovery Time Lines 5A-5E